COMPARATIVE GENOMIC, TRANSCRIPTOMIC AND PHENOMIC ANALYSES ON QUORUM SENSING OF *Hafnia alvei*

TAN JIA YI

FACULTY OF SCIENCE
UNIVERSITY OF MALAYA
KUALA LUMPUR

2019

COMPARATIVE GENOMIC, TRANSCRIPTOMIC AND PHENOMIC ANALYSES ON QUORUM SENSING OF *Hafnia alvei*

TAN JIA YI

THESIS SUBMITTED IN FULFILMENT OF THE REQUIREMENTS FOR THE DEGREE OF DOCTOR OF PHILOSOPHY

INSTITUTE OF BIOLOGICAL SCIENCES
FACULTY OF SCIENCE
UNIVERSITY OF MALAYA
KUALA LUMPUR

2019

UNIVERSITY OF MALAYA

ORIGINAL LITERARY WORK DECLARATION

Name of Candidate: **TAN JIA YI**

Matric No: **SHC150077**

Name of Degree: **DOCTOR OF PHILOSOPHY**

Title of Project Paper/Research Report/Dissertation/Thesis ("this Work"):

COMPARATIVE GENOMIC, TRANSCRIPTOMIC AND PHENOMIC ANALYSES ON QUORUM SENSING OF *Hafnia alvei*

Field of Study:

GENETICS AND MOLECULAR BIOLOGY

I do solemnly and sincerely declare that:

(1) I am the sole author/writer of this Work;
(2) This Work is original;
(3) Any use of any work in which copyright exists was done by way of fair dealing and for permitted purposes and any excerpt or extract from, or reference to or reproduction of any copyright work has been disclosed expressly and sufficiently and the title of the Work and its authorship have been acknowledged in this Work;
(4) I do not have any actual knowledge nor do I ought reasonably to know that the making of this work constitutes an infringement of any copyright work;
(5) I hereby assign all and every rights in the copyright to this Work to the University of Malaya ("UM"), who henceforth shall be owner of the copyright in this Work and that any reproduction or use in any form or by any means whatsoever is prohibited without the written consent of UM having been first had and obtained;
(6) I am fully aware that if in the course of making this Work I have infringed any copyright whether intentionally or otherwise, I may be subject to legal action or any other action as may be determined by UM.

Candidate's Signature Date:

Subscribed and solemnly declared before,

Witness's Signature Date:

Name:

Designation:

COMPARATIVE GENOMIC, TRANSCRIPTOMIC AND PHENOMIC ANALYSES ON QUORUM SENSING OF *Hafnia alvei*

ABSTRACT

Quorum sensing (QS) is the regulatory event achievable via cell-to-cell communication that involves release and detection of autoinducers (AIs), which occurs in a wide range of bacteria. To date, QS has been associated to events of pathogenesis, biofilm formation, antibiotic resistance in clinical, industrial, as well as agricultural aspects. The focus of this study lies on the acyl-homoserine lactone (AHL) type QS in *Hafnia alvei*, an opportunistic pathogen and potential spoilage agent. *H. alvei* FB1 was obtained in an attempt to isolate AHL-producing strains from "fish ball", a popular street food made of fish paste. The main objective of this study is to investigate the role of AHL type QS in FB1 via identification of QS core genes using genomic approach, followed by transcriptomic and phenomic comparative profiling between QS-deficient mutants and the wildtype strains. In this study, *H. alvei* FB1 has been found to produce two types of AHLs, namely, *N*-(3-oxohexanoyl) homoserine lactone ($3OC_6$-HSL) and *N*-(3-oxooctanoyl) homoserine lactone ($3OC_8$-HSL). Complete genome sequence of FB1 was obtained and a single pair of AHL synthase (*halI*) and its cognate receptor (*halR*) genes were identified. QS-deficient mutants of FB1 were constructed via λ-Red recombineering method. Comparative study showed that the removal of QS genes in FB1 affected mainly mechanisms in cell division, nutrient uptake, as well as resistance to a number of antibiotics, which were crucial for survival, adaptation and colonisation of the organism in both food and host gut environment. In conclusion, this study has served its role as a preliminary fundamental study with the hope to pave the advancement of more in depth study and application in future.

Keywords: Quorum sensing, *N*-acylhomoserine lactone, *Hafnia alvei*, food, opportunistic pathogen

ANALISIS PERBANDINGAN GENOMIK, TRANSKRIPTOMIK, DAN FEMONIK BAGI PENGESANAN KUORUM *Hafnia alvei*

ABSTRAK

Pengesanan kuorum (QS) adalah peristiwa kawalatur melalui komunikasi sel ke sel yang melibatkan pelepasan dan pengesanan autoinduser (AI) yang berlaku di sejulat lebar bakteria. Hingga hari ini, QS telah dikaitkan dengan kejadian patogenesis, pembentukan biofilm, resistans kepada antibiotik dalam aspek klinikal, industri, dan pertanian. Fokus kajian ini adalah pada QS jenis asil-homoserina lakton (AHL) dalam *Hafnia alvei*, sejenis patogen oportunis dan agen kerosakan makanan potensi. *H. alvei* FB1 telah diperolehi dalam satu percubaan untuk mengasingkan strain-strain penghasil AHL dari bebola ikan, sejenis makanan jalanan popular diperbuat daripada pes ikan. Objektif utama kajian ini adalah untuk mempersiasatkan peranan QS jenis AHL dalam FB1 melalui pengenalan gen-gen teras QS dengan pendekatan genomik, diikuti dengan pemprofilan perbandingan transkriptomik dan fenomik antara mutan-mutan defisien QS dengan strain jenis liar. Dalam kajian ini, *H. alvei* FB1 didapati menghasilkan dua jenis AHL, iaitu N-(3-oksoheksanoil) homoserina lakton (3-oxo-C6-HSL) dan N-(3-oxooktanoil) homoserina lakton (3-oxo-C8-HSL). Jujukan genom lengkap FB1 telah diperolehi dan sepasang tunggal sintase AHL (halI) dan reseptor seasalnya (halR) dikenali. Mutan-mutan defisien QS FB1 telah dihasilkan melalui cara λ-Red recombineering. Kajian perbandingan menunjukkan kekurangan gen-gen QS dalam FB1 menjejaskan terutamanya mekanisme dalam pembelahan sel, pengambilan nutrien, serta resistens terhadap sebilangan antibiotik. Ciri-ciri tersebut penting dalam survival, adaptasi dan kolonisasi organisme tersebut dalam persekitaran makanan dan salur makanan perumah. Sebagai kesimpulan, kajian ini telah memenuhi peranannya sebagai kajian asasi awal dengan harapan untuk menyumbang kepada kemajuan kajian yang lebih mendalam serta aplikasi pada masa depan.

Kata kunci: Pengesanan kuorum, *N*-asil-homoserina lakton, *Hafnia alvei*, makanan, patogen oportunis

ACKNOWLEDGEMENTS

First and foremost, I would like to express my heartiest appreciation to my supervisor, Assoc. Prof. Dr. Chan Kok Gan for his dedicated efforts in providing new ideas, valuable guidance, and constant encouragement from the process of preparation and throughout the completion of my Ph.D. research and thesis. My sincere thanks also go to my lab manager, Ms. Yin Wai Fong for her help in financial management and ensuring sufficient supplies of necessity, which allowed the research project to be carried out smoothly.

My appreciation also goes to University of Malaya for providing sufficient financial support, including High Impact Research (HIR) grants, Postgraduate Research Grant (PPP), and Graduate Research Assistantship Scheme (GRAS), as well as all the necessary facilities throughout the commencement of this research. I would also like to express my gratitude to the staff of Institute of Biological Sciences (ISB) for their assistance in the process of thesis submission and efficiency in processing various forms of paperwork.

Furthermore, I would like to acknowledge my lab mates and friends for their moral support and assistance in various ways that contributed to the research. Last but not least, I would like to express my heartfelt appreciation to my family members, who have been supported me unconditionally throughout the period of my study.

TABLE OF CONTENTS

LIST OF FIGURES

LIST OF TABLES

LIST OF SYMBOLS AND ABBREVIATIONS

°C	:	Degree Celcius
<	:	Less than
≤	:	Less than or equal
µg	:	Microgram
µL	:	Microliter
>	:	More than
%	:	Percent
×	:	Times
× *g*	:	Times gravity
$3OC_{10}$-HSL	:	*N*-3-oxodecanoyl-homoserine lactone
$3OC_{12}$-HSL	:	*N*-3-oxododecanoyl-homoserine lactone
$3OC_{6}$-HSL	:	*N*-3-oxohexanoyl-homoserine lactone
$3OC_{6}$-HSL	:	*N*-3-oxohexanoyl-homoserine lactone
$3OC_{8}$-HSL	:	*N*-3-oxooctanoyl-homoserine lactone
$3OC_{8}$-HSL	:	*N*-3-oxooctanoyl-homoserine lactone
$3OHC_{4}$-HSL	:	*N*-3-hydroxybutanoyl-homoserine lactone
ACN	:	Acetonitrile
ACP	:	Acyl carrier protein
AGE	:	Agarose gel electrophoresis
AHL	:	*N*-acyl-homoserine lactone
AI	:	Autoinducer
AI2	:	Autoinducer-2
AIP	:	Autoinducing peptide
ANI	:	Average nucleotide index

BASys	:	Bacterial Annotation System
BHI	:	Brain Heart Infusion
BLAST	:	Basic Local Alignment Search Tool
bp	:	Base pair
C_{10}-HSL	:	*N*-decanoyl-homoserine lactone
C_4-HSL	:	*N*-butanoyl-homoserine lactone
C_6-HSL	:	*N*-hexanoyl-homoserine lactone
C_8-HSL	:	*N*-octanoyl-homoserine lactone
Cas	:	CRISPR-associated
CDD	:	Conserved Domain Database
CDD	:	Conserved Domain Database
cDNA	:	Complementary DNA
CDS	:	Coding DNA sequence
ChIP	:	Chromatin immunoprecipitation
COG	:	Cluster of Orthologous Group
CRISPR	:	Clustered Regularly Interspaced Short Palindromic Repeats
DDH	:	DNA-DNA hybridisation
DEG	:	Differentially expressed gene
DMT	:	Drug/metabolite transporter
DNA	:	Deoxyribonucleic acid
dsDNA	:	Double-stranded DNA
DSMZ	:	German Collection of Microorganisms and Cell Cultures
EPS	:	Exopolysaccharide
EST	:	Expressed sequence tag
eV	:	Electronvolt
FC	:	Fold change

g	:	Gram
G6P	:	Glucose-6-phosphate
gDNA	:	Genomic deoxyribonucleic acid
GEO	:	Gene Expression Omnibus
Gepard	:	Genome Pair Rapid Dotter
GN	:	Gram-negative
GO	:	Gene Ontology
h	:	Hour
HGAP	:	Hierarchical Genome Assembly Process
HGT	:	Horizontal gene transfer
HS	:	High sensitivity
KanR	:	Kanamycin resistance cassette
kb	:	Kilobase
kDa	:	Kilodalton
kV	:	Kilovolt
LB	:	Luria-Bertani
LBA	:	Luria-Bertani agar
LBB	:	Luria-Bertani broth
LC-MS	:	Liquid chromatography-mass spectrometry
m/*z*	:	Charge-to -mass
MAC	:	MacConkey
MALDI	:	Matrix-assisted laser desorption
MEGA	:	Molecular Evolutionary Genetics Analysis
MFS	:	Major facilitator superfamily
min	:	Minute
mL	:	Milliliter

MLSA	:	Multilocus sequence analysis
mM	:	Millimolar
mm	:	Millimeter
MOPS	:	3-[*N*-morpholino] propanesufonic acid
MS/MS	:	Tandem mass spectrometry
MSA	:	Multiple sequence alignment
ng	:	Nanogram
NJ	:	Neighbour-joining
nm	:	Nanometer
OAT	:	Orthologous Average Nucleotide Identity Tool
OD	:	Optical density
OM	:	Outer membrane
PBS	:	Phosphate buffer saline
PCA	:	Principal component analysis
PCR	:	Polymerase chain reaction
PGAAP	:	Prokaryotic Genome Automatic Annotation Pipeline
pM	:	Picomolar
PM	:	Phenotype microarray
PMF	:	Peptide mass fingerprint
POCP	:	Percentage of conserved proteins
psi	:	Pound per square inch
PTS	:	Phosphotransferase system
qPCR	:	Quantitative polymerase chain reaction
QS	:	Quorum sensing
RAST	:	Rapid Annotation using Subsystem Technology
R_f	:	Retention factor

RIN	:	RNA integrity number
RM	:	Restriction-modification
RNA	:	Ribonucleic acid
rpm	:	Revolutions per minute
rRNA	:	Ribosomal RNA
RTC	:	Real time classification
SAM	:	*S*-adenosyl-L-methionine
sec	:	Second
SMRT	:	Single Molecule Real Time
SOC	:	Super Optimal broth with Catabolite repression
ssDNA	:	Single-stranded DNA
T6P	:	Trehalose-6-phosphate
T6SS	:	Type VI Secretion System
TBE	:	Tris-boric acid ethylenediaminetetraacetic acid
TLC	:	Thin layer chromatography
TOF	:	Time of flight
tRNA	:	Transfer RNA
UV	:	Ultraviolet
v/v	:	Volume over volume
w/v	:	Weight over volume
WGS	:	Whole genome sequencing
WT	:	Wild type

LIST OF APPENDICES

CHAPTER 1: INTRODUCTION

Quorum sensing (QS) is a form of cell-to-cell communication adapted by a wide range of bacterial species, achievable by release and detection of signaling molecules called autoinducers (AIs) (Miller & Bassler, 2001). *N*-acyl-homoserine lactone (AHL) is one of these AIs commonly produced by Proteobacteria. Individual cells monitor the changes in 'quorum' through detection of these small, often lipophilic molecules in the environment, and, in response, adjust the expression of a network of genes in a collective manner (Parsek & Greenberg, 2000). AHL-based QS has been reported to associate with various microbial activities of clinical, industrial, and agricultural importance, such as regulation on virulence expression (Duerkop et al., 2007; Hao & Burr, 2006; Pearson et al., 2000), production of antibiotics (Barnard et al., 2007; Pierson et al., 1995), biofilm formation (Rivas et al., 2007; TomLin et al., 2005; Labbate et al., 2004), and food spoilage (Blana & Nychas, 2014; Bruhn et al., 2004; Christensen et al., 2003).

The focus of this study, *Hafnia alvei* FB1 is one of such AHL-producing strains recovered from vacuum-packed refrigerated fish paste meatballs (commonly known as 'fish ball'), in an attempt to search for AHL-producing bacteria in food. 'Fish ball' or fish paste meatball, is a popular form of street food in Southern China and South-East Asia.

Hafnia, a genus establishing characteristics such as rod-shaped, motile, flagellated, and facultative anaerobic, belongs to the family *Hafniaceae*. *H. alvei* has been identified to be among the enteric bacteria commonly involved in food spoilage (Blana & Nychas, 2014; Bruhn et al., 2004; Gram et al., 1999; Ridell & Korkeala, 1997), and an opportunistic pathogen (Janda & Abbott, 2006). The ability of *H. alvei* to survive under low temperature (Ridell & Korkeala, 1997) has made it an interesting subject of study in controlling bacterial contamination in the food industry. In recent years, advancement in the technology of high-throughput sequencing and accessibility of powerful bioinformatics pipelines enable bacterial genomes and transcriptomes to be explored with

much ease. On the other hand, current DNA recombinant technology that allows precise genome editing provides a convenient tool in the study of QS regulons. This study investigated the profile of QS signalling molecules produced by *H. alvei*, as well as investigated the regulatory role of QS in *H. alvei* as a candidate of gut pathogen by studying the QS-deficient mutants in a comparative transcriptomics and phenotypic perspective.

The objectives of this study involve:

1. To isolate and identify AHL-producing bacteria in fish meatball samples
2. To characterise the AHL profile of the isolated foodborne AHL-producing bacteria
3. To sequence the whole genome of the isolated foodborne AHL-producing bacteria for identification of QS genes
4. To conduct functional study of the QS-genes in the bacterial strain

CHAPTER 2: LITERATURE REVIEW

2.1 Quorum Sensing (QS)

The term QS was first coined by Fuqua et al. (1994) to refer to the process of bacterial cell-to-cell communication. The phenomenon was first observed from a series of experiments conducted on the bioluminescent bacterium *Allivibrio fischeri* (formerly *Vibrio fischeri*), a symbiont of the Hawaiian bobtail squid, *Euprymna scolopes*. In the light organ of the squid, where the bacterial cell density is high and the signaling molecules abundant, LuxR, the AHL receptor protein, in its active form, binds to the promoter of *luxICDABEG* operon and induces bioluminescence (Fuqua et al., 1994). The same reaction does not occur in a low cell density planktonic state (Figure 2.1).

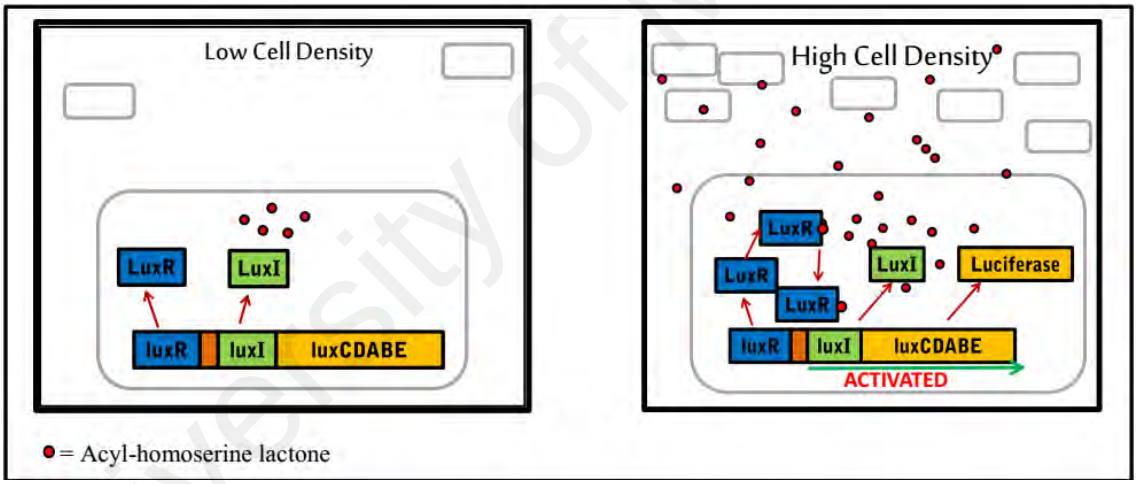

Figure 2.1: Model of QS system in *A. fischeri* which regulates bioluminescence activation. At high cell density, AHL binds to its cognate LuxR and subsequently activates transcription of LuxI and the luciferase operon.

To date, a variety of QS mechanisms and signalling molecules have been reported: The best characterized LuxI-LuxR type system that utilized AHLs (as in *A. fischeri*) in Proteobacteria (Case et al., 2008), the small post-translationally modified autoinducing peptides (AIPs) that are the main signalling molecules in Gram-positive bacteria (Sturme et al., 2002), and the "universal" Autoinducer-2 (AI2), the furanosyl borate diester, that exists in both Gram-positive and negative bacteria (Miller & Bassler, 2001; Bassler et al.,

1993). Classical examples of traits and cellular activities that have been associated to QS include virulence expression (Passador et al., 1993), biofilm formation (Davies et al., 1998), production of antibiotics (Bainton et al., 1992a; Bainton et al., 1992b), motility (Eberl et al., 1999; Eberl et al., 1996), and conjugation (Zhang et al., 1993).

It is generally agreed that the major role of QS lies in the regulation of gene expression in response to population density, in such a way that certain cellular function would not be induced until there is a sufficient quorum. There is also an alternative theory stating that QS has the potential to act as a mechanism for "environmental sensing", which utilizes the signaling molecules to detect the properties of diffusion flow of the environment (Redfield, 2002).

2.1.1 *N*-Acyl-Homoserine Lactones (AHLs)

AHL is a form of signalling molecules produced exclusively within Proteobacteria (Case et al., 2008). These signalling molecules share conserved structural characteristics: A homoserine lactone ring and an *N*-acyl side chain consisting of 4 to 18 carbons. There could be an oxo- or hydroxy- substituent at the C_3 position (Chhabra et al., 2005) (Figure 2.2). These small molecules are synthesized from their substrates, *S*-adenosyl-L-methionine (SAM) and acyl-acyl carrier protein (acyl-ACP) (Hanzelka & Greenberg, 1996; Moré et al., 1996). The reaction is catalysed by a wide range of AHL-synthase proteins that are homologous to LuxI in *A. fischeri*. AHL synthesis has also been reported to be catalysed less commonly by enzymes from other families, such as LuxM in *Vibrio harveyi* (Bassler et al., 1993) and HdtS in *Pseudomonas fluorescens* (Laue et al., 2000).

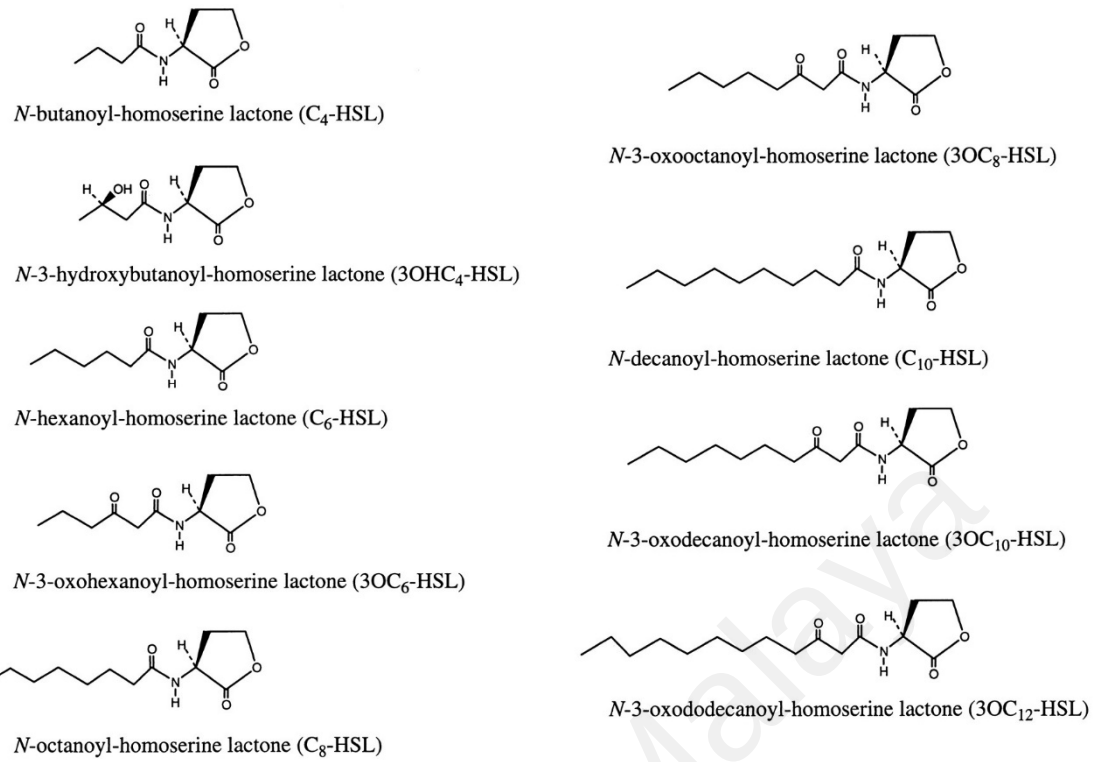

Figure 2.2: Structure of nine naturally occurring AHL molecules (Guan et al., 2000). Reproduced with permission (Appendix A).

The AHL molecules, once generated, travel across the cell membrane via either passive diffusion or active transport according to their length or degree of substitution (Pearson et al., 1999). The concentration of AHLs builds up along with the increase in cell density. Once a certain threshold is reached, these molecules bind to their receptors, a family of transcriptional regulators homologous to the LuxR protein, which, in turn, regulate the expression of certain genes within a microorganism. (Parsek & Greenberg, 2000).

2.1.1.1 Detection of AHLs

Production of AHLs by bacterial isolates was commonly detected using biosensors, which are bacterial strains that display a visible phenotypic change (pigment production or bioluminescence) in response to the presence of AHLs. At the same time, they must also not produce AHLs on their own. Construction of AHL biosensors was done via either

modification of QS system originally presents in a bacterial strain or insertion of reporter plasmid (Steindler & Venturi, 2007).

One example for the first type, *Chromobacterium violaceum* CV026, was constructed by disrupting the AHL-producing ability of *C. violaceum* ATCC 31532 with a mini-Tn*5* transposon mutation on the *cviI* gene, resulting in a mutant that forms white instead of dark purple colonies (McClean et al., 1997). This AHL biosensor works by showing purple pigmentation when extragenous AHLs (C_4 – C_8-HSL) are present. On the other hand, *E. coli* [pSB401], example for the second type, is a plasmid that harbours a *luxCDABE* operon of *Photorhabdus luminescens* that is activated upon exposure to a number of short-chain AHLs (Winson et al., 1998b). Application of AHL biosensors are usually carried out in four ways, namely, T-streak assay; thin layer chromatography (TLC) overlay; quantification assay; and *in vivo* assay (Steindler & Venturi, 2007). A range of currently available AHL biosensors, along with their usage and specificity, are listed in Table 2.1.

Detection of AHLs produced by bacterial strains can also be done using analytical approaches, such as liquid chromatography coupled with mass spectrometry (LC-MS), which combines the separation capabilities of LC and the analytical capabilities of MS. Application of this technique allows a wider detection range and more accurate quantitation that are limited in biosensors (Ortori et al., 2011). Targeted LC-MS methods for AHL identification have been applied for organisms such as *Pantoea stewartii* (von Bodman & Farrand, 1995), *Pseudomonas aureofaciens* (Wood et al., 1997), *Nitrosomonas europaea* (Burton et al., 2005), and *Pseudomonas fluorescens* (Liu et al., 2007). For unidentified AHLs, tandem mass spectrometry (MS/MS) analyses have proven useful in *Rhodobacter sphaeroides* (Puskas et al., 1997), *Methylobacterium extorquens* (Nieto Penalver et al., 2006) and *Bradyrhizobium japonicum* (Lindemann et al., 2011).

Table 2.1: AHL Biosensors.

Plasmid/Biosensor	Host	QS System Based on	Reporter System	Best Responds to	Good Detection	Common Application	Reference
C. violaceum CV026	N/A	CviI/R (*C. violaceum*)	Violacein pigment	C_6-HSL	C_4-HSL; 3OC_6-HSL; C_8-HSL; 3O C_8-HSL;	T-streak, TLC overlay	(McClean et al., 1997)
pSB401	*E. coli*	LuxI/R (*A. fisheri*)	*luxCDABE*	3OC_6-HSL	C_6-HSL; C_8-HSL; 3O C_8-HSL	TLC overlay, quantification assay	(Winson et al., 1998b)
pHV200I$^-$	*E. coli*	LuxI/R (*A. fisheri*)	*luxCDABE*	3OC_6-HSL	C_6-HSL; C_8-HSL; 3O C_8-HSL	TLC overlay, quantification assay	(Pearson et al., 1994)
pSB403	Broad host range	LuxI/R (*A. fisheri*)	*luxCDABE*	3OC_6-HSL	C_6-HSL C_8-3OHSL C_8-HSL	TLC overlay, quantification assay	(Winson et al., 1998b)
pSB536	*E. coli*	AhyI/R (*A. hydrophyla*)	*luxCDABE*	C_4-HSL		TLC overlay, quantification assay	(Swift et al., 1997)
pAL101	*E. coli* (*sdiA* mutant)	RhlI/R (*P. aeruginosa*)	*luxCDABE*	C_4-HSL		TLC overlay, quantification assay	(Lindsay & Ahmer, 2005)
pSB1075	*E. coli*	LasI/R (*P. aeruginosa*)	*luxCDABE*	3OC_{12}-HSL	3OC_{10}-HSL; C_{12}-HSL	TLC overlay, quantification assay	(Winson et al., 1998a)
pKDT17	*E. coli*	LasI/R (*P. aeruginosa*)	β-galactosidase	3OC_{12}-HSL	3OC_{10}-HSL; C_{10}-HSL; C_{12}-HSL	TLC overlay, quantification assay	(Pearson et al., 1994)
M71LZ	*P. aeruginosa lasI*$^-$	LasI/R (*P. aeruginosa*)	β-galactosidase	3OC_{12}-HSL	3OC_{10}-HSL	Quantification assay	(Dong et al., 2005)
pZLR4	*A. tumefaciens* NT1	TraI/R (*A. tumefaciens*)	β-galactosidase	3OC_8-HSL	All 3OC_n-HSLs; C_6-HSL; C_8-HSL; C_{10}-HSL; C_{12}-HSL; C_{14}-HSL; 3OHC_6-HSL; 3OHC_8-HSL; 3OHC_{10}-HSL	T-streak, TLC overlay, quantification assay	(Farrand et al., 2002)
pCF218 + pCF372	*A. tumefaciens* WCF47	TraI/R (*A. tumefaciens*)	β-galactosidase	As above with more sensitivity	As above with more sensitivity	TLC overlay, quantification assay	(Zhu et al., 1998)
pJZ384 + pJZ410 + pJZ372	*A. tumefaciens* KYC55	TraI/R (*A. tumefaciens*)	β-galactosidase	As above with more sensitivity	As above with more sensitivity	TLC overlay, quantification assay	(Zhu et al., 2003)

N/A: Non-applicable

Table 2.1, continued.

Biosensor	Host	QS System Based on	Reporter System	Best Responds to	Good Detection	Common Application	Reference
pSF105 + pSF107	*P. fluorescens* 1855	PhzI/R (*P. fluorescens* 2-79)	β-glucuronidase β-galactosidase	3OHC$_6$-HSL	3OHC$_8$-HSL	TLC overlay, quantification assay	(Khan et al., 2005)
S. melilotisinI::*lacZ*	*S. melilotisinI*::*lacZ*	SinI/R (*S. meliloti*)	β-galactosidase	3OC$_{14}$-HSL	3OC$_{16:1}$-HSL; C$_{16}$-HSL; C$_{16:1}$-HSL; C$_{14}$-HSL	T-streak, TLC overlay, quantification assay	(Llamas et al., 2004)
pJNSinR	*S. melilotisinI*::*lacZ*	SinI/R (*S. meliloti*)	β-galactosidase	As above with more sensitivity	As above with more sensitivity	T-streak, TLC overlay, quantification assay	(Llamas et al., 2004)
pAS-C8	Broad host range	CepI/R (*B. cepacia*)	Gfp	C$_8$-HSL	C$_{10}$-HSL	Single cell	(Riedel et al., 2001)
pKR-C12	Broad host range	LasI/R (*P. aeruginosa*)	Gfp	3OC$_{12}$-HSL	3OC$_{10}$-HSL	Single cell	(Riedel et al., 2001)
pJBA-132	Broad host range	LuxI/R (*A. fisheri*)	Gfp	3OC$_6$-HSL	C$_6$-HSL; C$_8$-HSL C$_{10}$-HSL	Single cell	(Andersen et al., 2001)

2.1.2 Types of AHL-Based QS

The LuxI-LuxR system found in the bioluminescent bacterium *A. fischeri* (Engebrecht et al., 1983; Engebrecht & Silverman, 1984) is the best-characterised AHL-based QS system. In this example, LuxI plays the role as *N*-3-oxohexanoyl-homoserine lactone ($3OC_6$-HSL) synthase (Eberhard *et al*., 1981); whereas LuxR the transcriptional regulator that, as the cell density increases, activates the luciferase operon in response to the abundance of $3OC_6$-HSL at a nanomolar level (Engebrecht & Silverman, 1987, 1984; Engebrecht et al., 1983). The LuxR protein contains an AHL-binding N-terminal domain along with a DNA-binding C-terminal domain, a feature that is conserved throughout the family of AHL-binding transcriptional regulators (Zhang et al., 2002; Hanzelka & Greenberg, 1995; Choi & Greenberg, 1991). In the presence of $3OC_6$-HSL, LuxR binds to the *lux* box, a site 20-nucleotide in length, centred 42.5 nucleotides upstream of the transcriptional start site of *luxI*, to activate the gene (Urbanowski et al., 2004; Devine et al., 1989). Unlike some other proteins in the family, the binding of $3OC_6$-HSL to LuxR is reversible by dilution, which is believed to be related to how these proteins respond to the drastic drop of population density (Urbanowski et al., 2004).

It was once believed that all LuxR homologues bound to the promoter regions only in the presence of AHLs. It was discovered later that, in some species, the LuxR counterparts could behave as 'quorum-hindered' apo-proteins, which bound DNA when the signaling molecules were absent. The first and best-characterised example of quorum-hindered transcriptional regulators was found in *Pantoea stewartii*. The LuxI-LuxR homologues in *P. stewartii* are known as EsaI and EsaR. A study observed a drastic decrease in exopolysaccharide (EPS) production following the disruption of *esaI* gene, which was reversible by the addition of $3OC_6$-HSL (von Bodman & Farrand, 1995). It was later reported in a subsequent study that, removal of EsaR caused an overproduction of EPS (von Bodman et al., 1998). This phenomenon of mutants in '*I*-gene' and '*R*-gene'

showing opposite phenotypes was later observed in a number of other organisms (Table 2.2). These proteins form a monophyletic clade in a phylogenetic tree and establish a few characteristics including: (i) Belong to order *Enterobacteriales*; (ii) bind $3OC_6$-HSL (SmaR as an exception); (iii) none activates or represses their cognate AHL synthase directly; (iv) function as both repressors or activators; (v) overlap their cognate synthase genes convergently (Winans, 2016; Tsai & Winans, 2010). A series of AHL-based QS systems that have been reported are listed in Table 2.2. Figure 2.3 demonstrates the modes of action of different types of LuxR homologues and their interaction with the cognate AHLs.

Table 2.2: AHL-based QS systems and the functions they regulate.

Organism	QS System	Orientation	AHL	Regulated Function	Quorum-Hindered Activity	Reference
α-Proteobacteria						
Agrobacterium tumefaciens	TraI-TraR	Non-adjacent	3OC$_8$-HSL	Conjugation	Not reported	(Piper et al., 1999)
Rhizobium leguminosarum	CinI-CinR	Tandem	3OHC$_{14:1}$-HSL	Regulation of cell cycle and nodulation in legumes; adaptation to starvation and salt stress	Not reported	(Edwards et al., 2009; Danino et al., 2003; Wisniewski-Dyé et al., 2002;Lithgow et al., 2000; Rodelas et al., 1999)
	RaiI-Rai-R	Tandem	C$_6$-HSL; C$_7$-HSL; C$_8$-HSL; C$_{10}$-HSL; 3OHC$_8$-HSL		Not reported	
	RhiI-RhiR	Non-adjacent	C$_6$-HSL; C$_7$-HSL; C$_8$-HSL		Not reported	
	TraI-TraR	Non-adjacent	3OC$_{10}$-HSL; C$_8$-HSL		Not reported	
Rhodobacter sphaeroides	CerI-CerR	Tandem	C$_{14:1}$-HSL	Regulation of cell aggregation	Not reported	(Puskas et al., 1997)
β-Proteobacteria						
Aeromonas hydrophila	AhyI-AhyR	Divergent	C$_4$-HSL; C$_6$-HSL	Biofilm formation; serine protease production	Not reported	(Lynch et al., 2002; Swift et al., 1997)
Aeromonas salmonicida	AsaI-AsaR	Divergent	C$_4$-HSL	Serine protease production	Not reported	(Swift et al., 1997)
Burkholderia cepacia	CepI-CepR	Divergent	C$_6$-HSL; C$_8$-HSL	Biofilm formation; siderophore production; swarming motility	Not reported	(Huber et al., 2001; Lewenza et al., 1999)
	CciI-CciR	Tandem	C$_6$-HSL; C$_8$-HSL	Protease production; swarming motility	Not reported	(Holden et al., 2009)
Chromobacterium violaceum	CviI-CviR	Convergent	C$_{10}$-HSL	Biofilm formation; chitinase; violacein production	Not reported	(Stauff & Bassler, 2011)

Table 2.2, continued.

Organism	QS System	Orientation	AHL	Regulated Function	Quorum-Hindered Activity	Reference
γ-Proteobacteria						
Erwinia chrysanthemi	ExpI-ExpR	Convergent	3OC$_6$-HSL; C$_6$-HSL	Swarming and swimming motility; cell aggregation; virulence factor	Yes	(Hussain et al., 2008; Andersson et al., 2000; Pirhonen et al., 1993)
Pantoea stewartii	EsaI-EsaR	Convergent	3OC$_6$-HSL	Adhesion; biofilm formation; host colonisation	Yes	(Schu et al., 2009; ; Minogue et al., 2005; von Bodman et al., 1998 von Bodman & Farrand, 1995)
Pectobacterium carotovorum subsp. *carotovora*	ExpI-ExpR	Convergent	3OC$_6$-HSL; 3OC$_8$-HSL	Carbapenem and exoenzyme production	Yes	(Andersson et al., 2000; Pirhonen et al., 1993 Bainton et al., 1992b;)
Pseudomonas aeruginosa	LasI-LasR	Tandem	3OC$_{12}$-HSL	Elastase, protease, and exotoxin A production	Not reported	(Passador et al., 1993)
	RhiI-RhiR	Tandem	C$_4$-HSL	Rhamnolipid and cyanide regulation	Not reported	(Pesci et al., 1997)
Pseudomonas aureofaciens	PhzI-PhzR	Convergent	C$_6$-HSL	Phenazine production	Not reported	(Whistler & Pierson, 2003)
Pseudomonas fluorescens	PhzI-PhzR	Convergent	3OHC$_6$-HSL; 3OHC$_8$-HSL; 3OHC$_{10}$-HSL; C$_6$-HSL; C$_8$-HSL	Antibiotic production	Not reported	(Khan et al., 2005)
Pseudomonas syringae	AhlI-AhlR	Convergent	3OC$_6$-HSL	Cell aggregation; epiphytic fitness	Not reported	(Quiñones et al., 2004; Dumenyo et al., 1998)

Table 2.2, continued.

Organism	QS System	Orientation	AHL	Regulated Function	Quorum-Hindered Activity	Reference
Serratia liquefaciens	SwrI-SwrR	Convergent	C_4-HSL; C_6-HSL	Biofilm formation	Not reported	(Labbate et al., 2004)
Serratia marcescens	SmaI-SmaR	Convergent	C_4-HSL; C_6-HSL	Haemolytic activity; swarming motility	Not reported	(Coulthurst et al., 2006)
	SpnI-SpnR	Convergent	$3OC_6$-HSL	Surfactant	Yes	(Horng et al., 2002)
Yersinia enterocolitica	YenI-YenR	Convergent	$3OC_6$-HSL; C_6-HSL	Swimming and swarming motility	Yes	(Atkinson et al., 2006; Tsai & Winans, 2011)

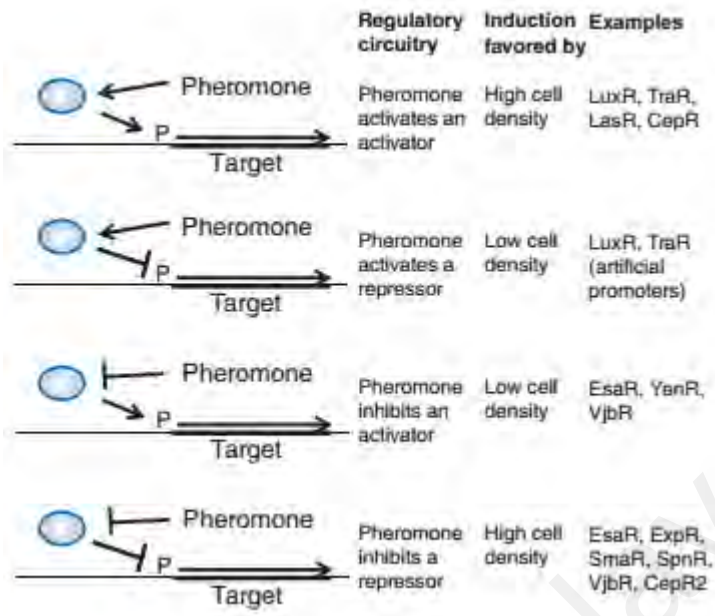

Figure 2.3: Possible scenarios showing interaction between AHL and different types of QS transcriptional regulators. Similar outcome, e.g., gene activation at high cell density, is achievable by opposite modes of action in both quorum-activated and quorum-hindered proteins (Winans et al., 2016). Reproduced with permission (Appendix A).

2.2 The Genus *Hafnia*

The genus *Hafnia* belongs to the recently founded family *Hafniaceae* (formerly part of *Enterobacteriaceae*) aside of *Edwardsiella* and *Obesumbacterium* (Adeolu et al., 2016). The name *Hafnia* was first inaugurated by Møller (1954), and first appeared as an official taxonomic classification in the Approved Lists of Bacterial Names in 1980 ("Approved lists of bacterial names," 1980). Currently, the genus comprises three species, namely, *H. alvei*, *H. paralvei*, and *H. psychrotolerans*. Up to the point when one of its subgroups became officially classified as *H. paralvei* in 2010 (Huys et al., 2010), *H. alvei* remained the only species that belonged to the genus *Hafnia*. Therefore, all literature referring to '*H. alvei*' before that were likely to refer to either species. The specific status of *H. psychrotolerans* was proposed in 2015 (Gu et al., 2015), and to date has not been referred in any further publication.

H. alvei is rod-shaped, motile, flagellated, and facultative anaerobic bacteria (Brenner & Farmer, 2005). As noted by Janda and Abbott (2006), isolation of *H. alvei* has been reported from a wide range of sources such as soil, water, fish, birds, and reptiles (Farmer, 2003; Stiles & Ng, 1981), but robust and repeatable reports were scarce.

2.2.1 *Hafnia* spp. and Food

Hafnia spp. has been commonly reported to be isolated from foods of animal origin, such as meat (Höll et al., 2016; Bruhn et al., 2004; Ridell & Korkeala, 1997; Stiles & Ng, 1981), seafood (Hou et al., 2017; Papadopoulou et al., 2007), and dairy products (Odenthal et al., 2016; Trmčić et al., 2016; Viana et al., 2009). Members of genus *Hafnia* have been commonly identified among the dominating spoilage microbiota in meat products in various storage conditions (Blana & Nychas, 2014; Bruhn et al., 2004; Gram et al., 1999; Ridell & Korkeala, 1997). One report stated that *Hafnia* spp. made up a majority of 49% of all enteric bacterial species isolated from a total of 88 refrigerated meat samples, and some strains were able to survive temperature as low as 0.2°C (Ridell & Korkeala, 1997). It was also found to be most competitive under a low oxygen atmosphere at temperature around 10°C (Höll et al., 2016 Doulgeraki et al., 2012; Doulgeraki et al., 2011; Borch et al., 1996). Although *H. alvei* was often referred to as an AHL-producing spoilage bacterium, Bruhn et al. (2004) has reported that removal of AHL-producing gene did not affect the rate of spoilage caused by *H. alvei* alone. However, the AHLs produced by *H. alvei* were able to induce protease activity in AHL-deficient *Serratia proteamaculans*. The authors postulated that the role of AHLs produced by *H. alvei* in meat spoilage was therefore indirect (Bruhn et al., 2004).

2.2.2 Clinical Association of *Hafnia* spp.

A number of clinical cases have been linked to *H. alvei* and *H. paralvei*, for instance, bacteraemia (Osuka et al., 2011; Moreno et al., 2010; Rodríguez-Guardado et al., 2006),

urinary tract infection (Rahman et al., 2014; Liu et al., 2007; Ramos & Dámaso, 2000), respiratory tract infection (Redondo et al., 2005), and various other infections (Vieira Colombo et al., 2016; Yap et al., 2010; Savini et al., 2008). Despite being commonly isolated from food and human stool samples, the association of *Hafnia* spp. with gastrointestinal diseases is still rare (Janda & Abbott, 2006). Studies on the attachment-effacement gene (*eaeA*)-positive *H. alvei* that caused diarrhoeal disease was once popular (Ridell et al., 1995; Ridell et al., 1994), but the strains were later re-assessed and identified to be *Escherichia albertii* (Huys et al., 2003)

2.2.3 Identification of *Hafnia* spp.

Members of the genus *Hafnia* are generally viewed as opportunistic pathogens and are usually associated with nosocomial infections or immunocompromised patients. To date, the pathogenesis of *Hafnia* spp. and its association with hosts remain largely unclear. In part, this is due to the lack of clarity in identification methods and good taxonomic literature. Traditional methods that identify bacterial isolates based on biochemical tests and phenotypic observation are still widely used in clinical testing and food industry. However, these methods tend to become insufficient over time as the taxonomical groupings expand with the rapid encounter of new species (McNally et al., 2016; Janda & Abbott, 2002). For instance, a study attempting to differentiate between attachment-effacement gene (*eaeA*)-positive (later classified as *E. albertii*) and *eaeA*-negative *H. alvei* demonstrated that biochemical tests alone were not very reliable even when applied on two groups that were later found to be different genera (Ridell et al., 1995). The results of phenotypic tests can also be considerably biased if the traits being tested were altered by mutations, especially in the case of emerging pathogens, where horizontal transfer of genetic materials tends to occur more frequently (Engering et al., 2013).

Over the years, standards for bacterial species identification and classification have been gradually shifting from phenotypic to genomic-based (Rosselló-Mora & Amann, 2001). Being one of the earliest taxonomic methods that classify prokaryotic species at the genome level, DNA-DNA hybridisation (DDH) has served as a gold standard in species identification for nearly 60 years (Brenner et al., 1969). It had remained the only method that offered numerical determination on species boundary until the measurement of relatedness based on whole genome sequences were introduced (Richter & Rosselló-Móra, 2009). In more recent years, with the advancement in DNA sequencing technologies, application of approaches that involve whole genome sequences like average nucleotide index (ANI) in determination of species boundary have been on the rise (See-Too et al., 2017; Vandamme & Dawyndt, 2011; Richter & Rosselló-Móra, 2009).

In recent times, a technology for rapid microbial identification that makes use of matrix-assisted laser desorption/ionisation-time of flight mass spectrophotometry (MALDI-TOF MS) has been introduced. In this method, bacterial identity was determined by comparing the peptide mass fingerprint (PMF), which is a characteristic spectrum of mass-to-charge (m/z) ratios that reflects the unique proteome profile of a species (Singhal et al., 2015). Identification by MALDI-TOF MS has been demonstrated to have high concordance with the microbial identification 'gold standard' 16S rDNA gene sequencing method (Suzuki et al., 2018; Timperio et al., 2017; Loucif et al., 2014). With the availability of automated platforms and updated reference database, this method is emerging as a time-saving alternative alongside the conventional methods.

2.3 Whole Genome Sequencing (WGS) for Bacteria

In August 1995, the completion of the first bacterial genome sequence of *Haemophilus influenza* marked the beginning of an era of 'real' genomics (Fleischmann et al., 1995).

Since then, the number of bacterial genomes sequenced has been on the rise with the advancement in whole-genome shotgun approach (Koonin & Galperin, 2003; Venter et al., 1996). The availability of sequence data that covers the entire genome of various organisms enable analysis to be performed with a comparative approach, based on the neutral theory of molecular evolution that the functionally important sequences were conserved across species (Kimura, 1983). This process, referred to as genome annotation, can now be performed at much ease on various freeware and online platforms, such as Rapid Annotation using Subsystem Technology (RAST) (Aziz et al., 2008), Bacterial Annotation System (BASys) (Van Domselaar et al., 2005), and Rapid Prokaryotic Genome Annotation (Prokka) (Seemann, 2014). At present, technical advances and their affordability, along with the development of powerful bioinformatic tools, have made systematic characterisation at the genome level possible. The large volume of WGS data made available in 'open access' databases also allows large scale genome comparison with functional elucidation to be performed in order to explore the underlying mechanisms of survival and adaptation in an evolutionary context.

2.4 Mutational Study of QS Regulon

2.4.1 λ-Red Recombineering

Recombineering, a termed coined by Donald L. Court (Ellis et al., 2001), refers to the approach of *in vivo* genetic engineering mediated by phage recombination systems, such as the λ Red (Yu et al., 2000) and RecET systems (Zhang et al., 1998). Instead of relying on restriction enzymes as in classical *in vitro* methods, recombineering makes use of phage-encoded 'recombinases'. For instance, the λ-Red system comprises three phage proteins: Gam, Exo, and Beta, which work as linear DNA exonuclease inhibitor, double-stranded DNA (dsDNA) exonuclease, and single-stranded DNA (ssDNA) stabilising protein, respectively (Ellis et al., 2001). The three phage proteins each plays its role in facilitating homologous recombination of the linear dsDNA substrate to the target site.

An advantage of this method is that the design of drug markers can be carried out without the need to consider of the location of restriction sites. In short, recombineering allows introduction of a wide range of desired changes, including deletions, point mutations, duplications, and inversions, into a bacterial genome using linear DNA substrates flanked with short sequences overlapping those at the upper and lower boundary of the targeted site.

2.4.2 RNA-Seq

A 'transcriptome' refers to the quantity of the complete set of transcripts in a cell captured at a time point. Transcriptomic studies allow one to investigate factors that affect the gene expression profile by manipulating the growth condition, time point, and regulatory genes. The first attempt to capture a partial transcriptome of human brain using expressed sequence tag (EST) method, which involved a total of 609 mRNA, was reported in 1991 (Adams et al., 1991).

At present, microarray and RNA-Seq are the two technologies most commonly used in transcriptomic studies. The former detects and quantify a defined set of transcripts with an array of hybridization probes. To date, thousands of transcripts can be assayed in a low-cost and labour-saving manner (Heller, 2002). Alternatively, RNA-Seq can now be performed using any high-throughput sequencing technology (Holt & Jones, 2008). This method involves sequencing of cDNA libraries generated from populations of RNAs. The resulting reads are later mapped to a reference genome or assembled de novo without the genomic sequence to reveal the expression level of each gene or transcript. With the key advantage of high dynamic range and low input volume over microarray, RNA-Seq has been seen to be overtaking microarray as the mainstream technique in transcriptomic studies (Su et al., 2014).

In the studies of QS regulons, gene knockout is a useful approach to identify the cellular function under the influence of QS. Followed by the removal of the genes responsible in signalling molecule production and reception, any changes in phenotypes or global gene expression can then be observed. QS has been reported to affect different sets of genes in different organisms, which often involved complicated networks of metabolic and regulatory pathways. Therefore, global transcriptomic study of knockout mutants is very useful in providing an overview of QS regulatory network in a microorganism.

Transcriptomic study of QS-deficient mutants by means of RNA-Seq has been performed on a wide range of AHL-producing bacteria. In recent years, global transcriptomic studies have been performed on various species of soil-associated genus *Burkholderia* (Gao et al., 2015; Kim et al., 2014; Majerczyk et al., 2014; Goo et al., 2012), which revealed a number of shared roles of QS in the closely related species, for instance, secondary metabolite biosynthesis, oxalogenesis as a means of survival of stationary-phase stress, toxin production, and motility. In the case of *P. stewartii*, the species that harbours the representative quorum-hindered transcriptional regulator, RNA-Seq has not only been performed on its QS-deficient mutants (Ramachandran et al., 2014), but also transcription factors that were under QS regulation (Burke et al., 2015).

2.4.3 Biolog Phenotype Microarrays (PMs)

Biolog PM technology provides a platform for high-throughput phenotyping of cells that enables simultaneous biochemical testing with multiple substrates on 96-well plates. The system records the biochemical reaction, either as end-point values or respiration kinetics, in a colorimetric manner. A tetrazolium dye is added to each well, of which the reduction results in the irreversible formation of a purple colour that accumulates over

time, generating a curve that corresponds to the respiratory rate of the cells that reflects the rates of electron flow (Bochner et al., 2001).

In mutant-wild type (WT) comparison studies, assays on individual strains performed in parallel can be analysed by overlapping the kinetic curves from different plates to reveal the phenotypic changes. At present, PM is often used in complement to genomic, transcriptomic, and proteomic studies. This approach has the advantage of recording the changes across the bacterial growth phases instead of a single time point. It also reveals the manifestation of changes in gene expression in the ultimate form of gain/loss in phenotypes, which facilitates the studies in a more practical sense towards application. This method has been applied in studies on QS-regulated traits in *Burkholderia thailandensis* (Chandler et al., 2009), *P. aeruginosa* (García-Contreras et al., 2015), and *C. violaceum* (de Oca-Mejía et al., 2015).

CHAPTER 3: MATERIALS AND METHODS

3.1 Bacterial Isolation

Refrigerated fish ball samples of different commercial brands were collected from local supermarkets in Klang Valley area. The samples were processed within half an hour following collection. Five grams of each fish ball sample along with 45 mL of Phosphate Buffer Saline (PBS) solution (1×, pH 6.5, preparation method stated in Appendix B) were homogenised with Stomacher® 400 Circulator Lab Blender (Seward, UK) at 230 rpm for 2 min. Homogenised samples were inoculated into 50 mL of Brain Heart Infusion (BHI) broth and incubated overnight at 37°C with shaking (220 rpm).

A series of tenfold serial dilution of 10^{-1}, 10^{-2}, 10^{-3}, 10^{-4}, and 10^{-5} were made from the overnight cultures with PBS buffer (1×, pH 6.5). Each dilution was spread on a MacConkey (MAC) agar (Scharlau, Spain) plate. Colonies were picked according to the observed morphologies (lactose fermentation, mucoid, size, form, elevation, and margin) and sub-cultured on Luria-Bertani agar (LBA) (Merck, Germany; Scharlau, Spain) plates until pure cultures were obtained. Isolates were routinely maintained on LBA plates at 37°C and kept as 20% glycerol stocks for long term storage.

3.2 Identification of Bacterial Strains with Matrix-Assisted Laser Desorption/Ionisation-Time of Flight Mass Spectrophotometry (MALDI-TOF MS)

Bacterial strains isolated were identified via MALDI Biotyper System (Bruker, Germany) (Seng et al., 2009) using direct smeared method. Bacterial cells were picked from single colonies and smeared on wells on an MSP96 Target Polished Steel PC Plate. The smeared cells were then overlaid with MALDI-matrix (α-cyano-4-hydroxycinnamic acid in 50% Acetonitrile (ACN)/2.5% trifluoroacetic acid). The plate was left to be air-dried, and, subsequently, subjected to scanning under laser wavelength of 337 nm and acceleration voltage of 20 kV using Microflex MALDI-TOF Benchtop Mass Spectrophotometer (Bruker, Germany). The output was analysed with Bruker MALDI Biotyper Real Time Classification (RTC) version 3.1 (Build 65) Software, at mass range of 2 – 20 kDa.

3.3 Phylogenetic Analysis of 16S rDNA

PCR amplification of 16S rDNA was performed with primer pair 27F and 1525R (Table 3.1) on T100™ Thermal Cycler (Bio-Rad, USA) according to condition stated in Table 3.2.

Table 3.1: Oligonucleotides used in PCR amplification for 16S rDNA sequence analysis.

Primers	Sequence (5' – 3')	Annealing temperature (°C)	Length (-mer)	Reference
27F	AGA GTT TGA TCM TGG CTC AG	58	20	(Lane, 1991)
1525R	AAG GAG GTG WTC CAR CC		17	(Dewhirst et al., 2000)

Table 3.2: Reagents and thermocycling conditions for PCR carried out with OneTaq® DNA Polymerase.

PCR Components			
Reagent		Volume per 25 µL Reaction (µL)	Final Concentration
5× OneTaq Standard Reaction Buffer		5.000	1×
10 mM dNTPs		0.500	200 µM
10 µM Forward Primer		0.500	0.2 µM
10 µM Reverse Primer		0.500	0.2 µM
OneTaq DNA Polymerase		0.125	0.625 units
Template DNA		1.000	<1,000 ng
Nuclease-Free Water		17.375	-
Thermocycling Condition			
Step		Temperature (°C)	Time
Initial Denaturation		94	30 sec
30 cycles	Denaturation	94	30 sec
	Annealing	Variable	60 sec
	Extension	68	1 min per kb
Final Extension		68	5 min
Hold		10	-

3.3.1 Agarose Gel Electrophoresis (AGE)

Output of PCR were separated by means of AGE. Agarose gel was prepared by mixing agarose powder and Tris-boric acid ethylenediaminetetraacetic acid (TBE) buffer (1×, pH 8.0, method of preparation stated in Appendix B) of appropriate weight and volume, accordingly. Amplicons with sizes smaller than 250 bp were separated with 2% (w/v) agarose gel; whereas 1% (w/v) agarose gel was used for fragments of larger sizes. The mixture was melted by heating up in a microwave oven followed by addition of 0.5 µL of GelStar™ Nucleic Acid Gel Stain 10,000× (Lonza, Switzerland). The cooled molten agarose was then left for solidification in a gel cast.

Prior to loading, 6× bromophenol blue loading dye was mixed with each sample at a 1:5 ratio. The samples were then loaded to the wells on the agarose gel submerged in a tank of 1× TBE buffer (1×, pH 8.0). In one of the wells, 1 kb DNA ladder (Fermentas,Thermo Fisher Scientific, USA) was loaded to serve as a reference for the size of DNA fragments. Electrophoresis was performed at 80 V, until the loading dye

front approached about 1.0 cm from the edge of the gel. The agarose gel was then visualised under ultraviolet (UV) light using DigiDoc-It® Imaging System (UVP Inc., USA).

3.3.2 Purification of DNA Fragments from Agarose Gel

Each PCR amplicon band of interest was excised from the agarose gel with a gel extractor under a benchtop UV transilluminator (UVP, USA). The piece of agarose gel containing the DNA fragment was then transferred to a 2.0-mL microcentrifuge tube. The DNA fragments were then recovered using QIAamp® Gel Extraction Kit (Qiagen, Germany), according to the manufacturer's protocol.

3.3.3 Confirmation of Amplicon Sequences

Sequences of the amplified products from PCR were determined via Sanger sequencing performed by the service provider (1st BASE, Malaysia).

3.3.4 Analysis of 16S rDNA Sequences

The sequences returned were viewed and trimmed prior to analysis using Molecular Evolutionary Genetic Analysis (MEGA) software version 7 (Kumar et al., 2016). The 16S rDNA sequences were proceeded for identity matching on EzBioCloud 16S database (https://www.ezbiocloud.net/) (Yoon et al., 2017). Species identities were determined with a sequence similarity cut-off value of 97%.

Phylogenetic trees were constructed to demonstrate the relatedness of the isolates to their closest neighbours according to 16S rDNA sequences (sequences obtained from EzBioCloud 16S database). Neighbour-joining (NJ) method with bootstrap value 1,000 was used. In order to produce a rooted tree, a distantly related taxon that was sufficiently conserved to the ingroup taxa was used as an outgroup.

3.4 Characterisation of AHL Profile

3.4.1 AHL Detection of Bacteria Isolates

A preliminary screening for AHL production was performed on all bacterial isolates by cross-streaking with biosensor *C. violaceum* CV026. *P. carotovorum* GS101 and *P. carotovorum* PNP22 were used as positive and negative control, respectively (McClean et al., 1997). Only isolates that induced violacein production after 18 – 24 h incubation were selected for subsequent analyses. The test was done in triplicate for each isolate.

3.4.2 AHL Extraction

AHLs were extracted three times from 100 mL of overnight LBB culture (buffered with 50 mM of 3-[*N*-morpholino] propanesufonic acid, MOPS, pH 5.5) (Yates et al., 2002) of selected isolates with equal volume of acidified ethyl acetate (0.1% v/v glacial acetic acid). The culture and solvent were mixed by shaking vigorously in a conical flask. The immiscible solvent layer was then separated into a sterile beaker and left to dry in a fumehood. The extracts collected in the beaker were then resuspended in 2 mL acidified ethyl acetate and transferred into microcentrifuge tubes and left to dry. The dried extracts were stored for later usage at -20°C.

3.4.3 Thin Layer Chromatography (TLC)

TLC was performed using synthetic $3OC_6$-HSL (0.1 µg/µL) and *N*-3-oxooctanoyl-homoserine lactone ($3OC_8$-HSL, 5 µg/µL) as standards. Both synthetic AHLs were obtained from Sigma-Aldrich®, USA. AHL extracts obtained in Section 3.5.2 (reconstituted in 1 mL acetonitrile, ACN) were applied on a reverse phase C18 TLC plate (TLC aluminium sheets 20 cm × 20 cm, Merck, Darmstadt, Germany) along with the standards. Mixture of methanol:water (60:40, v/v) was used as mobile phase for TLC. The TLC plate was then air-dried in a fume hood. A thin film of LBA seeded with *C. violaceum* CV026 was overlaid on top of the dried TLC plate, followed by overnight

incubation at 28 °C. Formation of purple spots on the CV026 lawn on LBA indicated the presence of AHLs. Retention factor (R_f) of each spot was calculated with the equation as follows:

$$R_f = \frac{\text{distance from the starting point to the center of the spot}}{\text{distance from the starting point to the solvent front}}$$

3.4.4 Triple-Quadrupole Liquid Chromatography-Tandem Mass Spectrometry (LC-MS/MS)

The AHL extracts obtained in section 3.3.4.2 were reconstituted in 1 mL of ACN, and 100 µL of the reconstituted extracts was loaded for LC-MS/MS analysis on Agilent 6490 Triple Quadrupole LC/MS system (Agilent Technologies Inc., USA) equipped with ZORBAX Rapid Resolution High Definition SB-C18 Threaded Column (2.1 mm × 50 mm, 1.8 µm particle size) (Agilent, USA). Flow rate was set at 0.3 mL/min, temperature 37°C, and injection volume 2 µL. Water and ACN (both added with 0.1% v/v formic acid) were used as mobile phases A and B, respectively. Gradient profile was set at A:B 80:20 at 0 min, 50:50 at 7 min, 20:80 at 12 min, and 80:20 at 14 min. For precursor ion-scanning analysis in positive ion mode, Q1 was set to cover a mass range of *m*/*z* 80 – 400, whereas Q3 was set to detect *m*/*z* 102. Detection of *m*/*z* 102 indicated the presence of a lactone ring, hence the presence of AHLs. MS parameters were set as follow: probe capillary voltage 3 kV, sheath gas 11 mL/h, nebuliser pressure 20 psi, and desolvation temperature 200°C. In the collisionally-induced dissociation mode, nitrogen was used as the collision gas. Collision energy was set at 10 eV. The output was analysed with Agilent MassHunter software (Agilent, USA). Ten synthetic AHLs and oxo-derivatives of known carbon chain lengths (Sigma-Aldrich®, USA) were used as the standard for comparison.

3.5 Deposition to Culture Collector

H. alvei FB1 was deposited to culture collector German Collection of Microorganisms and Cell Cultures GmbH (Deutsche SammLung von Mikroorganismen und Zellkulturen GmbH, DSMZ) upon confirmation of the AHL-producing ability (Culture Collection Number: DSM 102038). API Biochemical Assay service was requested to be done by DSMZ to confirm the identity prior to the deposition.

3.6 Single Molecule Real-Time (SMRT) Sequencing

3.6.1 Genomic DNA (gDNA) Extraction

gDNA used in this study was extracted with MasterPure™ DNA Purification Kit (Epicentre, USA) according to the protocol provided by the manufacturer. Bacterial cells were harvested from overnight liquid culture by centrifugation at 10,000 × *g* for 10 min. Routine quantification was performed on Qubit® 2.0 Fluorometer with dsDNA High Sensitivity Assay Kit (Invitrogen, USA); whereas quality assessment was performed with NanoDrop™ 2000 Spectrophotometer (Thermo Scientific, USA) and gel electrophoresis.

3.6.2 Library Preparation

gDNA extracted as stated in Section 3.6.1 was subjected to routine checking according to "PACBIO® GUIDELINES FOR SUCCESSFUL SMRTbell™ LIBRARIES" (Appendix C) prior to library preparation for sequencing. Accurate quantity of dsDNA was determined using Qubit® dsDNA BR kit on Qubit® Fluorometer (Life Technologies, USA) according to manufacturer's protocol. Quality assessment of gDNA was performed by obtaining the A 260/280 (acceptable range: 1.8 – 2.0) and A 260/230 (acceptable range: 2.0 – 2.2) ratios. A total of 150 ng (measurement by Qubit) of gDNA samples were loaded on 0.8% (w/v) agarose gel and the integrity gDNA was evaluated by AGE. The AGE condition was according to that listed in Section 3.3.1. Only samples that met all the criteria were proceeded for library preparation.

A total of 10 µg of gDNA samples that passed the quality check were sheared into fragments of 17 – 20 kb in sizes. gDNA samples were eluted in 100 µL Buffer EB (Qiagen, Germany) and centrifuged in g-TUBE™ (Covaris, UK) at 4,800 rpm for 2 min. The sheared gDNA samples were then purified and concentrated with 0.45× volume of washed Agencourt AMPure XP magnetic beads (Beckman Coulter, USA). Fragment sizes in each sample were verified with DNA 12000 kit on Agilent 2100 Bioanalyzer (Agilent, USA). Subsequent preparation of SMRTbell template libraries was carried out with SMRTbell Template Prep Kit 1.0 (Pacific Biosciences, USA) according to the "Procedure & Checklist - 20 kb Template Preparation using BluePippin™ Size Selection". The sheared gDNA was subjected to steps of end repair, ligation of adapters, and exonuclease digestion of incompletely ligated products. In the following stage, samples were proceeded to annealing of the library sequencing primers, and subsequently binding of P6 DNA polymerase using DNA Polymerase Binding Reagent Kit (Pacific Biosciences, USA). Prior to sequencing, the bound complexes were immobilised onto Magbeads (Pacific Biosciences, USA). SMRT sequencing was performed using PacBio RSII Sequencer (Pacific Biosciences, USA) with 3 SMRT cells.

3.6.3 Genome Assembly

Quality filtering and *de novo* assembly the output reads generated from SMRT sequencing was performed using the Hierarchical Genome Assembly Process (HGAP) pipeline version 3.0 on the Pacific Biosciences' SMRT portal (Chin et al., 2013). Polished assemblies were generated from this module that incorporated Celera Assembler, BLASR mapper, and Quiver consensus caller algorithms. Short reads below 500 bp were removed at the quality filtering stage, and the minimum polymerase read quality was set at 0.80. The cut-off length of seeding reads serving as references for recruitment of shorter reads for pre-assembly were determined at the assembly stage, based on the subread length corresponding to sequencing coverage at an approximately 40× depth in the subread

length plot. The polished assembled contigs generated were then subjected to further validation for sequence accuracy. The circularity of the contigs was determined using Genome Pair Rapid Dotter (Gepard) version 1.3 (Krumsiek et al., 2007).

3.6.4 Genome Annotation

Contigs in fasta format acquired from the assembly step were subjected for gene prediction and annotation using Prokka (Seemann, 2014), and also uploaded for annotation and SEED-based subsystem characterisation on RAST server (Aziz et al., 2012; Aziz et al., 2008). Whole genome sequences were deposited to the GenBank database (https://www.ncbi.nlm.nih.gov/) and subjected to annotation via Prokaryotic Genome Automatic Annotation Pipeline (PGAAP) (Angiuoli et al., 2008). A circular genome map was constructed using CGView Server (Grant & Stothard, 2008). Annotated coding DNA sequences (CDSs) were sorted into functional categories based on Clusters of Orthologous Groups (COGs) using WebMGA server (Wu et al., 2011).

3.6.5 Taxonomic Circumscription

To verify the species circumscription, ANI was calculated with Orthologous Average Nucleotide Identity Tool (OAT), based on the OrthoANI algorithm (Lee et al., 2016), using type strains of each species as references. Any strain that shared an ANI value above 95% was considered to belong to the same species as the reference type strain (Goris et al., 2007).

In order to determine the genus boundary, percentage of conserved proteins (POCP) was calculated, using the type strain of the type species of a genus as a reference (Qin et al., 2014). First, the amino acid sequences of two genomes in .faa format were aligned against each other with Basic Local Alignment Search Tool for protein sequences (BLASTp) program (Altschul et al., 1997), using parameters as follow: E value < 1e-5, sequence identity > 40%, and alignable region of query protein sequence > 50%. The

BLASTp alignment was done twice, with each of the two genomes used as the query once. POCP was calculated with the equation as follows:

$$\text{POCP}=\left(\frac{\text{C1+C2}}{\text{T1+T2}}\right).100\%$$

Where,

*C*1 = conserved number of proteins in the first genome

*C*2 = conserved number of proteins in the second genome

*T*1 = total number of proteins in the first genome

*T*2 = total number of proteins in the second genome

3.6.6 Comparative genomics

Comparative analysis was performed between *H. alvei* FB1 and ten other closely related genomes obtained from the GenBank database (https://www.ncbi.nlm.nih.gov/) using sequence-based comparison function of RAST (Aziz et al., 2008). Genome sequences of closely related genomes were aligned to the predicted proteome of *H. alvei* FB1.

3.7 Identification of QS Genes

3.7.1 Identification of QS Genes from Annotated Data

Nucleotide and amino acid sequences of potential *luxI* and *luxR* homologues were identified from the annotated whole genome data. A search on BLAST and InterProScan (Jones et al., 2014) was performed to identify the signature conserved domains on the sequences. The sequences were aligned with other known homologues obtained from the GenBank database (https://www.ncbi.nlm.nih.gov/), and phylogenetic analysis was performed using MEGA7 (Kumar et al., 2016).

3.7.2 Cloning and Expression of the *luxI* homologue

Identity and function of the *luxI* homologue were determined via cloning and expression study using Gene Synthesis service (GenScript, USA). Target DNA sequence was first synthesised in vector pUC57, and then sub-cloned into *E. coli* expression vector pGS21a by the service provider. The expression vector carrying the target sequence was transferred into expression host *E. coli* BL21 Star (DE3). The expression of *luxI* homologue was examined via a cross-streak assay on the transformed host with CV026 biosensor. AHLs produced were then identified on LC-MS platform as described in Section 3.3.4.3.

3.8 Construction of QS Mutants

Replacement knockout of QS genes in *H. alvei* FB1 was carried out according to Court Lab's protocol "Recombineering: Using Drug Cassettes to Knock out Genes in vivo" downloadable from the official website (https://redrecombineering.ncifcrf.gov/).

3.8.1 Design and Construction of Linear DNA Substrates

Linear DNA substrate for recombineering was constructed through PCR amplification with 70-base hybrid primers. The primers were designed by joining 50 bases of homologous sequence that flanked the sequence to be replaced, and 20 bases at the 3' end that primed the amplification of Kanamycin resistance (KanR) cassette from the template strain (TKC) (Sharan et al., 2009). Schematic description on how the hybrid primers was created and their role in recombineering were shown in Figure 3.1. PCR conditions were set as described in Table 3.3. Primer pair *halI*-KanR-F and *halI*-KanR-R were used to construct linear substrate for replacement knockout of *halI* gene, whereas *halR*-KanR-F and *halR*-KanR-R for *halR*. Primer sequences were listed in Table 3.4.

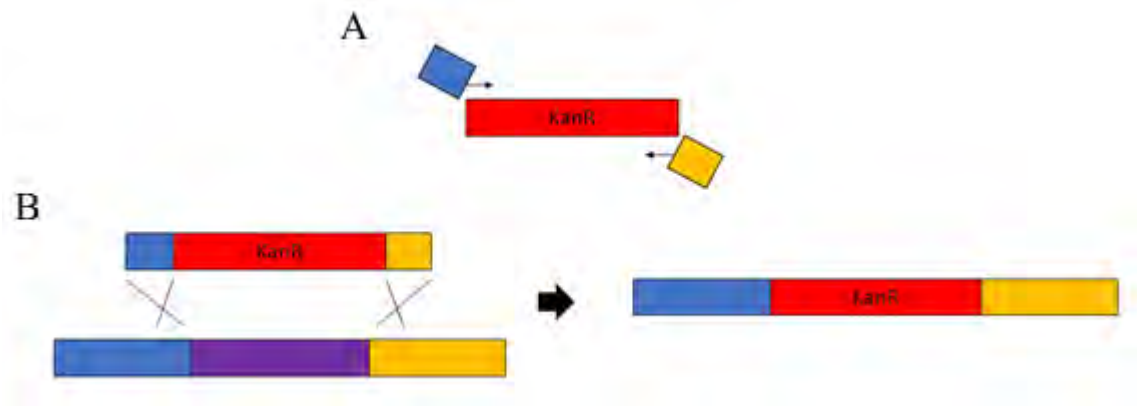

Figure 3.1: Schematic representation of the construction of a linear recombineering substrate. (A) Amplification of KanR cassette using hybrid primers. (B) Replacement knockout of the target sequence (purple) with the KanR cassette via homologous recombination. The blue and orange blocks represent regions of homology shared between the genome sequence and the cassette.

Table 3.3: Reagents and thermocycling conditions for PCR carried out with Q5® High-Fidelity 2X Master Mix.

PCR Components			
Reagent		**Volume per 25 µL Reaction (µL)**	**Final Concentration**
Q5 High-Fidelity 2× Master Mix		12.50	1×
10 µM Forward Primer		1.25	0.5 µM
10 µM Reverse Primer		1.25	0.5 µM
Template DNA		1.00	<1,000 ng
Nuclease-Free Water		9.00	-
Thermocycling Condition			
Step		**Temperature (°C)**	**Time**
Initial Denaturation		98	30 sec
30 cycles	Denaturation	98	10 sec
	Annealing	72	30 sec
	Extension	72	30 sec
Final Extension		72	2 min
Hold		10	-

Table 3.4: Oligonucleotides used in PCR amplification for mutant construction.

Primers	Sequence (5' – 3')	Annealing temperature (°C)	Length (-mer)	Reference
halI-KanR-F	ATA GCA GGA CGC GAA AAA CAC CAG CCA TAG ATA ATA TGG ATA GTA ACT AAA ATG TAA TCA AGG TGA TGG ATA TGG ACA GCA AGC GAA CCG	72	90	This study
halI-KanR-R	AGT AAG CAA CGC CCG ACA AGC AAT AAG GTT GGG CGT TGA ACT TGA TCT TAT TAC ACC AAT GCA GGC GTA ATC AGA AGA ACT CGT CAA GAA G		91	This study
halR-KanR-F	GTA CTT TGC GCC CTG TAC TTA AGT GCA TGT TGT CAC TCA GAC ATG GGA AAT TGA ACG TCT AGG AGC CCA ATA TGG ACA GCA AGC GAA CCG	72	90	This study
halR-KanR-R	AGT CGG TGG TAT TCA GTC CCA GAT GGT TAA TTG GCC AAT GTC GAT AGC CGT TAC GCC TGC ATT GGT GTA ATC AGA AGA ACT CGT CAA GAA G		91	This study
*halI*_u-F	CCA GCC ATA GAT AAT ATG GA	50 (with Screen_KanR-R)	20	This study
*halI*_d-R	AGT AAG CAA CGC CCG ACA AG	50 (with Screen_KanR-F)	20	This study
*halR*_u-F	AAG TGC ATG TTG TCA CTC AG	50 (with Screen_KanR-R)	20	This study
*halR*_d-R	AGT CGG TGG TAT TCA GTC CC	50 (with Screen_KanR-F)	20	This study
Screen_KanR-F	CAC TGA GTT TCA CGA GGA CT		20	This study
Screen_KanR-R	TGA ACG CAC CGT TAA ATT CC		20	This study

3.8.2 Preparation of Electrocompetent Cells for Transformation

Bacterial culture for electrocompetent cell preparation was prepared by adding 2 mL of fresh overnight *H. alvei* FB1 culture into 200 mL of LB broth in a conical flask. The cells were grown at 37°C with shaking (300 rpm) to an OD_{600} of 0.5 – 0.7. The flask containing the cells was then chilled on ice for 20 min. The cells were kept as close to 0°C as possible in the subsequent steps by handling with pipette tips and containers that were previously chilled. The chilled cells were washed by centrifugation for 4,000 x *g* for 15 min at 4°C in cold 50 mL conical tubes. The supernatant was then discarded, and the pellets were resuspended in equal volume of ice-cold 10% glycerol. The wash step as

above was repeated twice with the new suspensions. At the end of this step, the pellets were resuspended in 1 mL of ice-cold 10% glycerol and transferred to pre-chilled microfuge tubes. The suspensions were again centrifuged at 4,000 x *g* for 15 min at 4°C. This time, the cells were resuspended in 100 µL ice-cold 10% glycerol. The suspensions were then dispensed into 20 µL aliquots and stored at -70°C for further use.

3.8.3 Transformation of Bacterial Cells via Electroporation

Electrocompetent cells prepared as described in the previous section were thawed on ice. A 1.5 microfuge tube, a 0.1-cm electroporation cuvette (Bio-Rad, USA) and pipette tips were chilled on ice prior to the electroporation steps. For each transformation reaction in 0.1-cm cuvette, 20 µL electrocompetent cell suspension and 1 µL DNA were used. The two were mixed well and incubated in a microfuge tube on ice for 1 min. The mixture was then transferred to the 0.1-cm cuvette and the electroporation was carried out at 2.5 kV. After the electroporation step, the mixture was instantly transferred to a microfuge tube containing room temperature Super Optimal broth with Catabolite repression (SOC). The cells were then left for incubation at 37°C for an hour with shaking at 225 rpm.

3.8.4 Replacement Knockout

Plasmid (pSIM7) (Datta et al., 2006) that carried the recombinase genes was introduced into *H. alvei* FB1 competent cells through electroporation as described in Sections 3.8.2 and 3.8.3. The transformed cells were selected on chloramphenicol plate (20 µg/mL) and the subsequent culture was maintained at 32°C to avoid induction of the recombinase genes. Overnight culture of the cells that harboured pSIM7 (0.5 mL) was added into in 35 mL LBB containing 20 µg/mL chloramphenicol with shaking at 220 rpm in a 32°C water bath till OD_{600} 0.5, and the expression of recombinase genes were heat-induced by incubation at a 42°C water bath with shaking (220 rpm) for 15 min. Following this, the cell-containing flask was rapidly cooled by gently swirling in ice-water slurry.

The same process was carried out in parallel with an uninduced culture that served as negative control. Both flasks were left on ice for at least 5 min. The cells were then centrifuged at 4,600 x *g* at 4°C for 7 min, followed by removal of the supernatant. The pallets were resuspended first in 1 mL ice-cold distilled water by gently pipetting, followed by the addition of 30 mL ice-cold distilled water and gentle inversion for mixing. The centrifugation step was repeated once with the conditions stated as above. The pellets were resuspended in 1 mL ice-cold distilled water without vortexing, and then transferred into pre-chilled microfuge tubes. The tubes of resuspended cells were centrifuged at full speed at 4°C for 1 min, followed by the removal of supernatant. The cells were then resuspended in 200 µL ice-cold distilled water. The electroporation was carried out with mixture of 50 µL of electrocompetent cells from the previous step with 100 – 150 ng PCR-amplified linear substrate at 1.8 kV in 0.1-cm cuvette. Immediately after electroporation, the cells were transferred to microfuge tubes containing 1 mL LBB for recovery at 30°C for 2 h with shaking at 220 rpm. Two negative controls were prepared in parallel with the transformation of heat-induced cells, one contained heat-induced cells with no linear substrate while the other non-induced cells with substrates. The cells were then plated on kanamycin plate (35 µg/mL) to select for mutants that carried the KanR cassette in the place of QS genes. The results of recombineering were then confirmed by colony PCR using primers (*halI*_u-F, *halI*_d-R, *halR*_u-F, and *halR*_d-R with Screen_KanR-F and Screen_KanR-R as described in Table 3.4) that amplified the junctions where recombination took place. Cross-streaking with CV026 was also performed on the *H. alvei* FB1Δ*halI*::KanR to confirm the AHL synthase function was successfully removed.

3.9 RNA-Seq

3.9.1 RNA Extraction

H. alvei FB1 WT and mutant cells were grown in 200 mL LB broth at 37°C with shaking at 220 rpm. Readings of optical density (OD_{600}) were measured every hour. The total RNA was stabilised immediately using Qiagen RNAprotect bacterial reagent (Qiagen, USA) when the cells were harvested at the desired OD_{600} (0.5 and 1.5) according to the manufacturer's protocol. Total bacterial RNA was purified using Qiagen RNeasy kit (Qiagen, USA) according to the manufacturer's protocol. Purified RNA samples were eluted in 100 µL sterile RNase-free water. Total RNA from three biological replicates was obtained from independent cultures to evaluate the reproducibility of RNA-Seq data. Purity of RNA samples was assessed using Nanodrop spectrophotometer (Thermo Scientific, USA), while RNA quantification was carried out using Qubit® RNA HS Assay Kit (Invitrogen, USA). The quality of the extracted RNA samples was performed with Agilent RNA 6000 Nano Kit (Agilent Technologies, USA) using 2100 Bioanalyzer.

3.9.2 Library Preparation

RNA samples with RNA Integrity Number (RIN) of >7.0 were chosen to proceed to rRNA depletion using Ribo-Zero™ rRNA Removal Kits (Bacteria) (Epicentre, USA) prior to cDNA synthesis. The quality of the rRNA-depleted RNA was assessed with Agilent RNA 6000 Pico Chip (Agilent Technologies, USA) using 2100 Bioanalyzer. Library preparation was performed according to the manufacturer's protocol using the Illumina ScriptSeq™ v2 RNA-Seq Library Preparation Kit (Epicentre, USA). Quality of the RNA-Seq transcriptome library was examined using Agilent 2100 High Sensitivity DNA Kit. Quantification of the library was performed using Qubit® dsDNA HS Assay Kit (Life Technologies, USA) and qPCR (KAPA Biosystems) before subjected to normalisation. The normalised samples (4 nM) were denatured with 0.2 N NaOH and

diluted 20 pM using pre-chilled Hybridisation Buffer (HT1) (Illumina, USA). The 20 pM transcriptome libraries were further diluted to 10 pM with pre-chilled HT1 buffer prior to whole transcriptome sequencing on MiSeq platform.

3.9.3 Data Analysis

RNA-seq read quality assessment was done using FastQC (version 0.11.2) (Andrews, 2010). Rockhopper (McClure et al., 2014; Tjaden, 2015) was used to align the paired end reads against *H. alvei* FB1 reference genome (GenBank accession number CP009706). Differential expression analysis was then performed with DESeq2 package using raw counts generated from Rockhopper as inputs (p_{adjust} value/$q < 0.01$) (Love et al., 2014). Gene Ontology (GO) and pathway enrichment analysis of differentially expressed genes (DEGs) was performed using The Database for Annotation, Visualization and Integrated Discovery (DAVID) v6.8 (Huang et al., 2009a, 2009b). The sequencing output, along with the raw counts, were deposited to the Gene Expression Omnibus (GEO) database (https://www.ncbi.nlm.nih.gov/gds) under accession number GSE93000.

3.9.4 Result Validation using qPCR

Prior to qPCR, total RNA extracted in Section 3.3.12.1 was converted to cDNA using QuantiTect® Reverse Transcription Kit (Qiagen, Germany) according to manufacturer's protocol. qPCR was performed with CFX96 Touch™ Real-Time PCR Detection System (Bio-Rad, USA) according to the conditions described in Table 3.5, using primers listed in Table 3.6. Expression level in ΔΔCq of each gene was determined from analysis using Bio-Rad CFX Manager version 3.1 (Bio-Rad, USA).

Table 3.5: Reagents and thermocycling conditions for PCR carried out with QuantiNova® SYBR Green PCR Kit.

PCR Components			
Reagent		**Volume per 20 µL Reaction (µL)**	**Final Concentration**
2x QuantiNova SYBR Green RT-PCR Master Mix		10.00	1×
10 µM Forward Primer		1.75	0.7 µM
10 µM Reverse Primer		1.75	0.7 µM
Template cDNA		1.00	≤1,00 ng
Nuclease-Free Water		5.50	-
Thermocycling Condition			
Step		**Temperature (°C)**	**Time**
Initial Activation		95	2 min
35 cycles	Denaturation	95	5 sec
	Annealing/Extension	57	10 sec
Melting Curve Analysis		72	2 min
Hold		57 – 95	0.5°C increment

Table 3.6: Oligonucleotides used in qPCR validation of RNA-Seq results.

Primers	**Sequence (5' – 3')**	**Annealing temperature (°C)**	**Length (-mer)**	**Reference**
amyA-F	GCG TCT AAA TCG GGC AGT GA	57	20	This study
amyA-R	CAC CAG CGT GAC CGT ATT CT		20	This study
ffh-F	GGG TGG GAT GAC CTC AAT GC	57	20	This study
ffh-R	TCC ATG CGC ACC AAG AGT TT		20	This study
gyrA-F	CAC CCA AGG TGT TAC GCT GA	57	20	This study
gyrA-R	ATC GTC AGC GAC ATC AGC AA		20	This study
hemS-F	CTA CAC GGC CAT GCG GGT T	57	19	This study
hemS-R	TTG CGG CTC TCT TCG GTC AG		20	This study
hmuT-F	GTT CCG CGT ACC CCA CTC AA	57	20	This study
hmuT-R	TGT CTT GAC CTG CGG CCA TT		20	This study
lamB-F	ATC GCC GCA ACC CGT AAC AC	57	20	This study
lamB-R	GAC GTC GTT GGC GGT GTC TT		20	This study
malE-F	TAC CGG CGA TGG TCC TGA TA	57	20	This study
malE-R	AGG CCA GAC TGT GCA TAA CC		20	This study
potB-F	TTA GAG GCC GCA CGT GAT TT	57	20	This study
potB-R	ACA ATA CCG GGC ATG GTG AG		20	This study
potE-F	CGC CGT TTG GTT TAG CGT TT	57	20	This study
potE-R	CTG CCA ACC CAG CAA TGA AC		20	This study
prr-F	ACG TTC TGT TCG GTT TGG GT	57	20	This study
prr-R	AGA CGC CGT GTG CTC AAT AA		20	This study
rbsB-F	CGG CGA ATA AAG GCG TTG TGG	57	21	This study
rbsB-R	ATA AAC TCA CCC GCG GCC TT		20	This study
rpoD-F	CGA CCA ACG TCG GTT CTG A	57	19	This study
rpoD-R	GCG GCC ATG AGT TTT GAT CG		20	This study
speC-F	GGC GCG CAT GGA TGA TAT TG	57	20	This study
speC-R	AAT GGT GCT GAG AGC CTG AC		20	This study
tdcB-F	ACG CGA GCA GGG TGT GAT T	57	19	This study
tdcB-R	GCA TGG CAC AAG ACA GGG AAA C		22	This study

3.10 Biolog Phenotype Microarrays (PMs)

The PM assays were performed with Biolog OmniLog® automated incubator (Biolog Inc., Hayward, California) based on the PM procedures for *E. coli* and other Gram-Negative (GN) bacteria. WT and mutant strains of *H. alvei* FB1 were incubated overnight on TSA plates at 37°C. Cells were then swabbed from the overnight culture and suspended in appropriate Biolog medium containing Dye Mix A. The turbidity was adjusted to 85% according to the manufacturer's protocol. IF-0 GN Base was used for plates PM-1 and -2; IF-0 GN Base with 5mM sodium pyruvate added was used for PM-3 to -8; and IF-10 Base with 1:200 dilution of an 85% transmittance suspension of cells was used for PM-9 to -20. A total of 100 μL cell suspension was transferred to each well on the PM plates. The plates containing cell suspension were then incubated in the OmniLog® incubator at 37°C for 48 hours, with readings taken every 15 min. Analysis of the results was performed using Kinetic and Parametric software (Biolog Inc., Hayward, California). Phenotypes were determined based on the area difference under the kinetic curve of dye formation between the WT and mutant strains and a significant divergent phenotype was identified when a difference in OmniLog™ units of 20,000 or above was obtained.

CHAPTER 4: RESULTS

4.1 Isolation of Bacteria

A total of 13 bacterial colonies displaying distinctive morphologies were recovered from fish paste meatballs from four different commercial brands (A, B, C, and D). Four out of 13 isolates (FB5, FB6, FB12, and FB13) established swarming morphology on LBA. Colonial morphology of each isolate on MacConkey agar was recorded as shown in Table 4.1. Colony morphologies of isolates on LBA were listed in Appendix D.

Table 4.1: Colonial morphologies of bacterial isolates on MacConkey agar.

Brand	Isolate	Colour	Diameter (mm)	Mucoid	Form	Elevation	Margin	Lactose fermentation
A	FB1	Colourless	2 - 4	No	Circular	Convex	Entire	-
	FB2	Colourless	2 - 4	No	Circular	Convex	Entire	-
	FB3	Pink	3 - 5	Yes	Circular	Umbonate	Undulate	+
	FB4	Pink	2 – 4	No	Circular	Convex	Entire	+
B	FB5	Colourless	2 – 4	No	Circular	Flat	Undulate	-
	FB6	Colourless	2 – 4	No	Circular	Flat	Undulate	-
	FB7	Pink	2 – 4	No	Circular	Convex	Entire	+
C	FB8	Pink	3 – 5	Yes	Circular	Umbonate	Undulate	+
D	FB9	Colourless	2 – 4	No	Circular	Convex	Entire	-
	FB10	Pink	2 – 4	Yes	Circular	Convex	Entire	+
	FB11	Pink	3 - 5	Yes	Circular	Umbonate	Undulate	+
	FB12	Colourless	2 – 4	No	Circular	Flat	Undulate	-
	FB13	Colourless	2 - 4	No	Circular	Flat	Undulate	-

*: Unable to identify due to swarming morphology; N/A: Non-applicable; +: Positive; -: Negative

4.2 Identification of Bacterial Isolates

All 13 isolates were identified using MALDI-TOF MS. Secure genus identification was obtained for all isolates, of which 4 were identified up to species level with high confidence. Identity of each isolate was listed in Table 4.2 along with the score values.

Table 4.2: Identity of isolates based on MALDI-TOF MS.

Isolate	Identity	Score
FB1	*Hafnia alvei*	2.655
FB2	*Enterobacter gergoviae*	2.279
FB3	*Klebsiella pneumoniae*	2.074
FB4	*Raoultella ornithinolytica*	2.230
FB5	*Proteus vulgaris*	2.038
FB6	*Proteus mirabilis*	2.144
FB7	*Raoultella ornithinolytica*	2.352
FB8	*Klebsiella pneumoniae*	2.011
FB9	*Citrobacter fruendii*	2.168
FB10	*Enterobacter gergoviae*	2.354
FB11	*Klebsiella pneumoniae*	2.020
FB12	*Proteus mirabilis*	2.399
FB13	*Proteus vulgaris*	2.411

Score values of 2.300 – 3.000: Highly probable species identification; 2.000 – 2.299: Secure genus identification, probable species identification; 1.700 – 1.999: Probable genus identification; 0.000 – 1.699: Not reliable identification

4.3 Characterisation of AHL Profile

4.3.1 Preliminary Screening for AHL production

All 13 bacterial isolates were subjected to screening for AHL production with biosensor *C. violaceum* CV026. Presence of short chain AHL was indicated by the purple pigmentation (violacein) on the horizontal streak (Figure 4.1). Strain FB1 was the only one showing a positive reaction. The results of the preliminary screening were listed in Table 4.3.

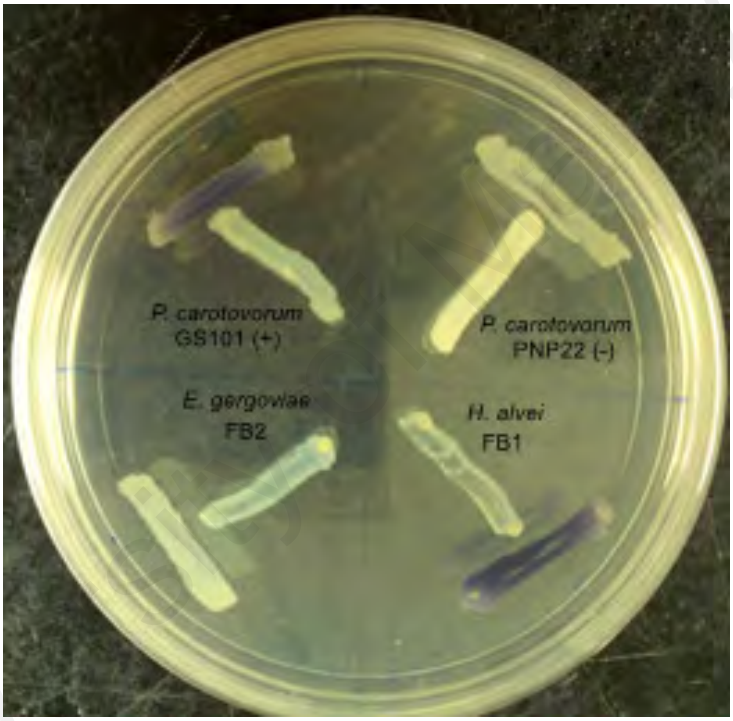

Figure 4.1: Screening for AHL production using *C. violaceum* CV026 cross streaking with *P. carotovorum* GS101 and PNP22 as positive and negative controls, respectively. *H. alvei* FB1 was found to induce the violacein production in CV026. The biosensor did not respond to the non-AHL-producing isolate, *E. gergoviae* FB2.

Table 4.3: Results from the preliminary screening for AHL production using CV026 biosensor.

Isolate	Violacein production
Hafnia alvei FB1	+
Enterobacter gergoviae FB2	-
Klebsiella pneumoniae FB3	-
Raoultella ornithinolytica FB4	-
Proteus vulgaris FB5	-
Proteus mirabilis FB6	-
Raoultella ornithinolytica FB7	-
Klebsiella pneumoniae FB8	-
Citrobacter freundii FB9	-
Enterobacter gergoviae FB10	-
Klebsiella pneumoniae FB11	-
Proteus mirabilis FB12	-
Proteus vulgaris FB13	-

+: Positive; -: Negative

4.3.2 AHL Identification by TLC

The AHL extracted from the spent supernatant of *H. alvei* FB1 was chromatographed on TLC. The result of TLC (Figure 4.2) showed the formation of two purple spots of R_f value similar to those formed by the known synthetic AHLs (approximately 10.0 for $3OC_6$-HSL and 14.2 for $3OC_8$-HSL).

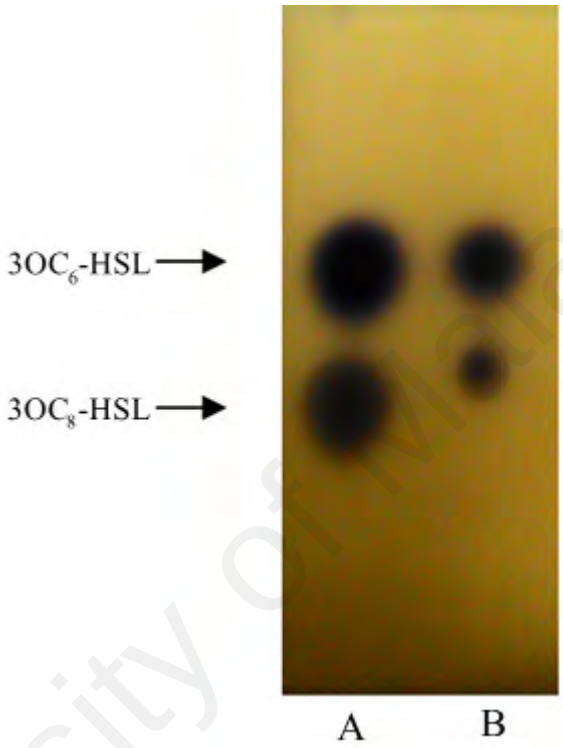

Figure 4.2: TLC separation of AHLs present in extract of the spent culture supernatant of *H. alvei* FB1, visualised with *C. violaceum* CV026. (A) Synthetic AHL standards; (B) AHLs extracted from *H. alvei* FB1

4.3.3 AHL Identification by LC-MS/MS

To further confirm the AHL profile of *H. alvei* FB1, the AHL extract was analysed using LC-MS/MS. Analysis of the spectra generated on the LC-MS/MS platform by comparing to a series of ten synthetic AHLs and oxo-derivatives with known chain lengths revealed that *H. alvei* FB1 produced two types of AHLs: $3OC_6$-HSL and $3OC_8$-HSL. The values of charge-to-mass (*m/z*) ratio of these detected AHLs (the former 214 and the latter 242) are consistent with those reported by Ortori et al. (2011). The total ion chromatograms and mass spectra are shown in Figure 4.3.

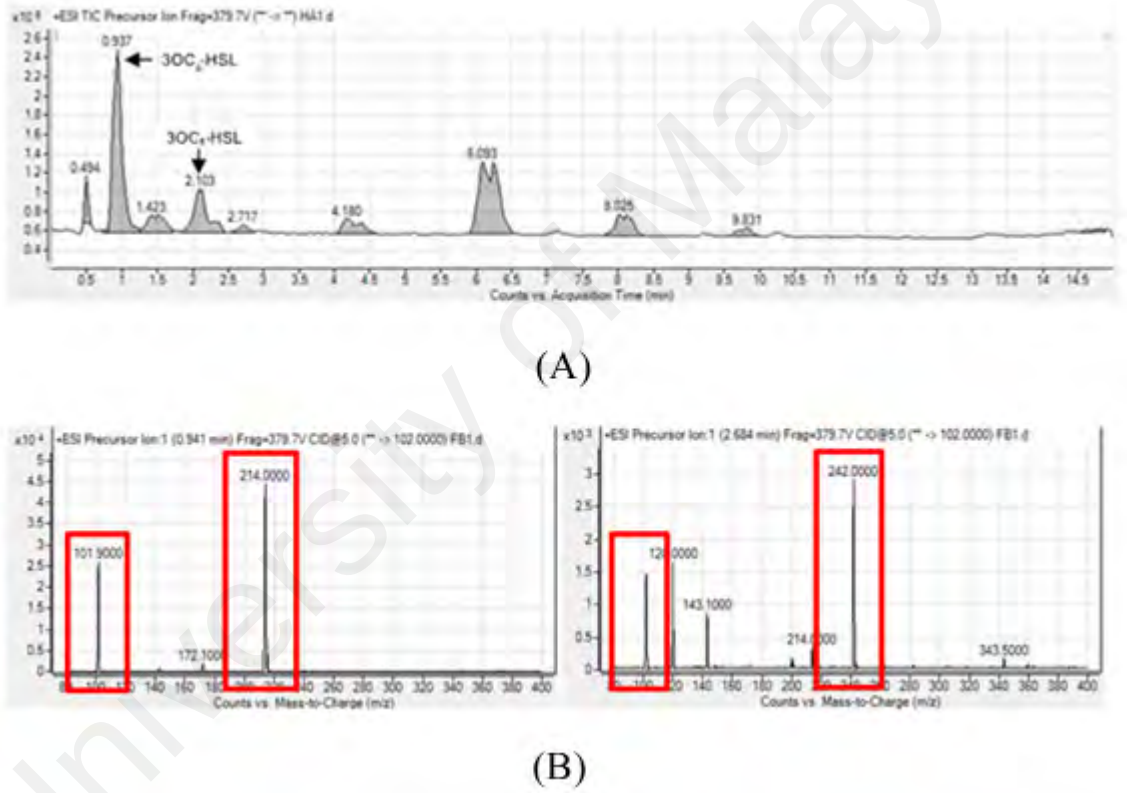

Figure 4.3: LC-MS/MS analysis of the crude AHL extract from the spent supernatant of *H. alvei* FB1. (A) Chromatograms showing the peaks of targeted AHLs extracted from the cell-free supernatant of *H. alvei* FB1 and (B) Mass spectra of AHLs extracted from the cell-free supernatant of *H. alvei* FB1, showing the presence of precursor ions $3OC_6$-HSL (*m/z* 214) and $3OC_8$-HSL (*m/z* 242) along with the product ion peaks (*m/z* 102.0 $\pm$ 0.1).

4.4 Characterisation of AHL-Producing Strain *H. alvei* FB1

4.4.1 Phylogenetic Analysis of *H. alvei* FB1 16S rDNA Sequence Phylogeny

Nucleotide sequences of *H. alvei* FB1 16S rDNA gene sequences obtained from the PCR product generated with primer pair 27F and 1525R was matched against the EzBioCloud 16S database, and 99.86% similarity with the type strain *H. alvei* ATCC 13337^T was returned. A phylogenetic tree was constructed using nine other 16S rDNA gene sequences with the highest similarity on MEGA7 (Figure 4.4). The evolutionary history was inferred using the Neighbour-Joining (NJ) method (Saitou & Nei, 1987).

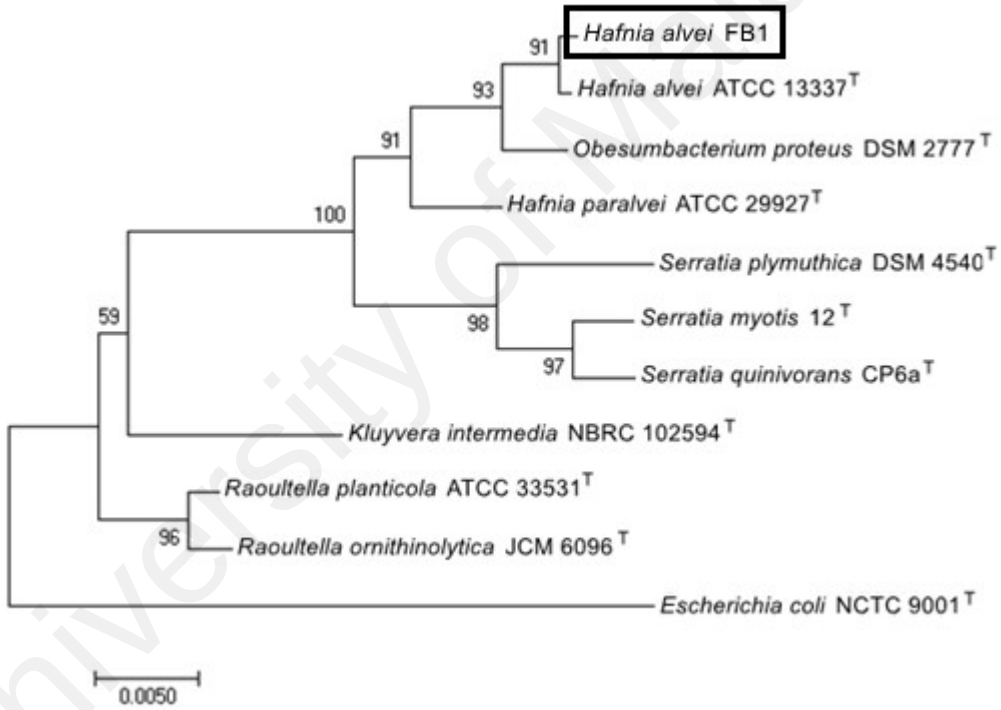

Figure 4.4: 16S rDNA genes phylogenetic analysis of *H. alvei* FB1 with *Escherichia coli* NCTC 9001^T as an outgroup. *H. alvei* FB1 is shown to be most closely related with the type strain of *H. alvei*. The scale bar represents 0.005 substitution per nucleotide position.

4.4.2 API Biochemical Assay

Biochemical assay using API strip was performed as a routine confirmation by the culture collector (DSMZ). The results in comparison with the type strain were listed in Table 4.4. *H. alvei* FB1 was found to lack urease activity as well as the ability to ferment amygdalin, of which both showed positive reactions in the type strain (*H. alvei* ATCC 13337^T).

Table 4.4: API Biochemical Assays.

Biochemical test	*H. alvei* FB1	*H. alvei* ATCC 13337^T
β-Galactosidase (ONPG)	+	+
Arginine dihydrolase (ADH)	-	-
Lysine decarboxylase (LDC)	+	+
Ornithine decarboxylase (ODC)	+	+
Citrate utilisation (CIT)	+	+
H_2S production (H2S)	-	-
Urease (URE)	-	+
Tryptophane deaminase (TDA)	-	-
Indole production (IND)	-	-
Voges-Proskauer (VP)	+	+
Mannitol (MAN)	-	-
Gelatinase (GEL)	+	+
Glucose (GLU)	+	+
Inositol (INO)	-	-
Sorbitol (SOR)	-	-
Rhamnose (RHA)	+	+
Saccharose (SAC)	-	-
Melibiose (MEL)	-	-
Amygdalin (AMY)	-	+
Arabinose (ARA)	+	+
Cytochrome oxidase (OX)	-	-

+: positive, -: negative

4.5 Whole Genome Sequencing (WGS)

The genome of *H. alvei* FB1 was sequenced on PacBio SMRT sequencer. A single contig of 4,712,721 bp with an average coverage of 68.46× was obtained from the HGAP assembly on SMRT portal. The circularity of the genome was confirmed by the presence of the two lines parallel to the main diagonal line at the upper right (Figure 4.5B) and lower left (Figure 4.5C) corners in dot plot analysis using Gepard (Krumsiek et al., 2007).

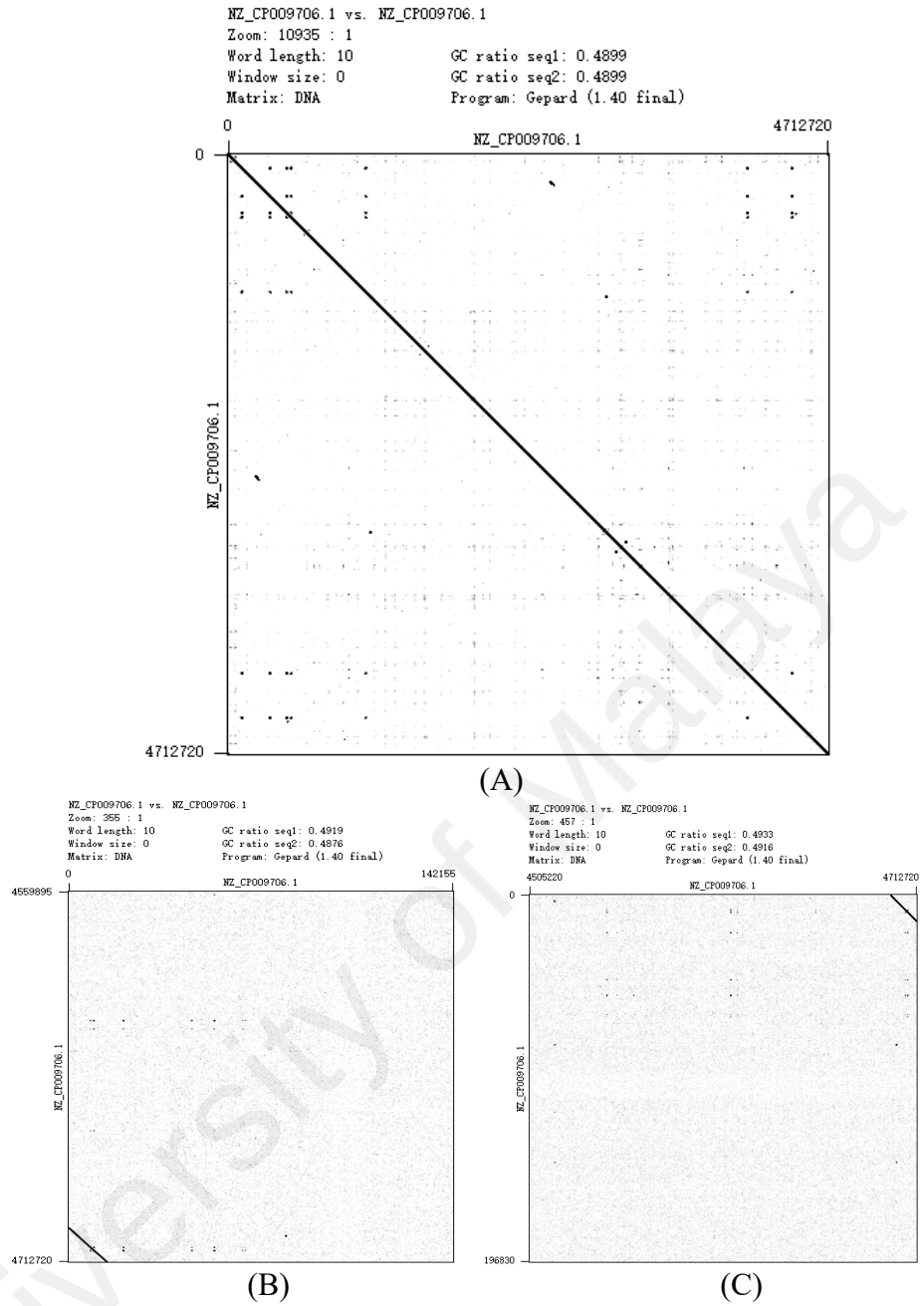

Figure 4.5: Circular chromosome of *H. alvei* FB1 represented in dot plot analysis. (A) Full dot plot showing the main diagonal line, (B) parallel line at the magnified lower left corner, and (C) parallel line at the magnified upper right corner.

The genome sequence of *H. alvei* FB1 was deposited to the GenBank depository under the accession number CP009706. A graphical representation of the distribution of genome features and GC content in the form of circular genome map was constructed based on PGAAP annotation (Figure 4.6). Basic features of this genome according to PGAAP annotation are summarised in Table 4.5.

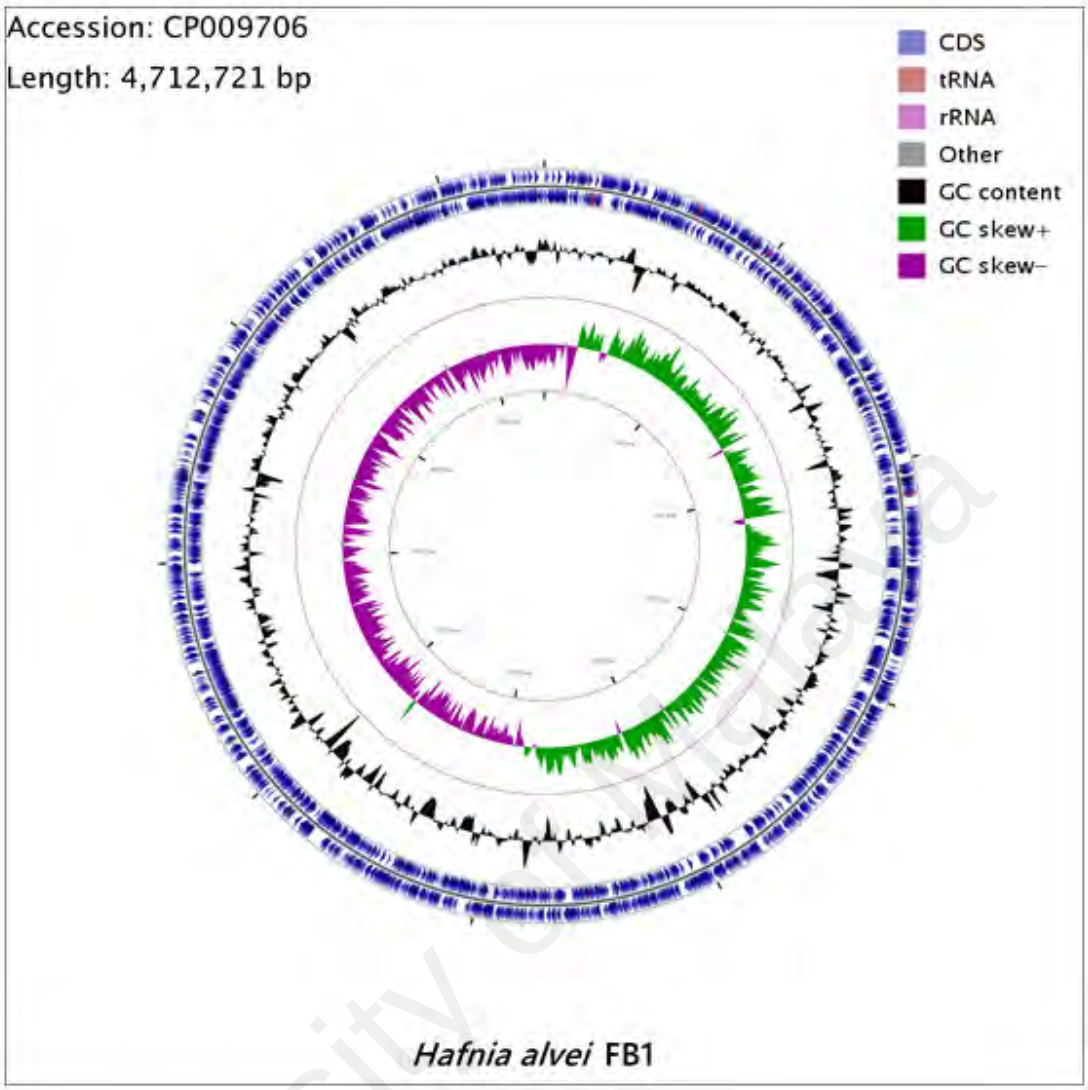

Figure 4.6: Circular genome map of *H. alvei* FB1 showing (from outermost to innermost): 1. CDS and genome features (forward strand); 2. CDS and genome features (reverse strand); 3. GC content; 4. GC skew.

Table 4.5: List of genome features.

Genome attribute	Number
DNA, total number of bases	4,712,721
DNA coding number of bases	4,088,435
DNA G+C number of bases	2,308,775 (49.0%)
Number of contigs	1
Genes total number	4,387
Protein coding genes	4,170
RNA genes	168
rRNA genes	25
5S rRNA	9
16S rRNA	8
23S rRNA	8
tRNA genes	91
Other RNA genes	52
Clustered Regularly Interspaced Short Palindromic Repeats (CRISPR) Count	3

Of all 4,712,721 bases of the genome, coding regions made up 86.8% (4,088,435). A total of 4,387 genes were predicted out of the genome sequence, of which 4,170 (95.1%) were protein-coding. All eight copies of 16S rDNA found in the FB1 genome shared similarity above 99% with that of *H. alvei* ATCC 13337^{T}, the type strain of *H. alvei* (Appendix E), hence confirmed that the genome belonged to *H. alvei* FB1 and there was no contamination by sequences from other organisms.

4.5.1 Clusters of Orthologous Groups (COGs)

The annotated gene sequences of FB1 genome were further assigned into functional categories based on the COGs. A summary of COG distribution displayed as a bar chart in Figure 4.7 shows that, aside of 17.84% of CDSs with ambiguous functions, a large portion of the genome was allocated to metabolic functions that maintain the wellbeing of the cell, with Amino acid transport and metabolism (E, 8.44%) and Carbohydrate transport and metabolism (G, 7.67%) topping the list. The category Defense mechanism (V), which comprised genes involved in drug resistance and DNA restriction-modification (RM), accounted for 1.2% of the whole genome.

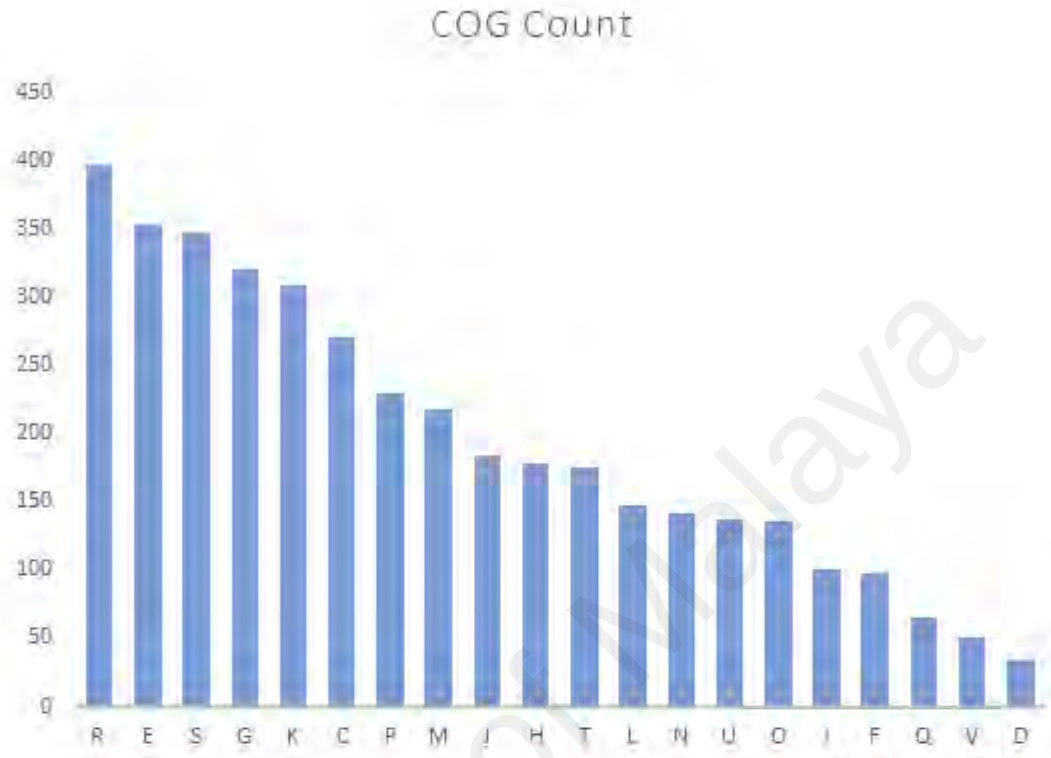

	Count	%
[R] General function prediction only	397	9.520384
[E] Amino acid transport and metabolism	352	8.441247
[S] Function unknown	347	8.321343
[G] Carbohydrate transport and metabolism	320	7.673861
[K] Transcription	308	7.386091
[C] Energy production and conversion	270	6.47482
[P] Inorganic ion transport and metabolism	229	5.491607
[M] Cell wall/membrane/envelope biogenesis	217	5.203837
[J] Translation, ribosomal structure and biogenesis	184	4.41247
[H] Coenzyme transport and metabolism	178	4.268585
[T] Signal transduction mechanisms	175	4.196643
[L] Replication, recombination and repair	148	3.549161
[N] Cell motility	141	3.381295
[U] Intracellular trafficking, secretion, and vesicular transport	137	3.285372
[O] Post-translational modification, protein turnover, and chaperones	136	3.261391
[I] Lipid transport and metabolism	100	2.398082
[F] Nucleotide transport and metabolism	97	2.326139
[Q] Secondary metabolites biosynthesis, transport, and catabolism	66	1.582734
[V] Defense mechanisms	50	1.199041
[D] Cell cycle control, cell division, chromosome partitioning	34	0.815348
Not in COG	639	15.32374

Figure 4.7: COG distribution statistics for *H. alvei* FB1 giving an overview of the COG coverage and the counts of each COG category.

4.5.2 Species Circumscription

To confirm the specific status of *H. alvei* FB1, a calculation of the ANI was performed, using the type strains of each species within the genus as references, based on the OrthoANI algorithm (Lee et al., 2016). The all-to-all ANI values among all genomes are presented in the form of clustered heatmap (Figure 4.8).

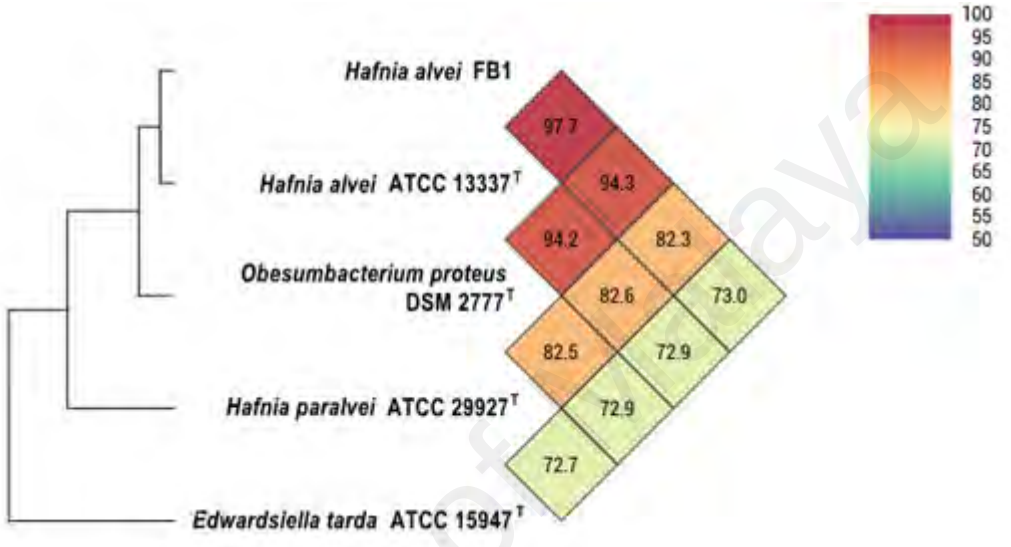

Figure 4.8: Clustering heatmap based on OrthoANI. The relatedness of *H. alvei* FB1 to the type strains within Hafniaceae family is demonstrated.

An ANI value of 97.7% shared between isolate FB1 and *H. alvei* ATCC 13337^T indicated that these two belonged to the same species (species cut-off value = 95%). Both strains also shared similar ANI values (82.3% and 82.6%, respectively) with the type strain of *H. paralvei*. Interestingly, the type strain of *Obesumbacterium proteus*, DSM 2777^T, which bears a different genus designation, shared much higher ANI values (94.3% and 94.2%) with *H. alvei* compared to *H. paralvei* (82.5%).

In order to determine the generic status of *Obesumbacterium*, POCP (Qin et al., 2014) between DSM 2777^T and *H. alvei* ATCC 13337^T was calculated. Values above the cut-off of 50% (82.35%) for DSM 2777^T were obtained, indicating that, instead of a separate genus, *O. proteus* should still belong under the genus *Hafnia*.

4.5.3 Comparison with Genomes of Other *H. alvei* Strains

Comparison of genomic content was carried out between *H. alvei* FB1 and *H. alvei* ATCC 13337^T, ATCC 29926, CBA7124, DSM 30098, DSM 30099, FDAARGOS_350, HUMV-5920, *O. proteus* DSM 2777^T, *H. paralvei* ATCC 29927^T, and *E. tarda* ATCC 15947^T using sequence-based comparison function of RAST server.

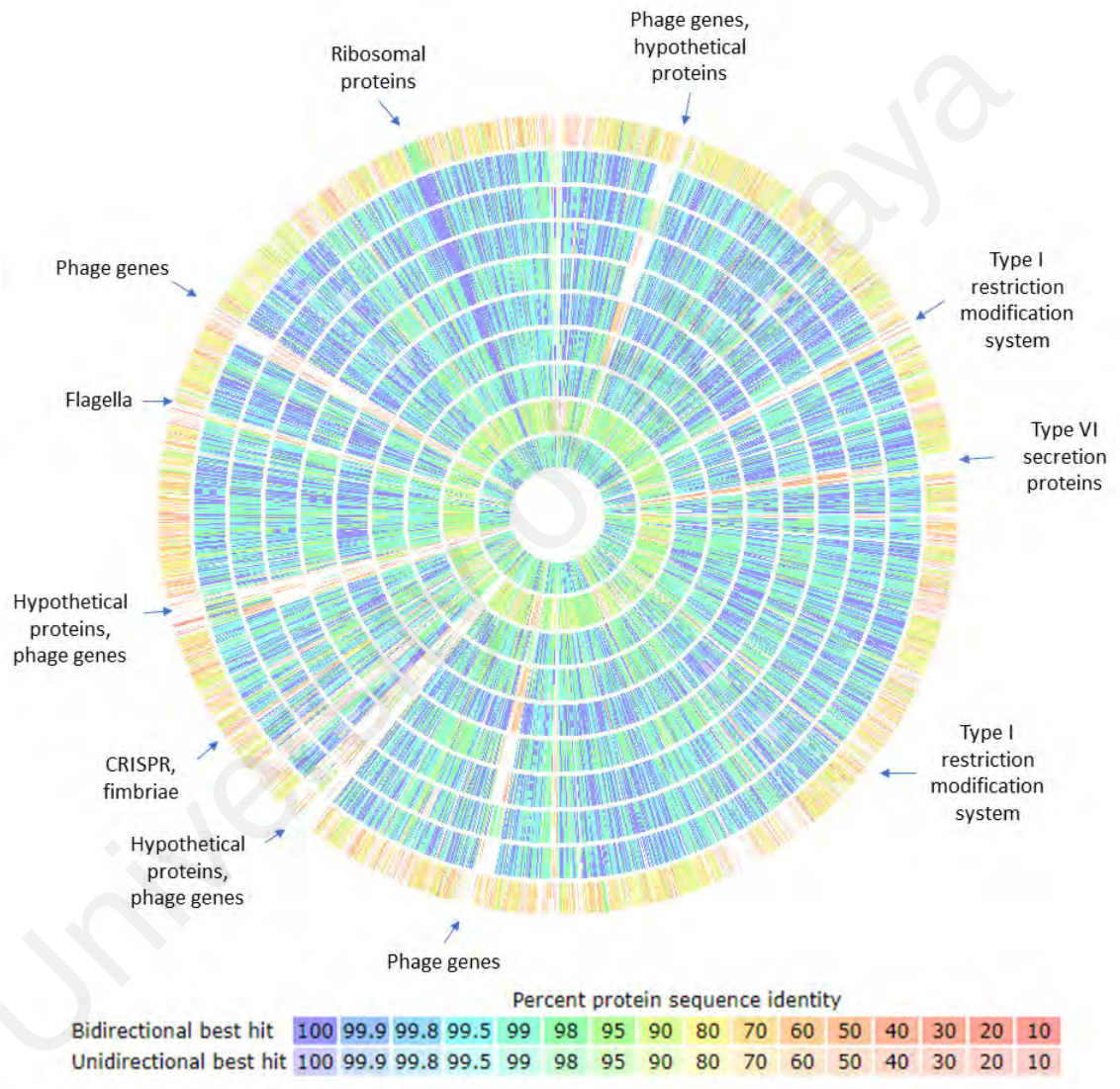

Figure 4.9: Predicted proteome sequence comparison between *H. alvei* FB1 and ten closely related strains. From innermost to outermost: *O. proteus* DSM 2777^T, *H. paralvei* ATCC 29927^T, *H. alvei* ATCC 13337^T, ATCC 29926, CBA7124, DSM 30098, DSM 30099, FDAARGOS_350, HUMV-5920, and *E. tarda* ATCC 15947^T. Protein sequences that do not find a match in *H. alvei* FB1 genome are shown as 'gaps'.

Comparison between *H. alvei* FB1 and seven other *H. alvei* genomes revealed that each genome shared average percentage of protein sequence identities ranging from 95.41% to 97.54% with *H. alvei* FB1, whereas *O. proteus* DSM 2777^T, *H. paralvei* ATCC 29927^T, and *E. tarda* ATCC 15947^T 94.51%, 86.87%, and 67.11%, respectively. This was represented as a colour-coded circular map as blue (*H. alvei* and *O. proteus*), green (*H. paralvei*), and orange (*E. tarda*) in Figure 4.9. Protein sequences that did not have a match in *H. alvei* FB1 genome are shown as 'gaps' in the circular map, the lowest identity that was shown as a match in this comparison is 19.52%. The 'gaps' consisted mainly of sequences annotated as 'hypothetical proteins' and genes associated with phages. Regions that display low protein identities on the map comprised genes encoding type I restriction-modification systems, a type VI secretion system, CRISPR-associated (Cas) proteins, fimbriae, and flagella.

A total of 3,102 protein coding sequences were shared among all genomes with *H. alvei* FB1, of which 1,906 (61.44%) were assigned to SEED subsystems. This subset of CDSs were found to be particularly low in subsystem category Phages, Prophages, Transposable elements, Plasmids (Figure 4.10). The list of genes found in *H. alvei* FB1 that were shared with only a fraction of other genomes comprised 1,307 sequences, of which only 320 were assigned to subsystems. In this subset, number of CDSs belonging to subsystem category Phages, Prophages, Transposable elements, Plasmids were exceptionally high (Figure 4.10). These CDSs were observed to be mainly of phage origins. On the other hand, 527 sequences shared among all *Hafnia* spp. genomes included in the comparison were not found in *E. tarda* ATCC 15947^T. Only 193 of these sequences were assigned to subsystems.

In Figure 4.10, it is shown that the high numbers of CDSs that belonged to certain subsystem categories in the subset "CDSs found in some of the genomes" were

contributed mainly by the lack thereof in *E. tarda* ATCC 15947^{T}, for instance, Amino Acids and Derivatives, Carbohydrates, Membrane Transport, Potassium Metabolism, Respiration, and Virulence, Disease and Defense.

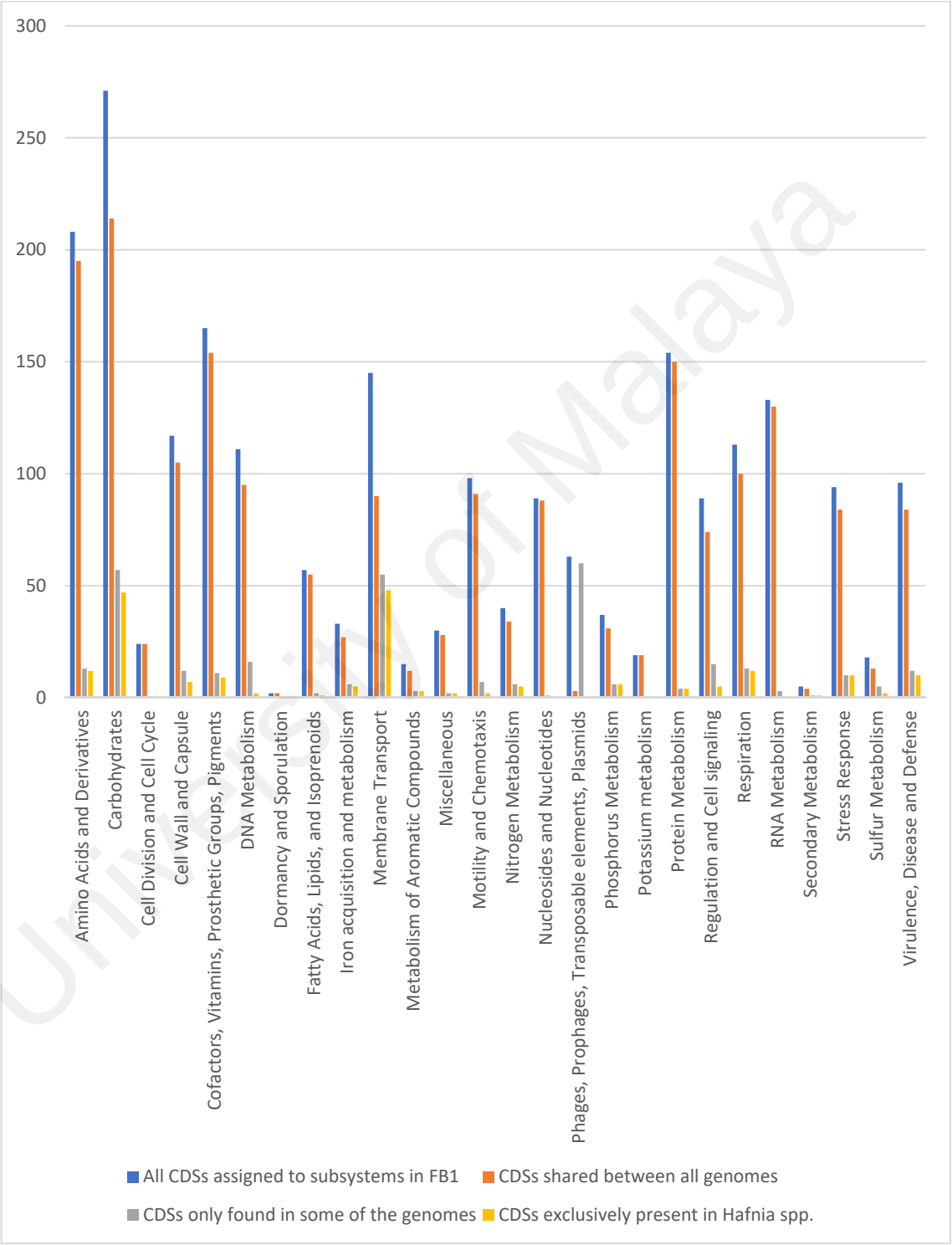

Figure 4.10: Bar chart displaying the distribution of subsystems in the genome of *H. alvei* FB1, CDSs found in all eleven genomes, CDSs with variable presence across the genomes, and CDSs that were shared among all *Hafnia* spp. but not found in *E. tarda* ATCC 15947^{T}.

4.6 QS System in *H. alvei* FB1

A homology search using LuxI and LuxR amino acid sequences via "BLAST search' function of RAST server revealed the presence of a pair of candidates at the position 2,668,370 – 2,669,738 in the genome of *H. alvei* FB1. The pair consisted of a 648-bp *luxI* homologue annotated as "acyl-homoserine-lactone synthase" by PGAAP (Locus tag AT03_RS12360) and "*N*-3-oxooctanoyl/*N*-3-oxohexanoyl-L-homoserine lactone synthase" by RAST; along with a 741-bp *luxR* homologue annotated as "LuxR family transcriptional regulator" by PGAAP (AT03_RS12355) and "Quorum sensing transcriptional regulator YspR" by RAST. The pair was found to be in convergent orientation, with 20-bp overlap at the 3'-ends (Figure 4.11).

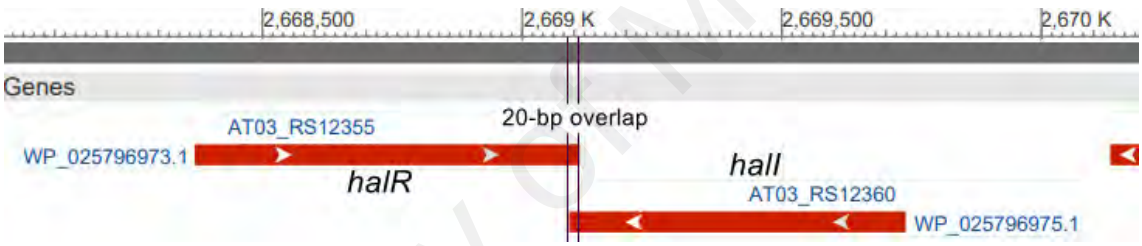

Figure 4.11: Orientation of *hall* and *halR* and their locations in *H. alvei* FB1 genome. A convergent transcriptional orientation with 20-bp overlapping region at the 3'-end is shown.

The pair was searched for the presence of signature domains carried on QS genes along with five other CDSs annotated as "LuxR family transcriptional regulator" against the Conserved Domain Database (CDD) (Marchler-Bauer et al., 2017). A domain that belonged to *N*-Acetyltransferase superfamily (pfam00765) was detected on the *hall* sequence (E-value = 1.05e-69) (Figure 4.12).

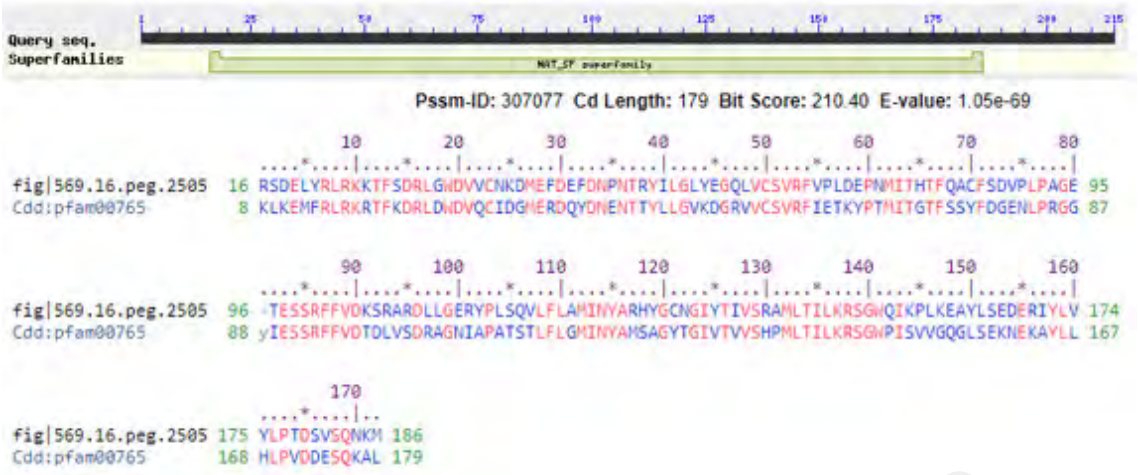

Figure 4.12: Signature conserved domain of *luxI* homologues on *halI*.

Among the six *luxR* candidates, only the one that flanked *halI* contained both signature domains that were conserved in AHL-dependent transcriptional regulators, namely, autoinducer binding domain (pfam03472, E-value = 2.02e-30) and a helix-turn-helix DNA binding domain (smart00421, E-value = 3.96e-18) (Figure 4.13).

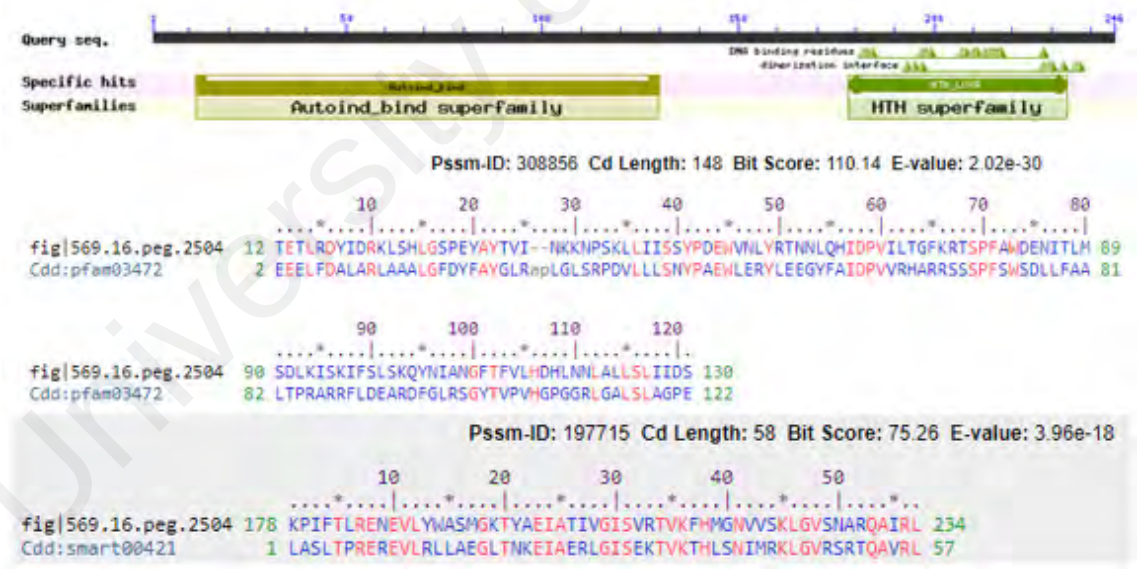

Figure 4.13: Signature conserved domain of *luxR* homologues on *halR*.

Multiple sequence alignment (MSA) was performed between HalI amino acid sequence and other known homologues of LuxI using MEGA7. The alignment along with conservation on each site was visualized using Jalview version 2 (Figure 4.14). Ten conserved key amino acid residues, namely, R25, F29, W35, E44, D46, D49, R70, F84, E101, and R104 according to their positions in TraI, as reported by Fuqua and Greenberg (2002) were identified in the sequence of HalI. Likewise, MSA on HalR and other known homologues of LuxR revealed the presence of six conserved key residues (W57, Y61, D70, P71, W85, and G113 according to their positions in TraR) within the autoinducer binding domain and three (E178, L182, and G188) within the DNA binding domain (Figure 4.15), as reported by Subramoni et al. (2015).

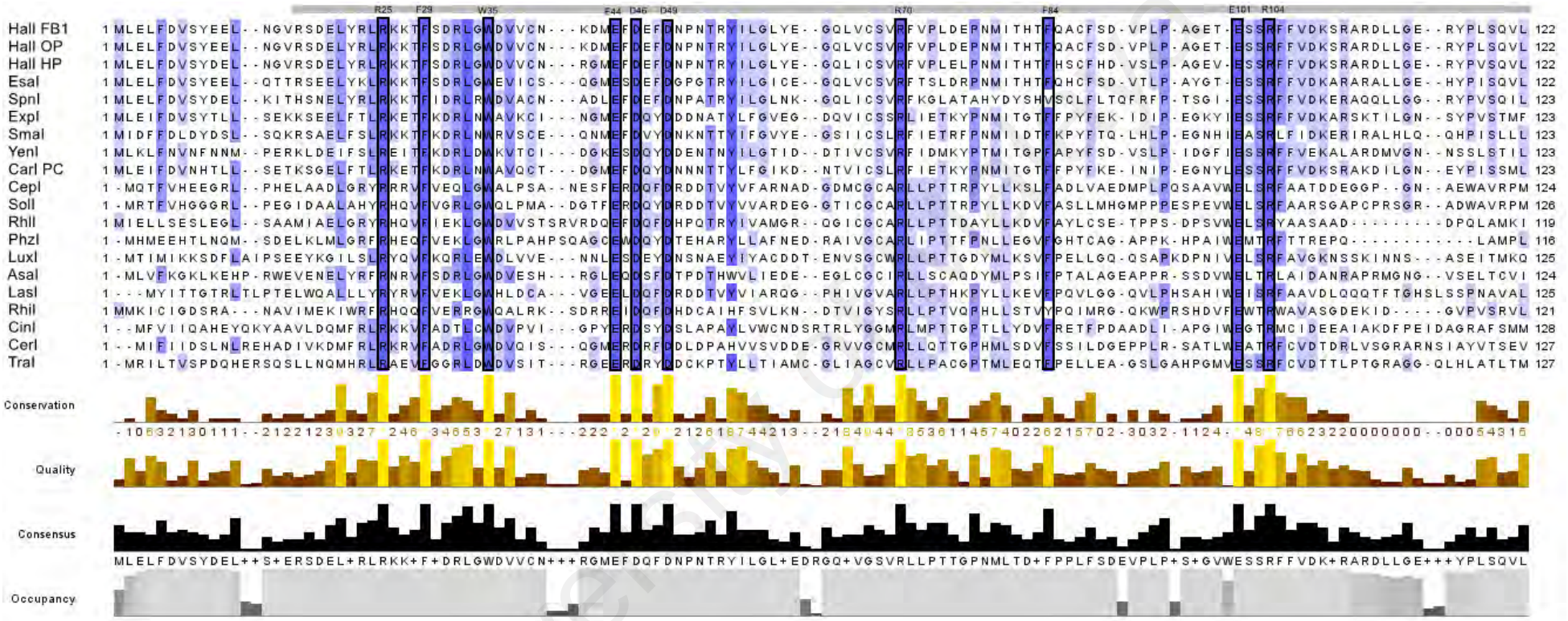

Figure 4.14: Multiple alignment of amino acid sequences of HalI and other known LuxI homologues. Ten key conserved residues according to their positions in TraI were highlighted. OP: *O. proteus*; HP: *H. paralvei*; PC: *P. carotovorum*.

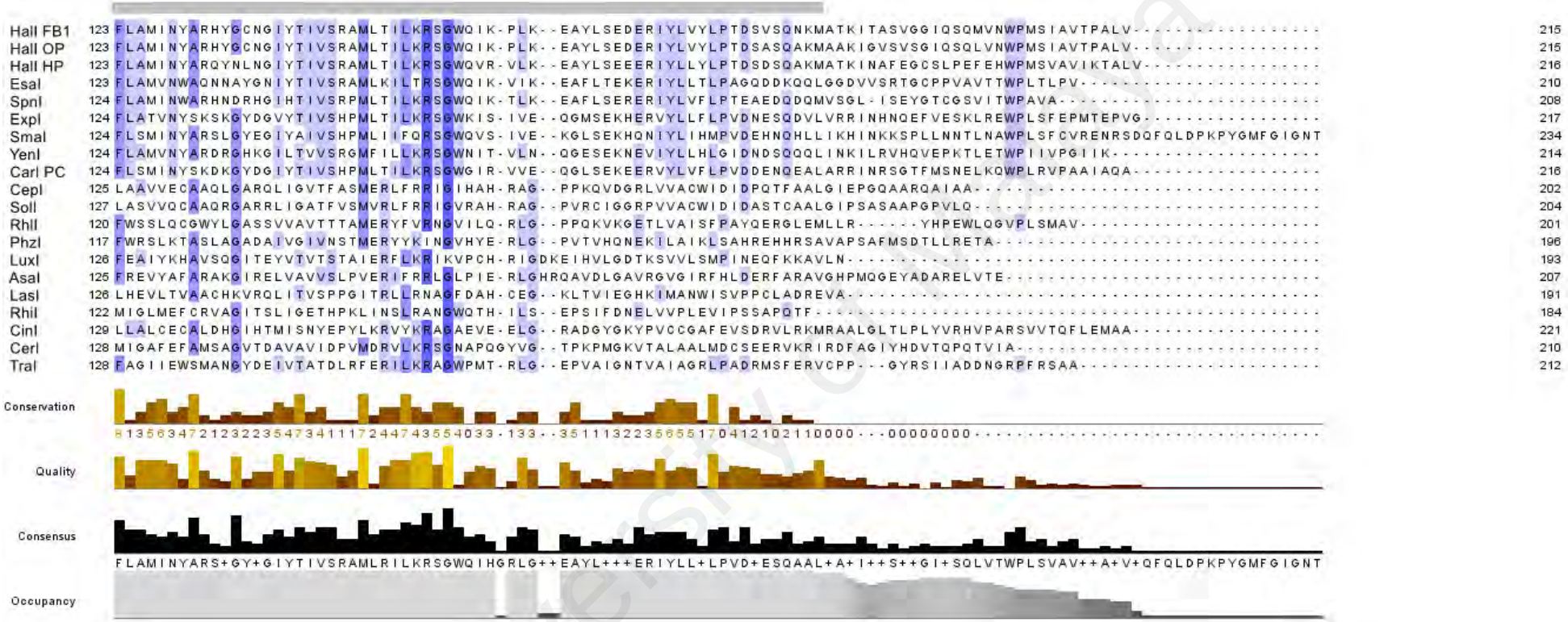

Figure 4.14, continued.

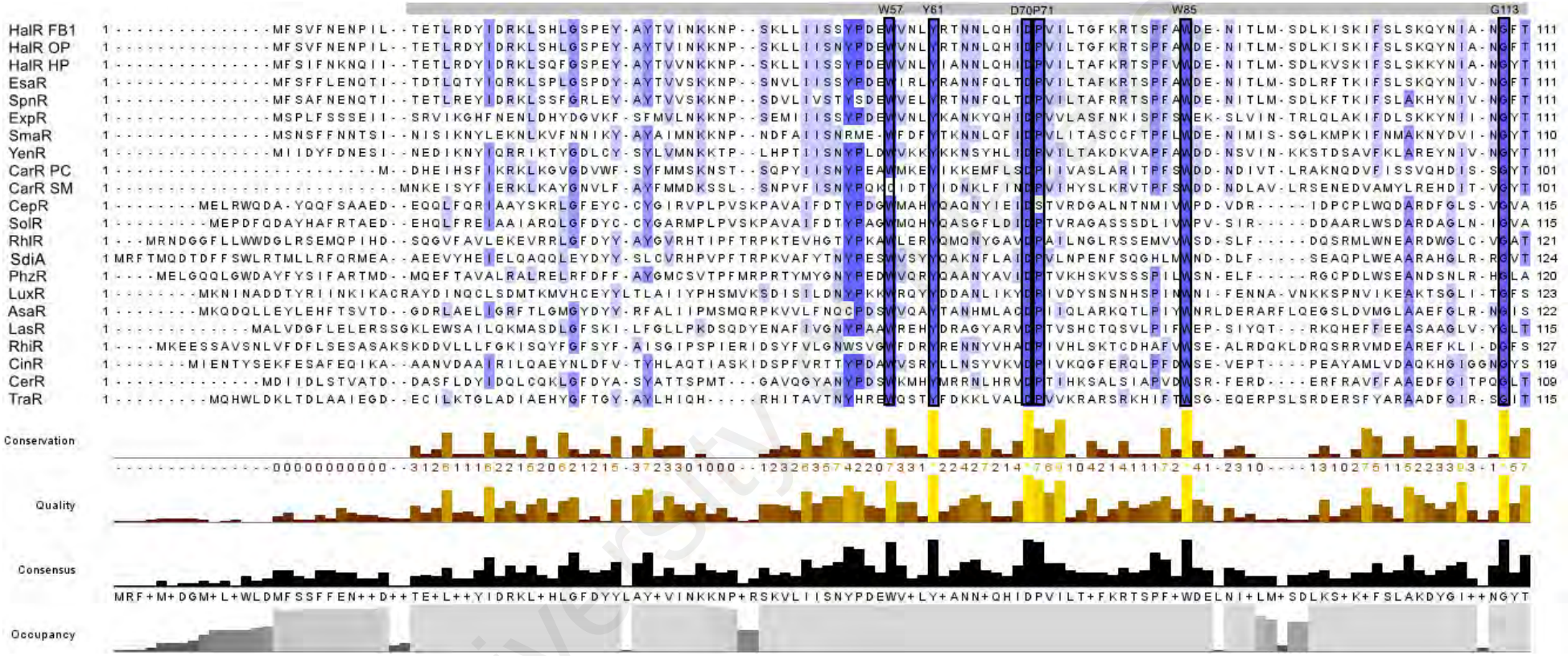

Figure 4.15: Multiple alignment of amino acid sequences of HalR and other known LuxR homologues. Nine key conserved residues within DNA binding domain according to their positions in TraR were highlighted. OP: *O. proteus*; HP: *H. paralvei*; PC: *P. carotovorum*.

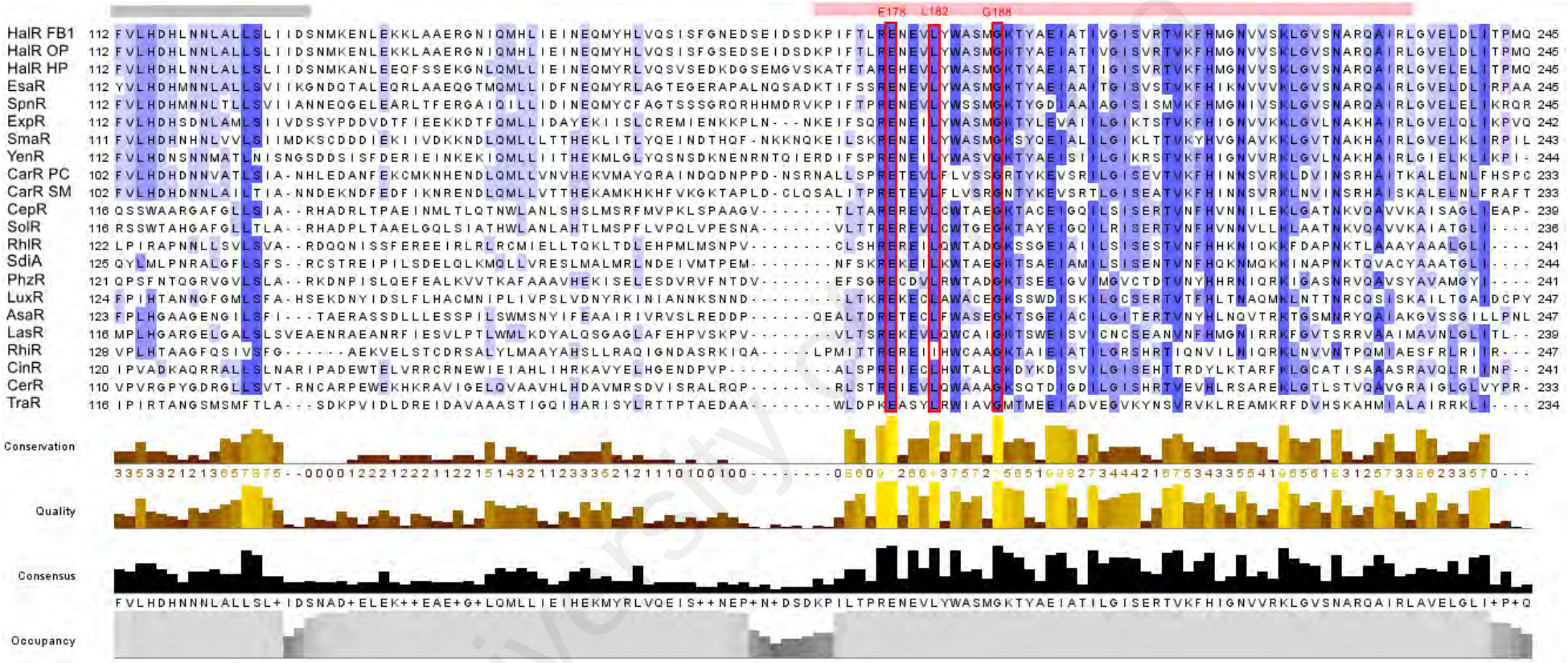

Figure 4.15, continued.

A single pair of *halI-halR* homologues was found in all seven other currently available *H. alvei* genomes, *O. proteus* DSM 2777^T, *H. paralvei* ATCC 29927^T, as well as *E. tarda* ATCC 15947^T. Coding regions flanking the two genes were largely conserved throughout the eight strains, except for the presence or absence of certain "blocks" of CDSs (Figure 4.16). Strain ATCC 29926 lacked a stretch of sequence encoding approximately 12 – 15 genes directly flanking the upstream of its *halR*. Albeit more distantly related, a certain degree of synteny was still observed between *O. proteus* DSM 2777^T and the *H. alvei* strains. A pair of CDSs putatively involved in multidrug resistance were found only in *O. proteus* DSM 2777^T and *H. alvei* FB1 but none others. No synteny was shared between the regions directly flanking the *halI-halR* pairs in *H. alvei* and *H. paralvei* ATCC 29927^T. Instead, genes located directly upstream of *H. paralvei* ATCC 29927^T found homologues in an inverted orientation at the upstream of *yspI*, the *luxI* homologue in *Yersinia pestis* KIM.

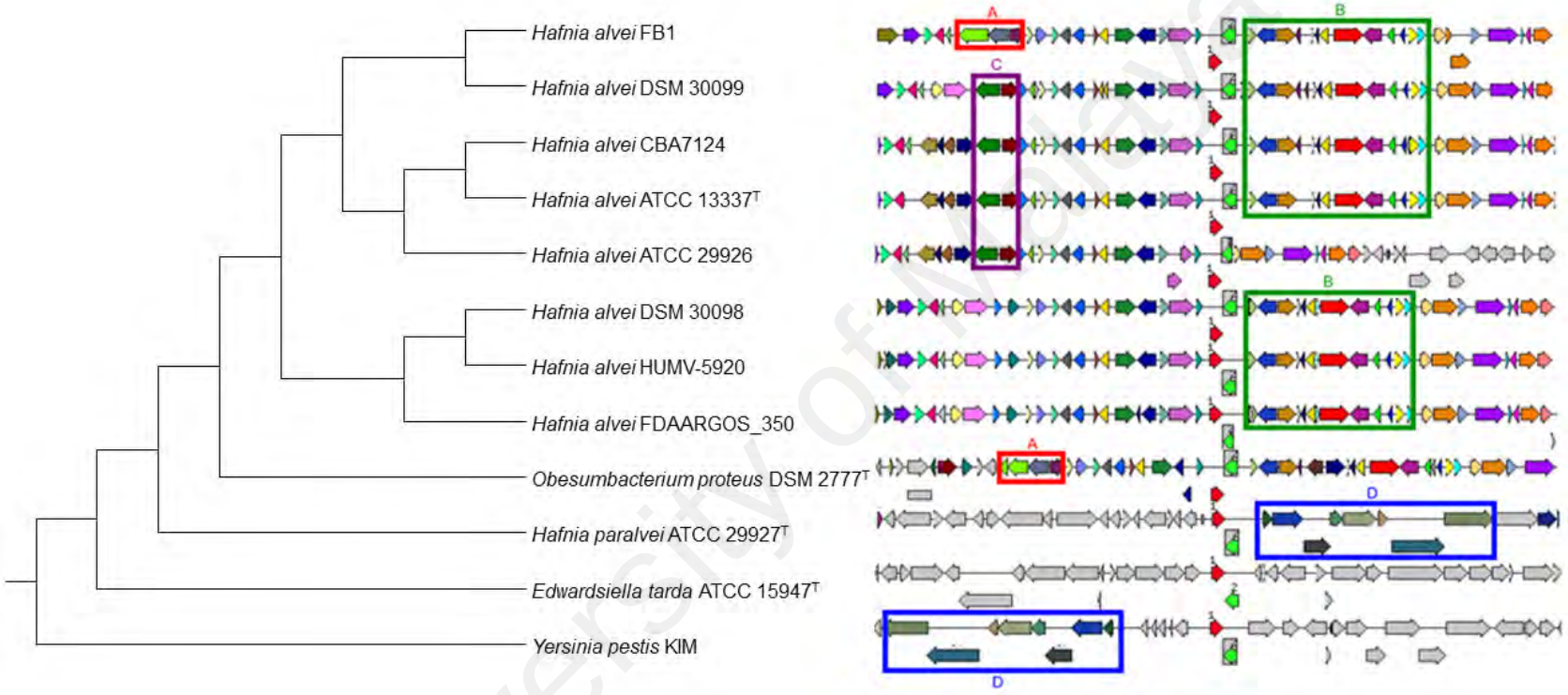

Figure 4.16: Synteny plot of regions flanking the putative QS genes (1: *hall*, 2: *halR*) in *H. alvei* FB1 and its close relatives. Homologous genes in different genomes were represented in same colours. Regions that show synteny in multiple genomes are highlighted in boxes of different colours, which contain, from left to right, A: Multidrug resistance protein (*ermB*), Membrane fusion component of tripartite multidrug resistance system, AraC family transcriptional regulator; B: Permease of the drug/metabolite transporter (DMT) superfamily, LysR family transcriptional regulator, putative *N*-acetyltransferase, Methyl-accepting chemotaxis protein I (serine chemoreceptor protein), LysR family transcriptional regulator, Ethidium bromide-methyl viologen resistance protein (*ermE*) Transcriptional regulator, AraC family; C: *mxcK*, putative LysR family transcriptional regulator; D (according to orientation in *H. paralvei* ATCC 29927^T: *impB*, *impC*, *impJ*, probable membrane protein, Outer membrane protein assembly factor YaeT precursor, putative cytoplasmic protein, *clpB*, *vgrG*. Genome regions were sorted according to whole genome phylogenetic tree generated using CVTree server.

Phylogenetic trees were built to demonstrate the phylogenies between HalI and HalR proteins with other LuxI and LuxR homologues of known functions (Figure 4.17 and Figure 4.18). Both trees shared roughly similar topologies, which consist of two major clusters. The top clusters are made up solely of members of γ-Proteobacteria, whereas the bottom ones contain those of α-, β-, and γ-Proteobacteria. All sequences from *Hafnia* spp. form a single clade in both trees, except for an orphan LuxI homologue (YspR) in *H. paralvei* bta3-1 that clusters with the more distantly related SmaR of *Serratia* sp. ATCC 39006. Both HalI and HalR were found to be more closely related to YspI-YspR in *Y. pestis* and YtbI-YtbR in *Y. pseudotuberculosis*, compared with *E. tarda* ATCC 15947^{T} that also belongs to the *Hafniaceae* family. The LuxR tree clearly shows that all the HalR sequences form a monophyletic clade with the sequences of LuxR homologues that were known to establish quorum-hindered activities.

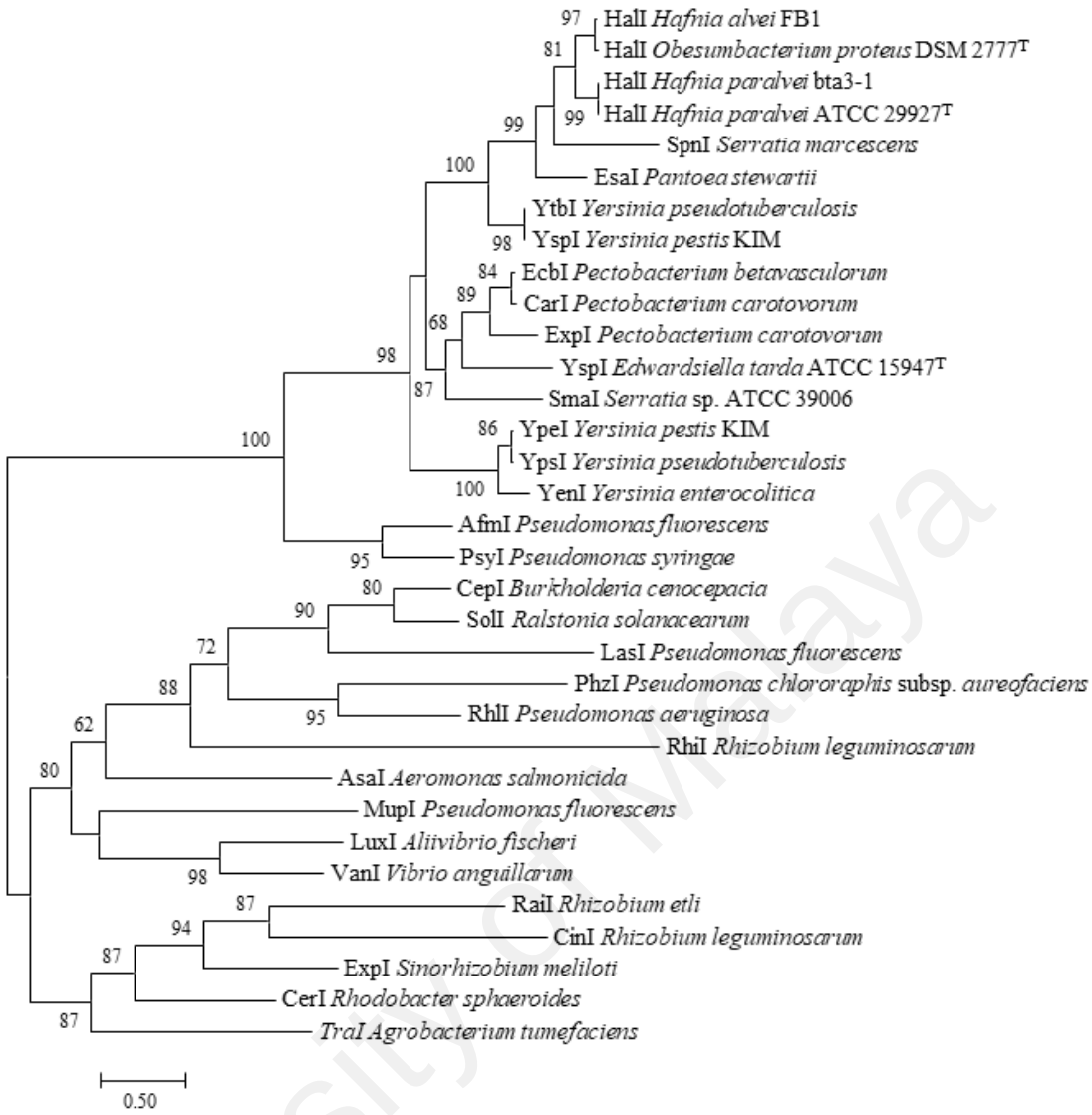

Figure 4.17: Phylogenetic tree showing the evolutionary distance of HalI of *H. alvei* FB1 and other LuxI homologues inferred using the Maximum Likelihood (PhyML) method based on the LG matrix-based model. The tree with the highest log likelihood (-11301.6) is shown. The aLRT branch support values are shown next to the branches. The tree is drawn to scale, with branch lengths measured in 0.5 substitutions per site (bar).

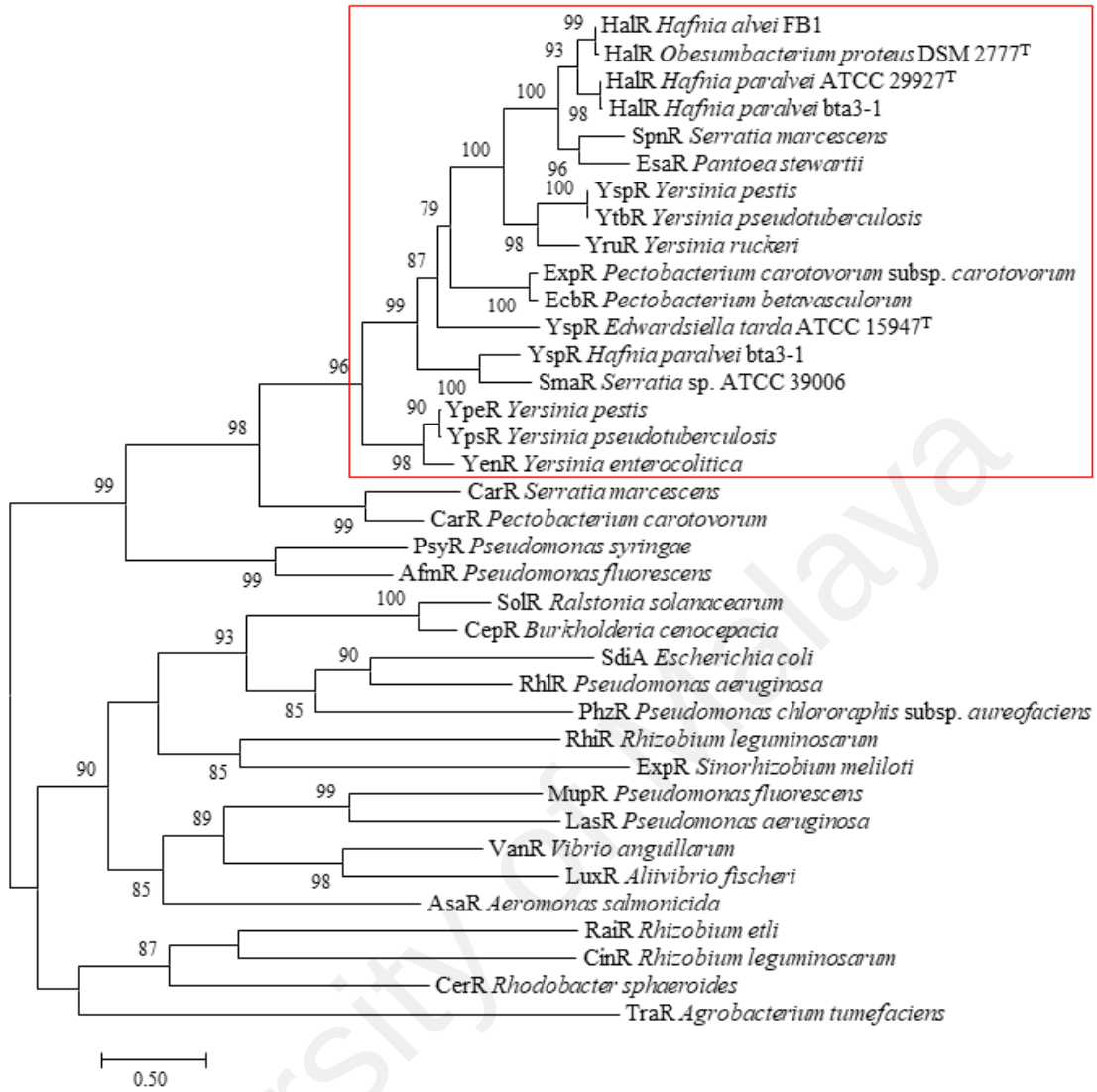

Figure 4.18: Phylogenetic tree showing the evolutionary distance of HalR of *H. alvei* FB1 and other LuxR homologues inferred using the Maximum Likelihood (PhyML) method based on the LG matrix-based model. The tree with the highest log likelihood (-14799.2) is shown. The aLRT branch support values are shown next to the branches. The tree is drawn to scale, with branch lengths measured in 0.5 substitutions per site (bar). The monophyletic clade that contained HalR and other LuxR homologues known to establish quorum-hindered properties were highlighted in red box.

4.6.1 Expression of *halI* in a Foreign Host

To prove the functionality of the identified AHL synthase, the *halI* sequence was cloned on a pGS-21a vector and expressed in host *E. coli* BL21 Star (DE3). Cross-streaking of the transformed BL21 Star (DE3) induced purple pigmentation of the CV026 biosensor (Figure 4.19). The same AHL profile produced by *H. alvei* FB1 ($3OC_6$-HSL and $3OC_8$-HSL) were detected using LC-MS/MS (Figure 4.20).

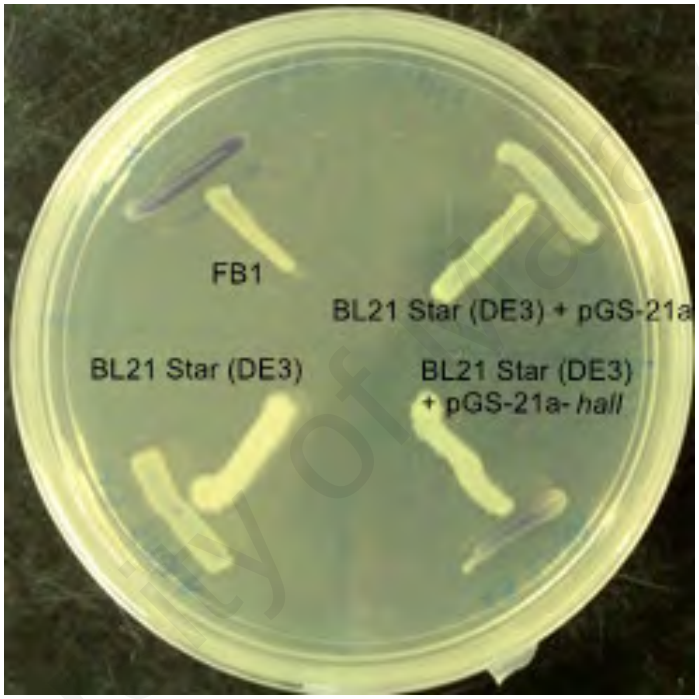

Figure 4.19: CV026 screening for AHL production in *E. coli* BL21 Star (DE3) harbouring pGS-21a-*halI*, with *H. alvei* FB1 as positive control, and BL21 Star (DE3) that was not transformed with a plasmid and BL21 Star (DE3) harbouring an native pGS-21a vector as negative controls. Violacein production by the streak of CV026 in perpendicular to BL21 Star (DE3) expressing the *halI* gene indicated the presence of AHLs.

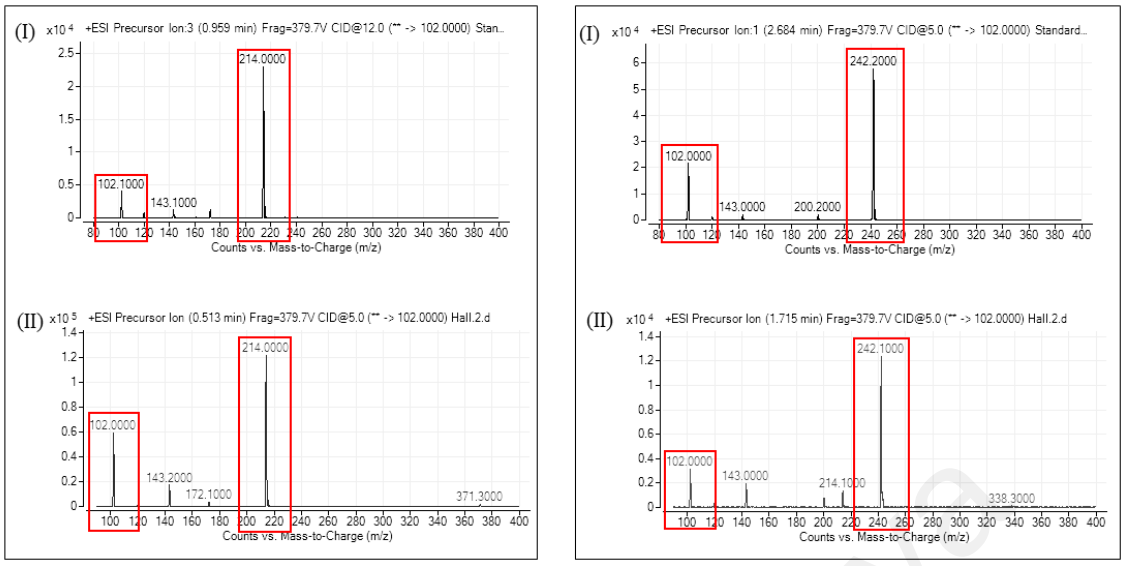

(A) (B)

Figure 4.20: LC-MS/MS analysis of the crude AHL extract from the spent supernatant of *E. coli* BL21 Star (DE3) harbouring pGS-21a-*hallI*. Mass spectra of AHLs extracted from the cell-free supernatant show the presence of (A) precursor ions $3OC_6$-HSL (*m/z* 214) and (B) and $3OC_8$-HSL (*m/z* 242), along with the product ion peaks (*m/z* 102). (I) Mass spectra of synthetic AHL standard; (II) Mass spectra of *E. coli* BL21 Star (DE3) harbouring pGS-21a-*hallI*.

4.6.2 Mutant Construction via λ-Red Recombineering

Two mutants, namely, Δ*hallI*::kanR and Δ*halR*::kanR were constructed using λ Red recombineering technique. In each mutant, either *hallI* or *halR* was replaced with a kanamycin resistance cassette. Verification of the mutants was performed via PCR on colonies picked from LBA plates containing 35 mg/mL kanamycin. The presence of amplification products encompassing the junctions between the flanking regions and a stretch of intragenic region of KanR cassette indicated the success of replacement knockout. The PCR products were then sent for Sanger sequencing to confirm the sequences (Figure 4.21). The Δ*hallI*::kanR mutants, when tested by cross-streaking with biosensor CV026, were found to be unable to induce purple pigment production (Figure 4.22).

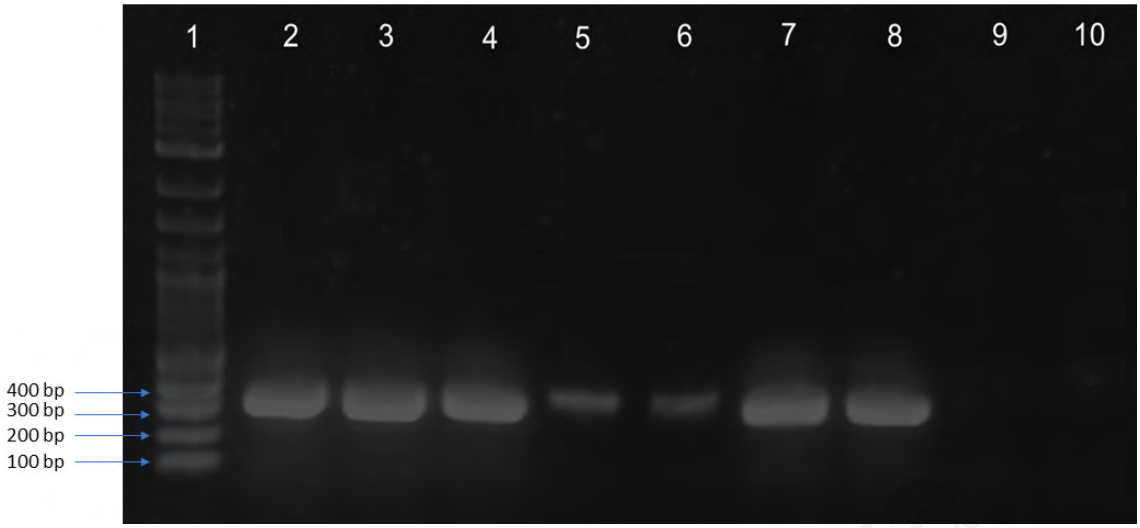

(A)

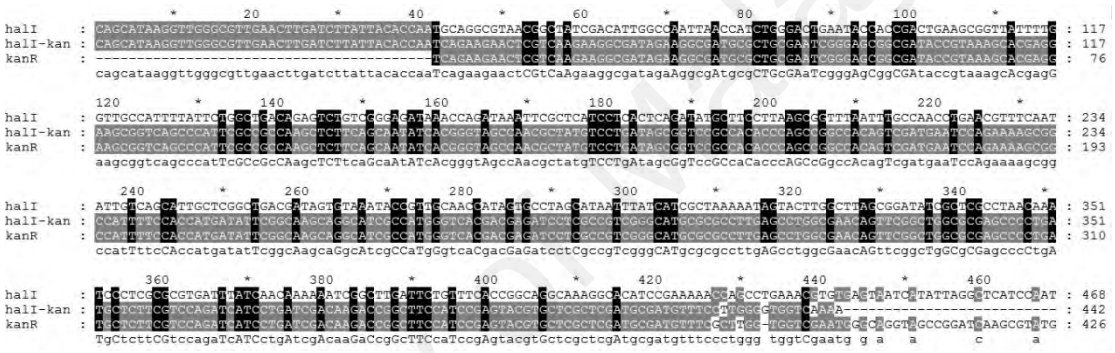

(B)

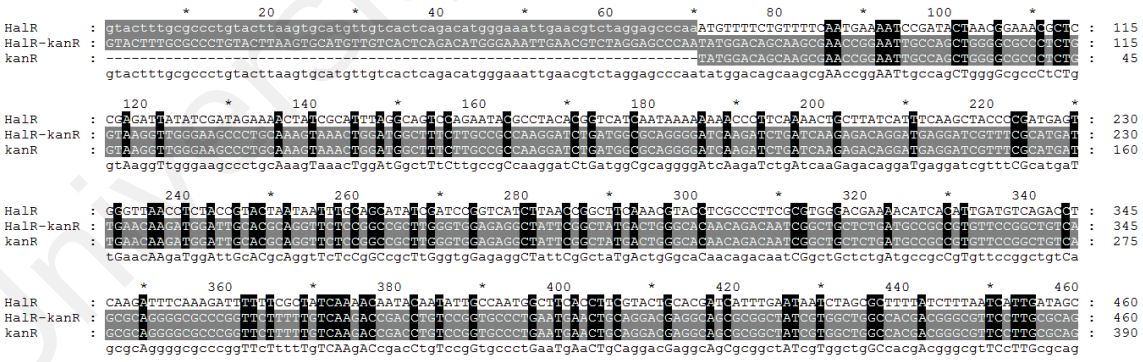

(C)

Figure 4.21: PCR verification of mutants. (A) 1. Ladder. 2, 3, 4. Amplification products encompassing 5'-flanking regions of *halI* and KanR cassette. 5, 6, 7, 8. Amplification products encompassing 5'-flanking regions of *halR* and KanR cassette. 9, 10. Amplification products of WT FB1. (B) Alignment of *halI*-KanR junction from Δ*halI*::KanR mutant to WT *halI* and KanR sequence. (C) Alignment of *halR*-KanR junction from Δ*halR*::KanR mutant to WT *halR* and KanR sequence.

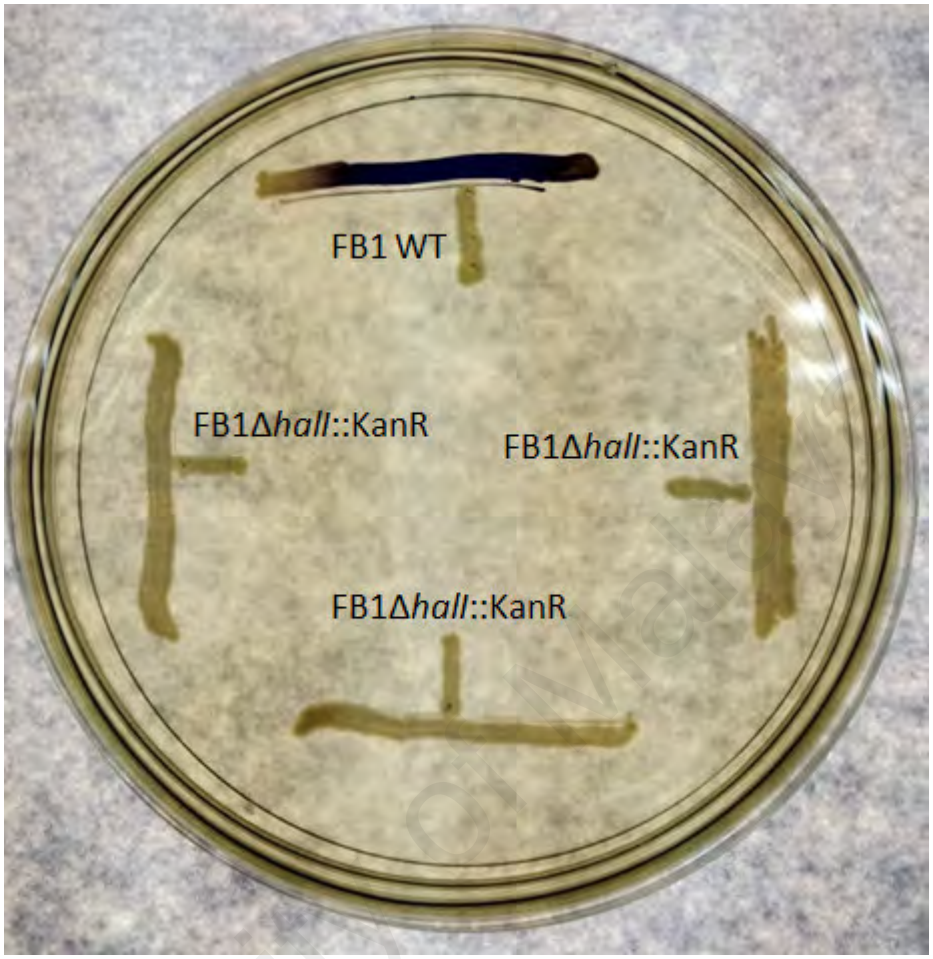

Figure 4.22: CV026 screening for AHL production in mutants with *hallI* gene replaced with a kanamycin resistance cassette (FB1Δ*hallI*::KanR). WT *H. alvei* FB1 (FB1 WT) was used as positive control. No violacein production was induced in horizontal streaks perpendicular to the mutants, indicating loss of the ability of AHL production.

4.7 RNA-Seq

To look into the pattern of global gene expression affected by the HalR regulon, RNA-Seq was performed for the two mutants using FB1 WT as a control. Transcriptomes of each strain were acquired at early and mid-exponential phase (OD_{600} = 0.5 and 1.5, respectively). Three libraries of FB1 WT, Δ*halI*::KanR, and Δ*halR*::KanR were generated for each growth phase, which yielded total reads ranging from 2,124,060 – 4,957,038. The Rockhopper software was able to map 504,685 – 3,344,049 reads to the reference genome. Quality Assessment of the Replicates

Principal component analysis (PCA) plot based on the raw counts showed that, for the samples harvested at OD_{600} 0.5, the three replicates of Δ*halR*::KanR samples were clearly separated from the WT and Δ*halI*::KanR samples along the PC1 axis, which contained as high as 94.662% of the variation; whereas the other two were found to be clustered close to each other on the said axis (Figure 4.23A). For the samples harvested at OD_{600} 1.5, replicates of each samples formed distinct clusters in different quadrants of the plot, with Δ*halI*::KanR mutant forming a more distinct cluster to WT samples along the PC1 axis (79.838% variants) compared with Δ*halR*::KanR samples (Figure 4.23B).

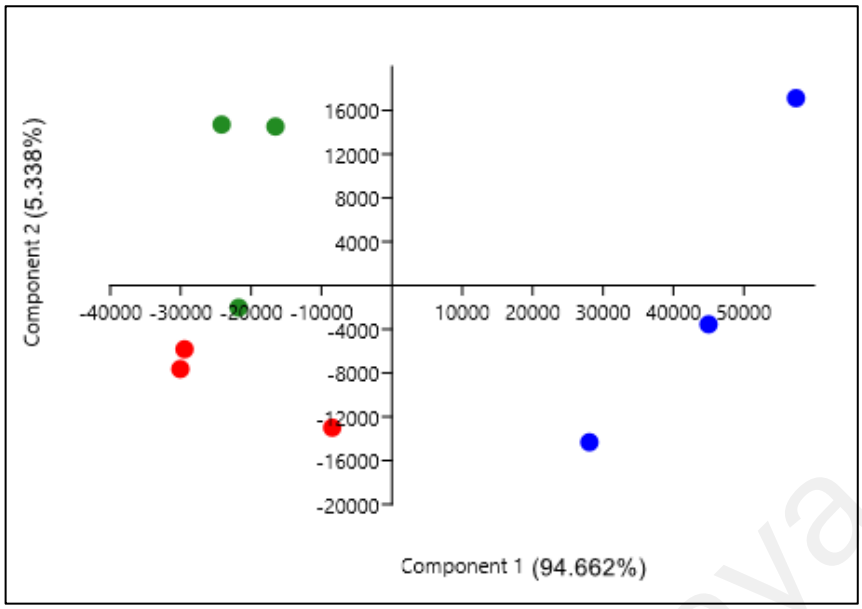

(A)

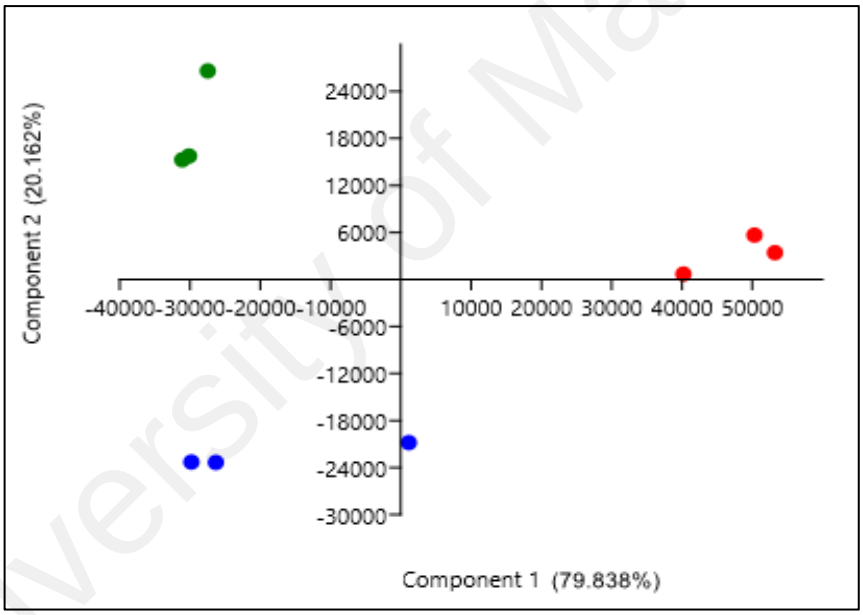

(B)

Figure 4.23: PCA scatter plots showing the variation between samples and persistency between replicates. Triplicates of *H. alvei* FB1 WT, Δ*halI*::KanR, and Δ*halR*::KanR are represented as green, red, and blue dots, respectively. (A) Samples harvested in early exponential phase. (B) Samples harvested in mid-exponential phase.

4.7.1 GO and Pathway Enrichment Analysis of QS-Dependent Genes

GO enrichment analysis was performed on the DEGs to gain an insight into the QS-regulated genes. At the early exponential phase, out of the 511 up-regulated genes in Δ*halR*::KanR mutant, 438 were assigned to 197 GO terms, of which five terms were found to be enriched (q-value < 0.01). As for the 176 down-regulated genes, 114 genes were assigned to 58 terms, of which only two were enriched (Figure 4.27). The GO terms enriched in the up-regulated DEGs included fatty acid biosynthetic process, cytoplasm, ATP binding, RNA binding, and tRNA binding, whereas those among the down-regulated ones were phosphoenolpyruvate-dependent sugar phosphotransferase system and response to stress.

In the mid-exponential phase, 304 out of 371 up-regulated genes in Δ*halR*::KanR mutant were assigned to 180 GO terms, two (phosphoenolpyruvate-dependent sugar phosphotransferase system and cobalamin biosynthesis process) were found to be significantly enriched. On the other hand, among the 263 GO terms accounted for the 317 out of 369 down-regulated genes, only one (TCA cycle) was significantly enriched. In the *halI* mutant, genes with positive and negative FCs were assigned to 132 and 138 GO terms, respectively. None of these terms were found to be enriched at q-value = 0.01.

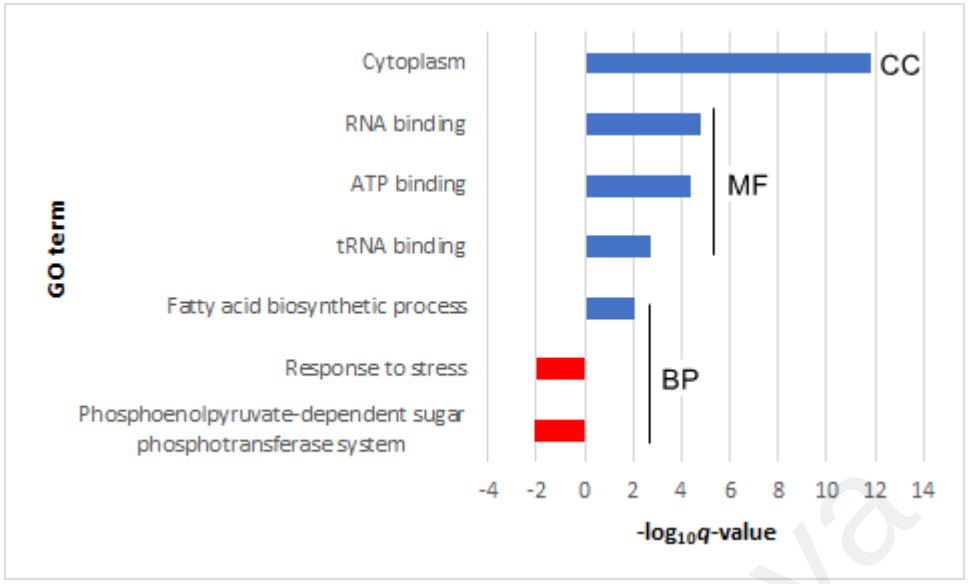

(A)

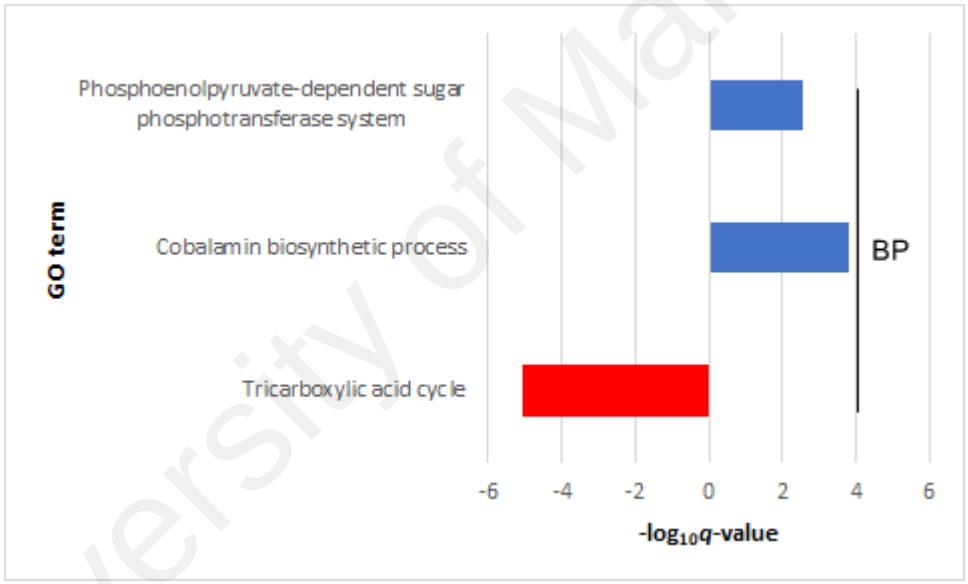

(B)

Figure 4.24: GO enrichment grouping of QS-dependent genes in *halR*::KanR in (A) early exponential phase and (B) mid-exponential phase. CC: Cellular content; MF: Molecular function; BP: Biological process.

DEGs were also mapped into the KEGG pathway database to identify pathways that were significantly enriched in each experimental condition (Figure 4.28). In early exponential phase, the up-regulated genes in Δ*halR*::KanR mutant were assigned to a total of 80 pathways, of which 12 were significantly enriched at the cut-off of *q*-value = 0.01. These pathways were made up primarily of those involved in biosynthesis of molecules and functions that involved nucleotides. On the other hand, six out of 59 pathways to

which the down-regulated genes in Δ*halR*::KanR mutant were assigned were found to be significantly enriched. As in GO ontology, phosphotransferase system (PTS) was involved, along with several other pathways involved in carbohydrate metabolism.

In mid-exponential phase, down-regulated pathways in Δ*halR*::KanR mutant far outnumbered the up-regulated ones. A total of 30 out of 80 pathways were found to be significantly enriched. The affected pathways were mostly responsible in amino acid metabolism. Δ*halI*::KanR mutant in the same growth phase accounted for a much smaller number of enriched pathways compared with Δ*halR*::KanR, but they were still dominated by down-regulated genes. Most of these pathways overlapped those affected in its *halR* counterpart, except for beta-lactam resistance.

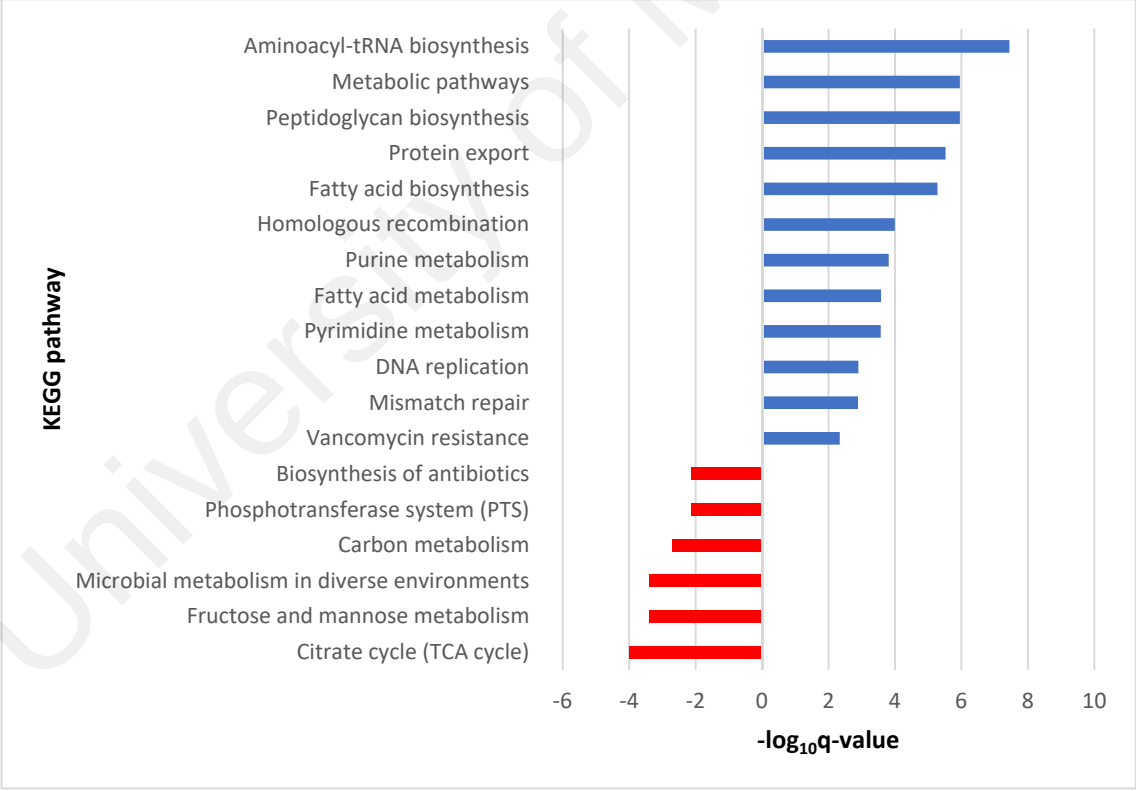

(A)

Figure 4.25: KEGG pathways enriched in (A) Δ*halR*::KanR mutant in early exponential phase, (B) Δ*halR*::KanR mutant in mid-exponential phase, and (C) Δ*halI*::KanR mutant in mid-exponential phase.

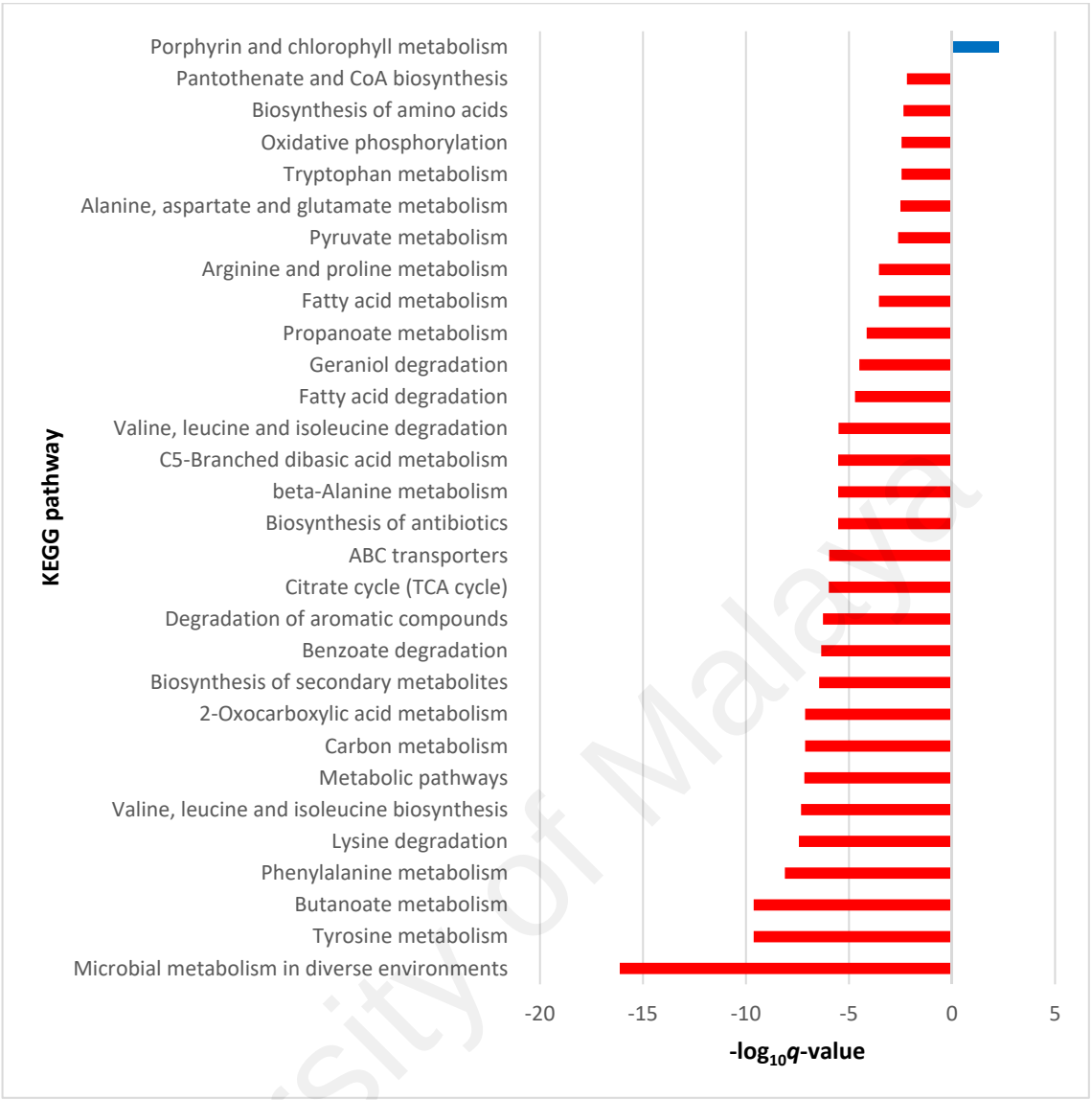

(B)

Figure 4.28, continued.

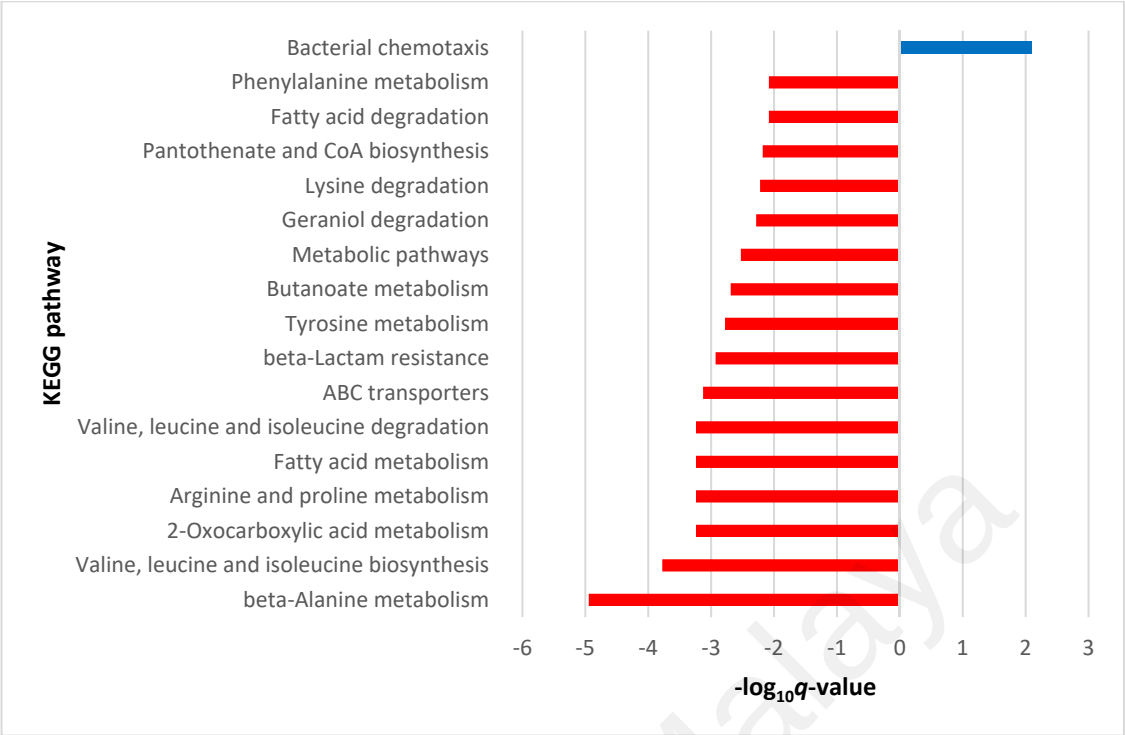

(C)

Figure 4.25, continued.

4.7.2 Transcriptomic Analysis of QS Mutants

No significant differential expression ($\log_2$ fold change [FC] > 1 or < -1) was observed in Δ*hall*::KanR mutant at a *q*-value of 0.01, aside from *hall*. A total of 687 genes were found to be differentially expressed in Δ*halR*::KanR mutant, of which 511 were up-regulated while 176 were down-regulated. The distribution of DEGs was demonstrated in the form of MA plots (Figure 4.24).

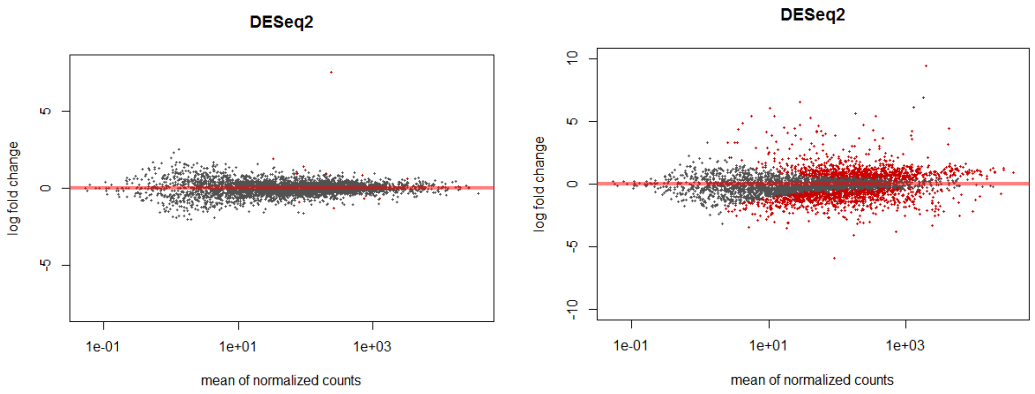

(A) (B)

Figure 4.26: MA plots showing the distribution of DEGs in (A) Δ*halI*::KanR and (B) Δ*halR*::KanR against WT in early exponential phase. Grey dots: genes with $\log_2$ FCs below 1 and above -1; red dots: genes with $\log_2$ FCs above 1 and below -1.

A total of 825 and 740 genes were found to be differentially expressed in Δ*halI*::KanR and Δ*halR*::KanR mutant, respectively. In the former, 392 were up-regulated while 433 were down-regulated; whereas in the latter, 371 showed positive fold-changes against the WT strain while 369 showed negative. The distribution of DEGs was demonstrated in the form of MA plots (Figure 4.25), and the overlapping genes between both mutants are shown in Venn diagrams (Figure 4.26)

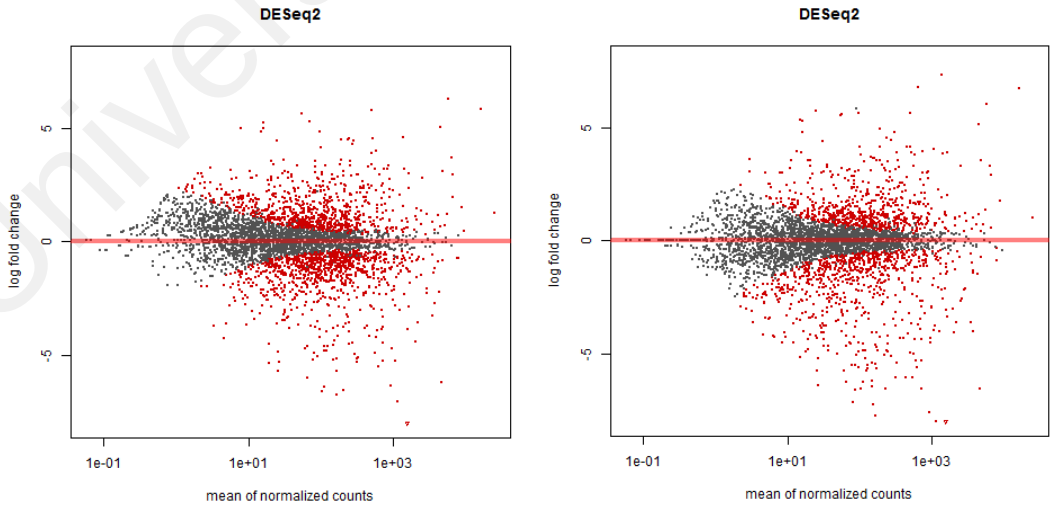

(A) (B)

Figure 4.27: MA plots showing the distribution of DEGs in (A) Δ*halI*::KanR and (B) Δ*halR*::KanR against WT in mid-exponential phase. Grey dots: genes that show $\log_2$ FCs below 1 and above -1; red dots: genes that show $\log_2$ FCs above 1 and below -1.

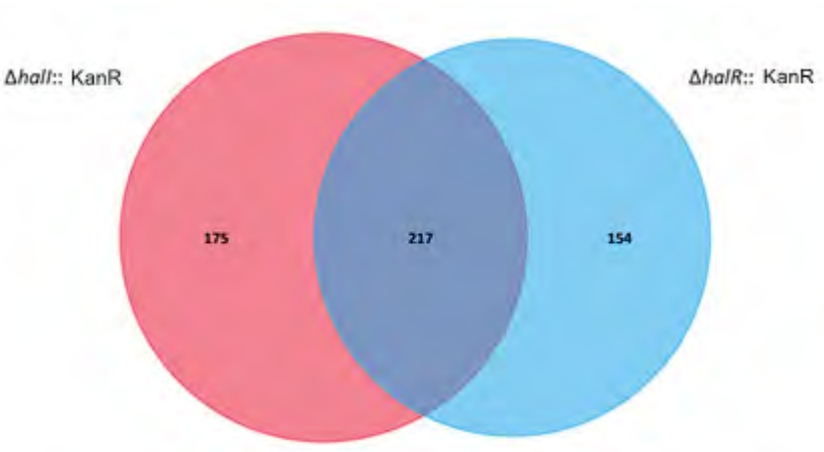

(A)

(B)

Figure 4.28: Venn diagram showing the overlapping DEGs between Δ*halI*::KanR and Δ*halR*::KanR mutants in mid-exponential phase. (A) A total of 217 up-regulated genes ($\log_2$ FC > 1, *q*-value < 0.01) are shared between Δ*halI*::KanR (red circle) and Δ*halR*::KanR (blue circle), which contain 175 and 154 unique up-regulated genes, respectively, (B) A total of 273 down-regulated genes ($\log_2$ FC < -1, *q*-value < 0.01) are shared between Δ*halI*::KanR (red circle) and Δ*halR*::KanR (blue circle), which contain 160 and 96 unique down-regulated genes, respectively.

Genes with the highest FC in each experimental condition were listed in Tables 4.6 – 4.11. For Δ*halR*::KanR mutant in exponential phase, both up- and down-regulated gene lists were topped by genes involved in Carbohydrate transport and metabolism. On the list for up-regulated genes, genes involved in this category were mainly those involved with ribose metabolism, whereas in the case of the down-regulated gene list, genes involved in mannitol, maltose and galactose uptake were among those with the highest FCs. In mid-exponential phase, genes involved in Amino acid transport and metabolism

were most abundant in the lists of both mutants. Interestingly, genes involved with maltose transport, for instance, maltoporin, which were down-regulated in the early exponential phase, were found to be up-regulated in the mid-exponential phase.

Table 4.6: List of 20 most up-regulated genes in Δ*halR*::KanR mutant in early exponential phase.

Locus Tag	Annotation	COG	Log_2FC	*q*-value
AT03_RS 00525	Ribose ABC transporter ATP-binding protein RbsA	Carbohydrate transport and metabolism	945.87	<0.01
AT03_RS 00530	D-ribose pyranase	Carbohydrate transport and metabolism	135.02	<0.01
AT03_RS 01140	Replication protein B	Nil	98.52	<0.01
AT03_RS 00520	Ribose ABC transporter permease	Carbohydrate transport and metabolism	78.70	<0.01
AT03_RS 01155	Regulatory protein	Nil	48.43	<0.01
AT03_RS 01065	Terminase	Nil	37.00	<0.01
AT03_RS 00505	Transcriptional regulator RbsR	Transcription	32.63	<0.01
AT03_RS 00990	Major tail tube protein	General function prediction only	31.23	<0.01
AT03_RS 04040	TonB-dependent receptor	Inorganic ion transport and metabolism	26.46	<0.01
AT03_RS 10685	Hemin transporter	Inorganic ion transport and metabolism	25.68	<0.01
AT03_RS 00515	D-ribose ABC transporter substrate-binding protein	Carbohydrate transport and metabolism	25.62	<0.01
AT03_RS 10710	Putative heme utilization radical SAM enzyme HutW	Coenzyme transport and metabolism	24.86	<0.01
AT03_RS 01075	Capsid scaffolding protein	Nil	21.90	<0.01
AT03_RS 14005	Catecholate siderophore receptor CirA	Inorganic ion transport and metabolism	19.45	<0.01
AT03_RS 00510	Ribokinase	Carbohydrate transport and metabolism	18.39	<0.01
AT03_RS 10230	Transporter	Inorganic ion transport and metabolism	17.25	<0.01
AT03_RS 08320	Cold-shock protein	Transcription	15.42	<0.01
AT03_RS 16895	Cold-shock protein	Transcription	11.95	<0.01
AT03_RS 14020	Iron ABC transporter substrate-binding protein	Inorganic ion transport and metabolism	11.39	<0.01
AT03_RS 14270	ATP-dependent RNA helicase RhlE	Replication, recombination and repair; Transcription; Translation, ribosomal structure and biogenesis	11.29	<0.01

Table 4.7: List of 20 most down-regulated genes in Δ*halR*::KanR mutant in early exponential phase.

Locus Tag	Annotation	COG	Log_2FC	*q*-value
AT03_RS 12355	LuxR family transcriptional regulator	Transcription	-6.65	<0.01
AT03_RS 16550	Cysteine synthase	Amino acid transport and metabolism	-4.39	<0.01
AT03_RS 00820	PTS mannitol transporter subunit IICBA	Carbohydrate transport and metabolism	-3.90	<0.01
AT03_RS 14820	PTS mannitol transporter subunit IIB	Carbohydrate transport and metabolism	-3.70	<0.01
AT03_RS 20910	DsdX permease	Carbohydrate transport and metabolism; Amino acid transport and metabolism	-3.66	<0.01
AT03_RS 19975	Sigma-54-dependent Fis family transcriptional regulator	Transcription; Signal transduction mechanisms	-3.32	<0.01
AT03_RS 07480	Galactose/methyl galactoside ABC transporter ATP-binding protein MglA	Carbohydrate transport and metabolism	-3.27	<0.01
AT03_RS 02730	Ornithine decarboxylase	Amino acid transport and metabolism	-3.22	<0.01
AT03_RS 14825	PTS ascorbate transporter subunit IIA	Carbohydrate transport and metabolism; Signal transduction mechanisms	-3.22	<0.01
AT03_RS 00815	Mannitol-1-phosphate 5-dehydrogenase	Carbohydrate transport and metabolism	-3.13	<0.01
AT03_RS 19940	Hydroxylase	Nil	-3.03	<0.01
AT03_RS 18510	N-acetylneuraminate lyase	Amino acid transport and metabolism; Cell wall/membrane/envelope biogenesis	-2.81	<0.01
AT03_RS 07475	Galactose ABC transporter substrate-binding protein	Carbohydrate transport and metabolism	-2.72	<0.01
AT03_RS 21335	Serine/threonine dehydratase	Amino acid transport and metabolism	-2.55	<0.01
AT03_RS 02545	Maltoporin	Carbohydrate transport and metabolism	-2.48	<0.01
AT03_RS 02530	Maltose transporter membrane protein	Carbohydrate transport and metabolism	-2.47	<0.01
AT03_RS 18240	Membrane protein	Nil	-2.44	<0.01
AT03_RS 06090	Urocanate hydratase	Amino acid transport and metabolism	-2.41	<0.01
AT03_RS 13030	Selenium-binding protein	Nil	-2.38	<0.01
AT03_RS 02535	Maltose ABC transporter substrate-binding protein MalE	Carbohydrate transport and metabolism	-2.37	<0.01

Table 4.8: List of 20 most up-regulated genes in Δ*halI*::KanR mutant in mid-exponential phase.

Locus Tag	Annotation	COG	Log_2FC	*q*-value
AT03_RS 02730	Ornithine decarboxylase	Amino acid transport and metabolism	6.52	<0.01
AT03_RS 09475	Oxalyl-CoA decarboxylase	Amino acid transport and metabolism; Coenzyme transport and metabolism	6.36	<0.01
AT03_RS 02735	Putrescine-ornithine antiporter	Amino acid transport and metabolism	6.07	<0.01
AT03_RS 17370	Lysine decarboxylase LdcC	Amino acid transport and metabolism	6.05	<0.01
AT03_RS 17365	Peptide permease	Amino acid transport and metabolism	5.75	<0.01
AT03_RS 17375	Lysine/cadaverine antiporter	Amino acid transport and metabolism	5.23	<0.01
AT03_RS 02545	Maltoporin	Carbohydrate transport and metabolism	4.96	<0.01
AT03_RS 20515	Nitrite reductase large subunit	Energy production and conversion	4.88	<0.01
AT03_RS 04205	Glycine radical enzyme activase	Posttranslational modification, protein turnover, chaperones	4.81	<0.01
AT03_RS 04645	Formate dehydrogenase subunit alpha	General function prediction only	4.79	<0.01
AT03_RS 08130	Hydroxylamine reductase	Energy production and conversion	4.77	<0.01
AT03_RS 09495	Arginine decarboxylase	Amino acid transport and metabolism	4.73	<0.01
AT03_RS 14605	Hydrogenase 2 b cytochrome subunit	Energy production and conversion	4.52	<0.01
AT03_RS 08225	Dimethylsulfoxide reductase	General function prediction only	4.49	<0.01
AT03_RS 09480	Formyl-CoA transferase	Energy production and conversion	4.36	<0.01
AT03_RS 21325	Propionate kinase	Energy production and conversion	4.21	<0.01
AT03_RS 08220	Dimethylsulfoxide reductase, chain B	Energy production and conversion	3.91	<0.01
AT03_RS 21335	Serine/threonine dehydratase	Amino acid transport and metabolism	3.86	<0.01
AT03_RS 15770	Cytochrome c-type protein NapC	Energy production and conversion	3.72	<0.01
AT03_RS 15785	Ferredoxin-type protein NapG	Energy production and conversion	3.61	<0.01

Table 4.9: List of 20 most down-regulated genes in Δ*halI*::KanR mutant in mid-exponential phase.

Locus Tag	Annotation	COG	Log_2FC	*q*-value
AT03_RS 05225	Gamma-aminobutyraldehyde dehydrogenase	Energy production and conversion	-7.29	<0.01
AT03_RS 05230	Spermidine/putrescine ABC transporter substrate-binding protein	Amino acid transport and metabolism	-7.18	<0.01
AT03_RS 05220	LysR family transcriptional regulator	Transcription	-6.86	<0.01
AT03_RS 12360	Acyl-homoserine-lactone synthase	Signal transduction mechanisms, Secondary metabolites biosynthesis, transport and catabolism	-6.64	<0.01
AT03_RS 07360	Indolepyruvate decarboxylase	Carbohydrate transport and metabolism; Coenzyme transport and metabolism; General function prediction only	-6.27	<0.01
AT03_RS 21240	Peptide transporter	Amino acid transport and metabolism; Inorganic ion transport and metabolism	-6.22	<0.01
AT03_RS 21145	E3 ubiquitin--protein ligase	Nil	-6.06	<0.01
AT03_RS 05245	Spermidine/putrescine ABC transporter permease	Amino acid transport and metabolism	-5.52	<0.01
AT03_RS 14980	Glyoxalase	Nil	-5.51	<0.01
AT03_RS 02995	Lysine/cadaverine antiporter	Amino acid transport and metabolism	-5.35	<0.01
AT03_RS 08830	Alpha-amylase	Carbohydrate transport and metabolism	-5.35	<0.01
AT03_RS 05235	Polyamine ABC transporter ATP-binding protein	Amino acid transport and metabolism	-5.34	<0.01
AT03_RS 05240	Spermidine/putrescine ABC transporter permease	Amino acid transport and metabolism	-5.32	<0.01
AT03_RS 09960	SpoVR family protein	Function unknown	-5.30	<0.01
AT03_RS 21245	Peptide transporter	Amino acid transport and metabolism; Inorganic ion transport and metabolism	-5.28	<0.01
AT03_RS 06585	Amino acid transporter	Amino acid transport and metabolism; Signal transduction mechanisms	-5.17	<0.01
AT03_RS 21235	Peptide ABC transporter ATP-binding protein	Amino acid transport and metabolism; Inorganic ion transport and metabolism	-5.04	<0.01
AT03_RS 14880	Histidine ABC transporter substrate-binding protein HisJ	Amino acid transport and metabolism; Signal transduction mechanisms	-4.98	<0.01
AT03_RS 11765	Transcriptional regulator	Translation, ribosomal structure and biogenesis	-4.86	<0.01
AT03_RS 02990	Lysine decarboxylase LdcC	Amino acid transport and metabolism	-4.86	<0.01

Table 4.10: List of 20 most up-regulated genes in Δ*halR*::KanR mutant in mid-exponential phase.

Locus Tag	Annotation	COG	Log_2FC	*q*-value
AT03_RS 02545	Maltoporin	Carbohydrate transport and metabolism	7.57	<0.01
AT03_RS 02550	Maltose operon protein MalM	Nil	6.97	<0.01
AT03_RS 17370	Lysine decarboxylase LdcC	Amino acid transport and metabolism	6.80	<0.01
AT03_RS 17365	Peptide permease	Amino acid transport and metabolism	6.43	<0.01
AT03_RS 02730	Ornithine decarboxylase	Amino acid transport and metabolism	6.14	<0.01
AT03_RS 02525	Maltose transporter permease	Carbohydrate transport and metabolism	5.94	<0.01
AT03_RS 02735	Putrescine-ornithine antiporter	Amino acid transport and metabolism	5.72	<0.01
AT03_RS 17375	Lysine/cadaverine antiporter	Amino acid transport and metabolism	5.16	<0.01
AT03_RS 04645	Formate dehydrogenase subunit alpha	General function prediction only	5.07	<0.01
AT03_RS 02530	Maltose transporter membrane protein	Carbohydrate transport and metabolism	5.07	<0.01
AT03_RS 04205	Glycine radical enzyme activase	Posttranslational modification, protein turnover, chaperones	4.69	<0.01
AT03_RS 14605	Hydrogenase 2 b cytochrome subunit	Energy production and conversion	4.45	<0.01
AT03_RS 08225	Dimethylsulfoxide reductase	General function prediction only	4.30	<0.01
AT03_RS 08220	Dimethylsulfoxide reductase, chain B	Energy production and conversion	4.26	<0.01
AT03_RS 09625	Metal transporter	Inorganic ion transport and metabolism	4.23	<0.01
AT03_RS 19580	Glucohydrolase	Carbohydrate transport and metabolism	4.22	<0.01
AT03_RS 19310	Electron transfer flavoprotein	Energy production and conversion	4.13	<0.01
AT03_RS 14600	Hydrogenase 2 large subunit	Energy production and conversion	3.99	<0.01
AT03_RS 02535	Maltose ABC transporter substrate-binding protein MalE	Carbohydrate transport and metabolism	3.95	<0.01
AT03_RS 08130	Hydroxylamine reductase	Energy production and conversion	3.95	<0.01

Table 4.11: List of 20 most down-regulated genes in Δ*halR*::KanR mutant in mid-exponential phase.

Locus Tag	Annotation	COG	Log_2FC	*q*-value
AT03_RS 05230	Spermidine/putrescine ABC transporter substrate-binding protein	Amino acid transport and metabolism	-8.18	<0.01
AT03_RS 07360	Indolepyruvate decarboxylase	Carbohydrate transport and metabolism; Coenzyme transport and metabolism; General function prediction only	-7.59	<0.01
AT03_RS 05995	Phenylacetic acid degradation protein PaaD	Secondary metabolites biosynthesis, transport and catabolism	-7.35	<0.01
AT03_RS 05225	Gamma-aminobutyraldehyde dehydrogenase	Energy production and conversion	-7.29	<0.01
AT03_RS 21230	Dipeptide ABC transporter ATP-binding protein	Amino acid transport and metabolism	-7.27	<0.01
AT03_RS 21240	Peptide transporter	Multiple classes	-7.22	<0.01
AT03_RS 06020	Phenylacetate-CoA oxygenase subunit PaaJ	General function prediction only	-7.04	<0.01
AT03_RS 05220	LysR family transcriptional regulator	Transcription	-6.86	<0.01
AT03_RS 18550	NAD-dependent succinate-semialdehyde dehydrogenase	Energy production and conversion	-6.86	<0.01
AT03_RS 18545	4-aminobutyrate aminotransferase	Amino acid transport and metabolism	-6.84	<0.01
AT03_RS 06035	Phenylacetate-CoA oxygenase subunit PaaA	Function unknown	-6.82	<0.01
AT03_RS 06585	Amino acid transporter	Amino acid transport and metabolism; Signal transduction mechanisms	-6.79	<0.01
AT03_RS 06025	Phenylacetic acid degradation protein	Function unknown	-6.76	<0.01
AT03_RS 21145	E3 ubiquitin--protein ligase	Nil	-6.64	<0.01
AT03_RS 18560	Carbon starvation induced protein	Nil	-6.63	<0.01
AT03_RS 09960	SpoVR family protein	Function unknown	-6.62	<0.01
AT03_RS 06015	Phenylacetic acid degradation protein	Energy production and conversion	-6.52	<0.01
AT03_RS 06030	Phenylacetate-CoA oxygenase subunit PaaB	Secondary metabolites biosynthesis, transport and catabolism	-6.37	<0.01
AT03_RS 21235	Peptide ABC transporter ATP-binding protein	Amino acid transport and metabolism; Inorganic ion transport and metabolism	-6.19	<0.01

4.7.3 Validation of RNA-Seq Data by qPCR

To validate the RNA-Seq results, six genes were randomLy chosen for qPCR. The log_2 FCs of qPCR were calculated and plotted against that of RNA-Seq (Figure 4.29). The correlation coefficients were all found to be above 0.99, indicating that the results obtained were reliable.

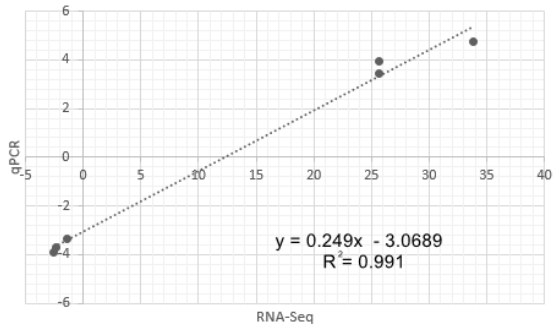

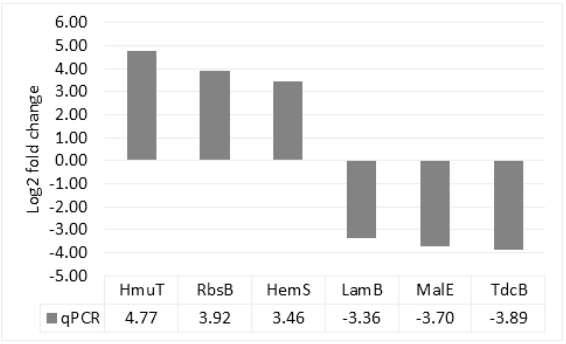

(A) (B)

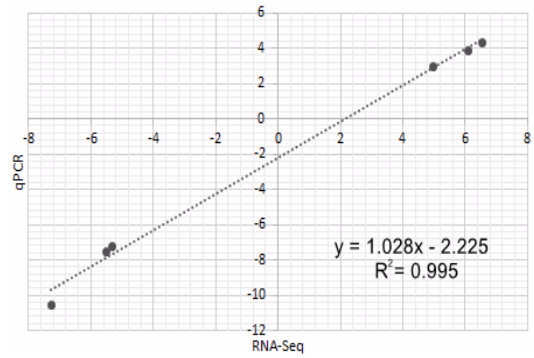

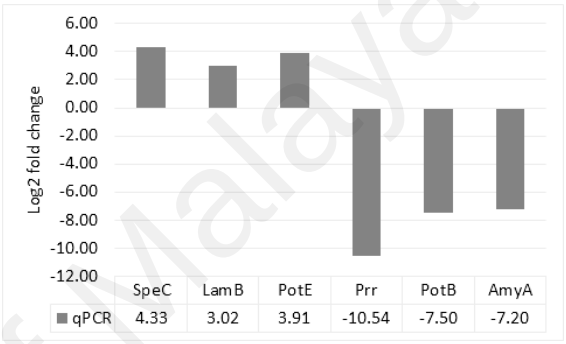

(C) (D)

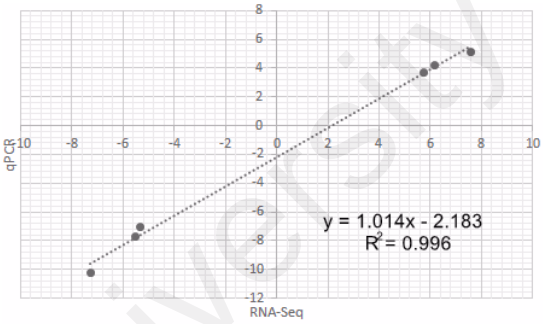

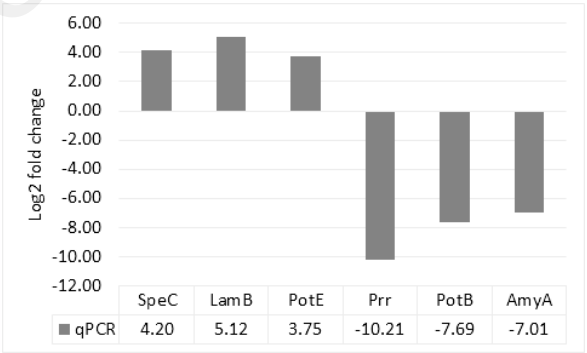

(E) (F)

Figure 4.29: qPCR validation of RNA-Seq results. Each $\log_2$ ratio of FCs calculated from qPCR was compared with that of the RNA-seq data. (A) Correlation of the FCs between RNA-seq (x-axis) and qPCR (y-axis) of Δ*halR*::KanR in the early exponential phase. (B) Log_2 FCs of Δ*halR*::KanR in the early exponential phase. (C) Correlation of FCs between RNA-seq (x-axis) and qPCR (y-axis) of Δ*halR*::KanR in the mid-exponential phase. (D) Log_2 FCs of Δ*halR*::KanR in the mid-exponential phase. (E) Correlation of foldchanges between RNA-seq (x-axis) and qPCR (y-axis) of Δ*halI*::KanR in the mid-exponential phase. (F) Log_2 FCs of Δ*halI*::KanR in the mid-exponential phase.

4.8 Biolog Phenotype Microarrays (PMs)

4.8.1 Carbon Source Utilisation

An overview of phenotypic changes in carbon source utilisation for both mutants in comparison to WT is presented as heatmaps in Figure 4.30. Of all 190 substrates tested, only three wells showed significant changes when incubated with Δ*halR*::KanR mutant.

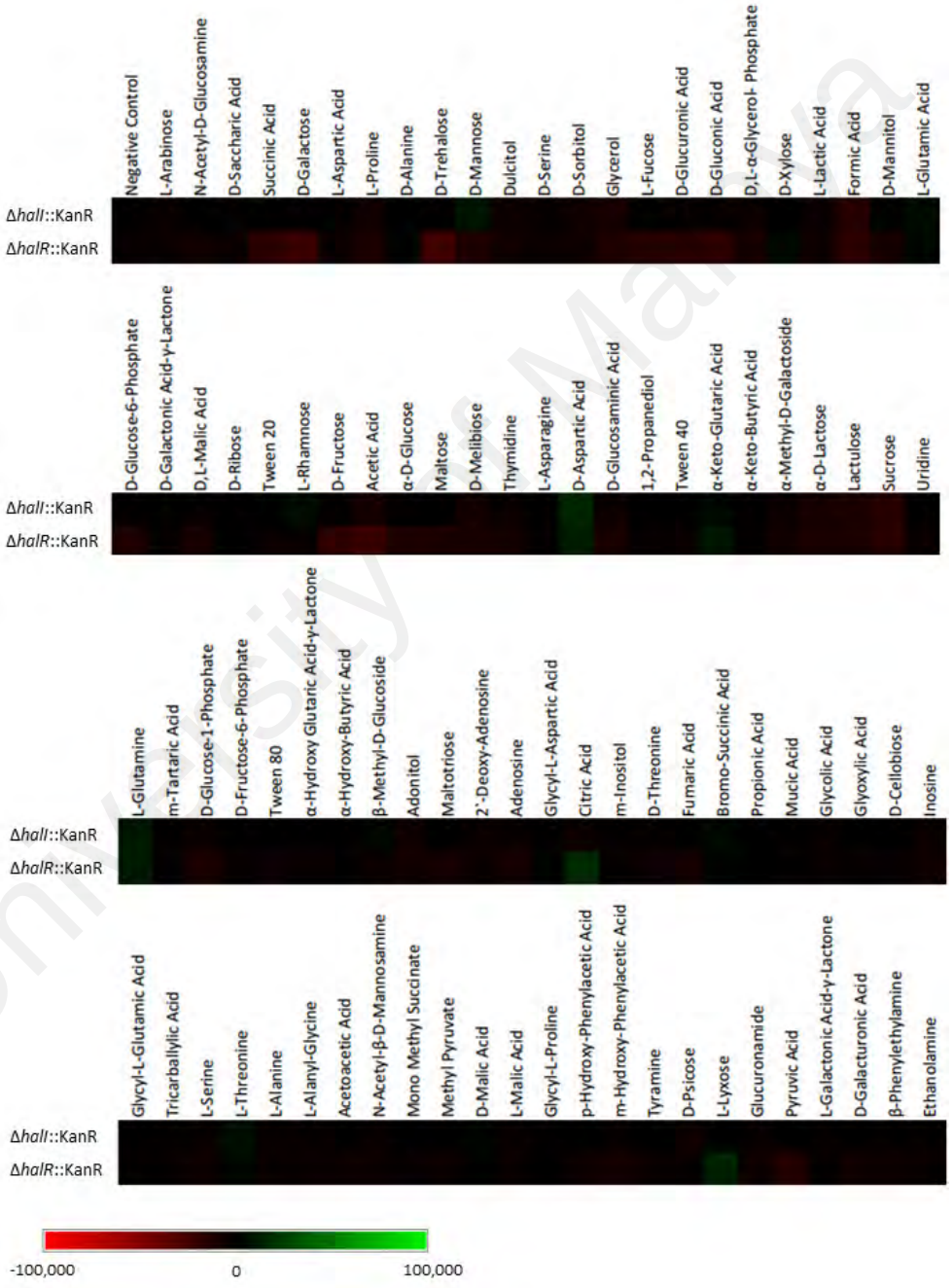

Figure 4.30: Heatmap showing the changes in respiratory kinetics in both Δ*halI*::KanR and Δ*halR*::KanR mutants when utilizing each substrate as the sole carbon sources. The colour scheme represents the magnitude of positive and negative changes in phenotypes.

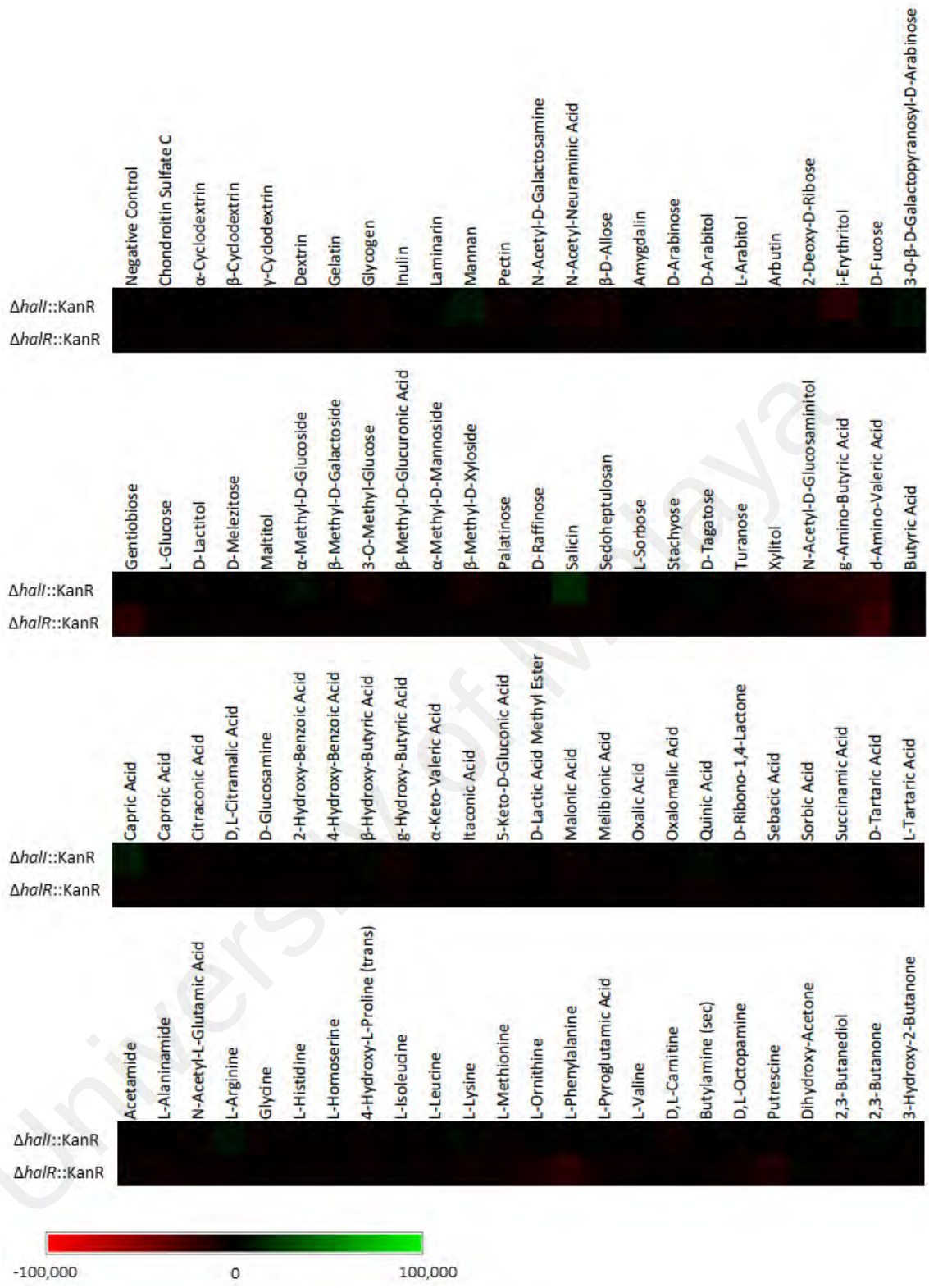

Figure 4.30, continued.

Out of all 190 substrates tested, Δ*halI*::KanR showed no significant changes in the ability to utilise any of these substrates, whereas significant decrease (-21,992, -23,155, and -21,083) was observed in Δ*halR*::KanR in D-galactose, D-trehalose, and acetic acid utilisation (Figure 4.31), respectively. In D-galactose and D-trehalose, the curves shared a similar biphasic pattern, whereby the respiratory rates of Δ*halI*::KanR started off slightly higher than WT at the beginning, and later converged with the curves of WT upon a time point from which the respiratory rates increased. Δ*halR*::KanR showed a similar pattern of changes albeit at much lower values. Such changes in respiratory rate were not observed in the kinetic curves obtained from wells containing acetic acid, in which the Δ*halI*::KanR curve was slightly lower than the WT curve throughout the time points. In all cases, Δ*halR*::KanR curves remained much lower than as compared to the WT and Δ*halI*::KanR.

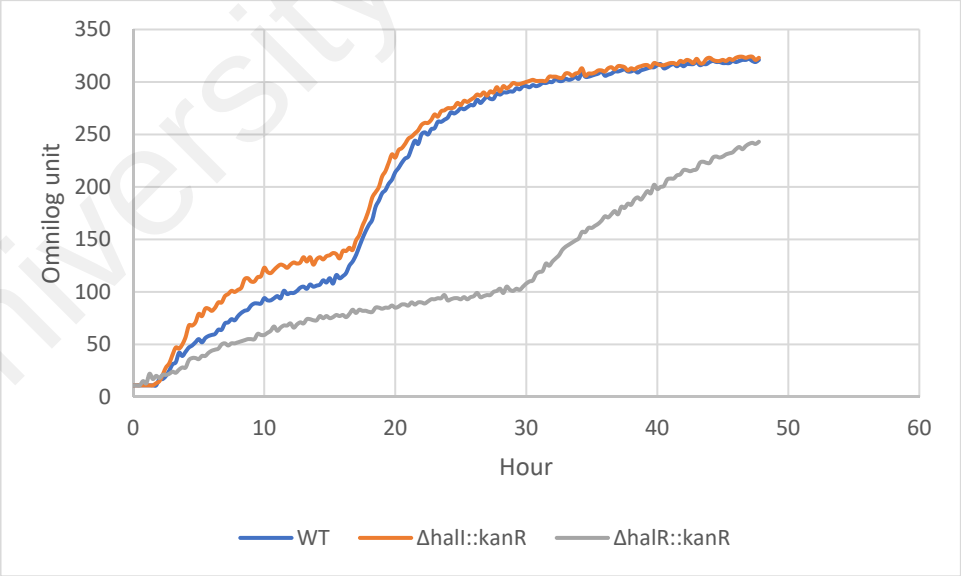

(A)

Figure 4.31: Respiratory curve of WT and two QS mutant strains (Δ*halI*::KanR and Δ*halR*::KanR) of *H. alvei* FB1 when utilising different carbon sources. (A) D-Galactose. (B) D-Trehalose. (C) Acetic acid.

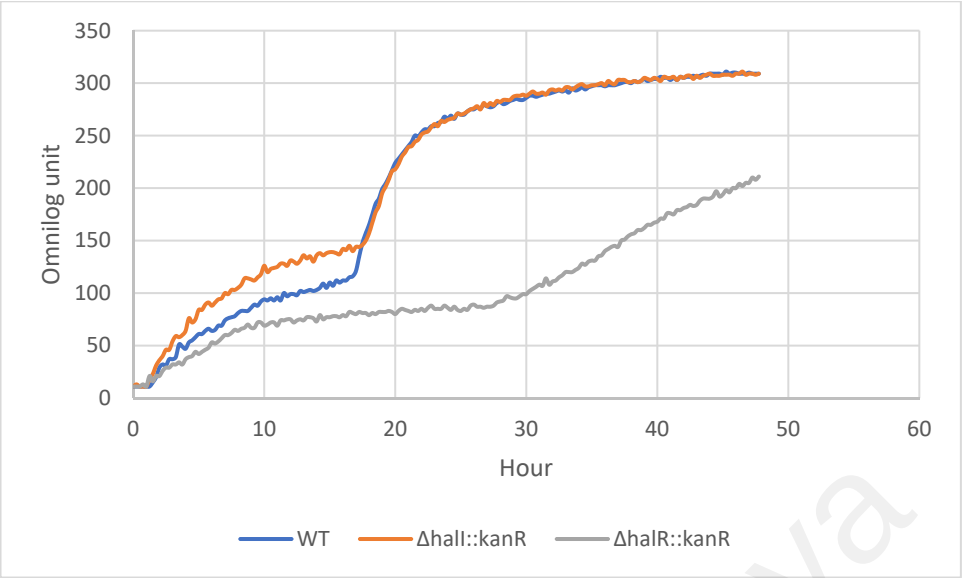

(B)

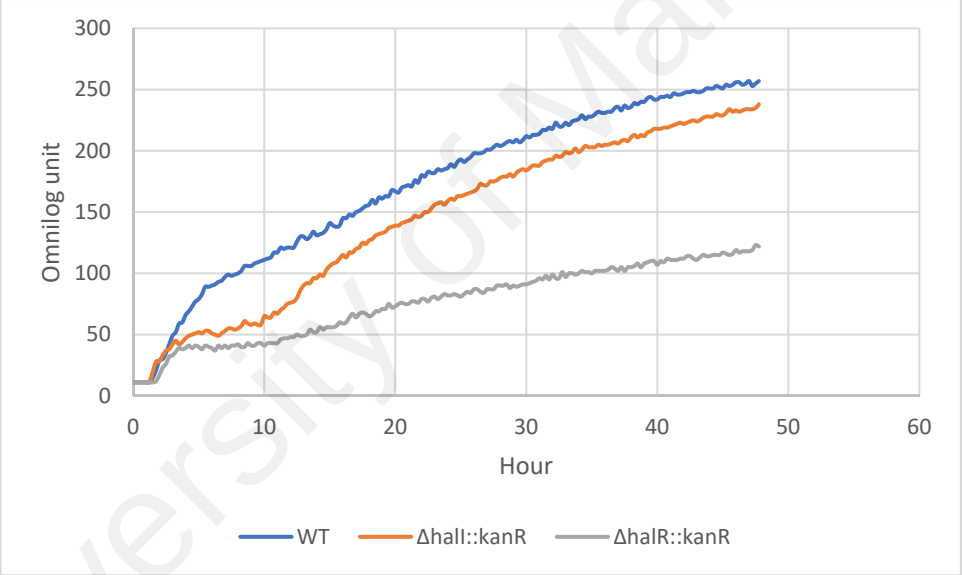

(C)

Figure 4.31, continued.

4.8.2 Antibiotic Resistance

Changes in sensitivity of Δ*halI*::KanR and Δ*halR*::KanR mutants were tested against a total of 67 antibiotics of seven classes using Biolog PM assays. An overview of the results is displayed in the form of heatmaps in Figure 4.32. Significant changes in antibiotic resistance are summarised in Table 4.12 according to classes and mode of actions. Significant changes in sensitivity were observed towards 23 antibiotics. In most cases, Δ*halR*::KanR mutant showed reduced resistance except for two aminoglycosides (Paromomycin and Tobramycin) and Ofloxacin. Significantly reduced resistance was observed in seven lactam antibiotics in Δ*halR*::KanR, which was not observed in Δ*halI*::KanR.

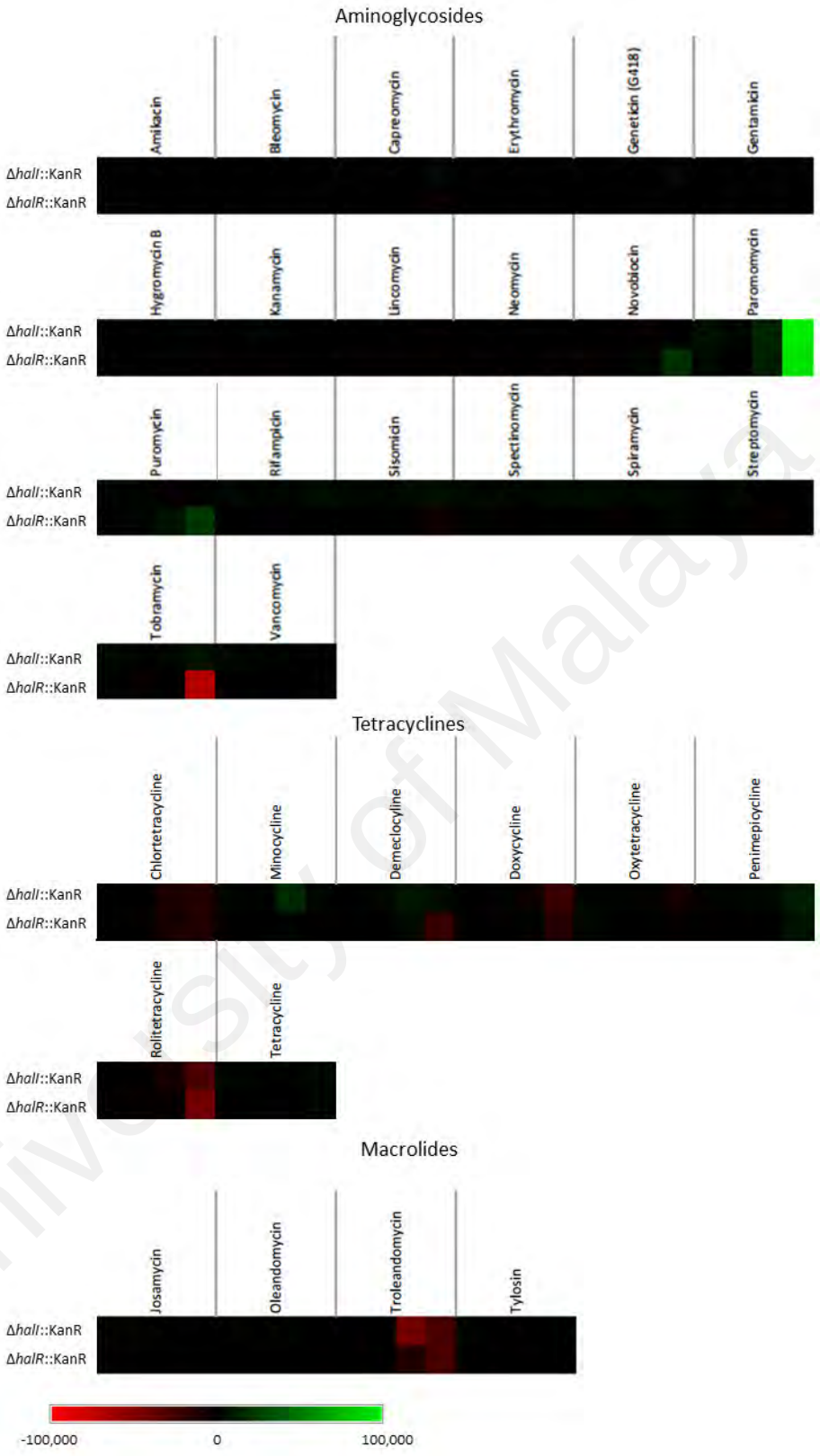

Figure 4.32: Heatmaps displaying changes in resistance to antibiotics in Δ*halI*::KanR and Δ*halR*::KanR mutants compared to WT. Wells are sorted according to classes of antibiotics. Each antibiotic was tested on four different concentrations (from left to right: lowest to highest). The colour scheme represents the magnitude of positive and negative changes in phenotypes. Overall, decrease in resistance (red) was observed in all classes, except for individual antibiotics, such as Paromomycin, Carbenicillin, Ofloxacin, and Pipemidic acid.

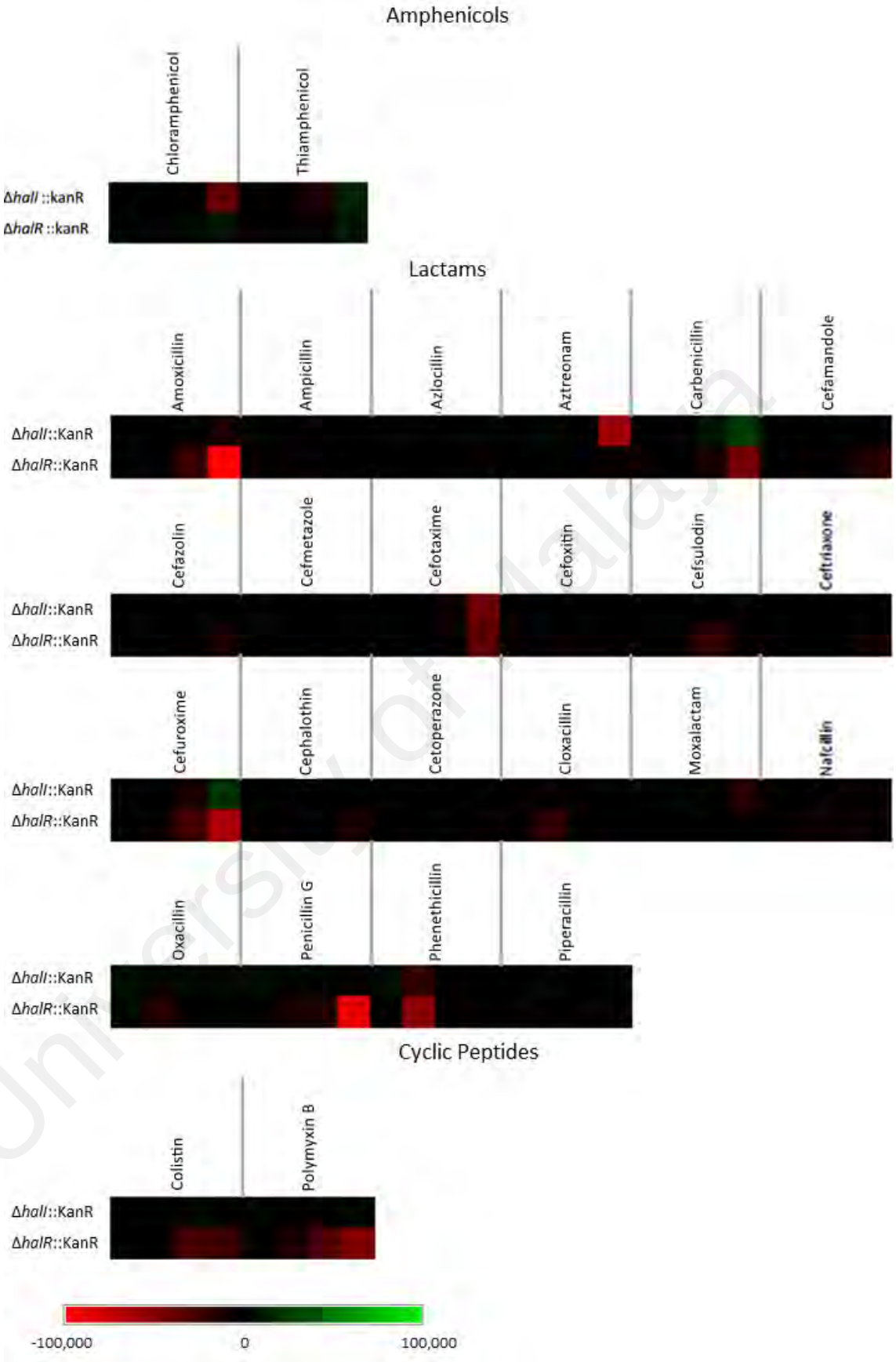

Figure 4.32, continued.

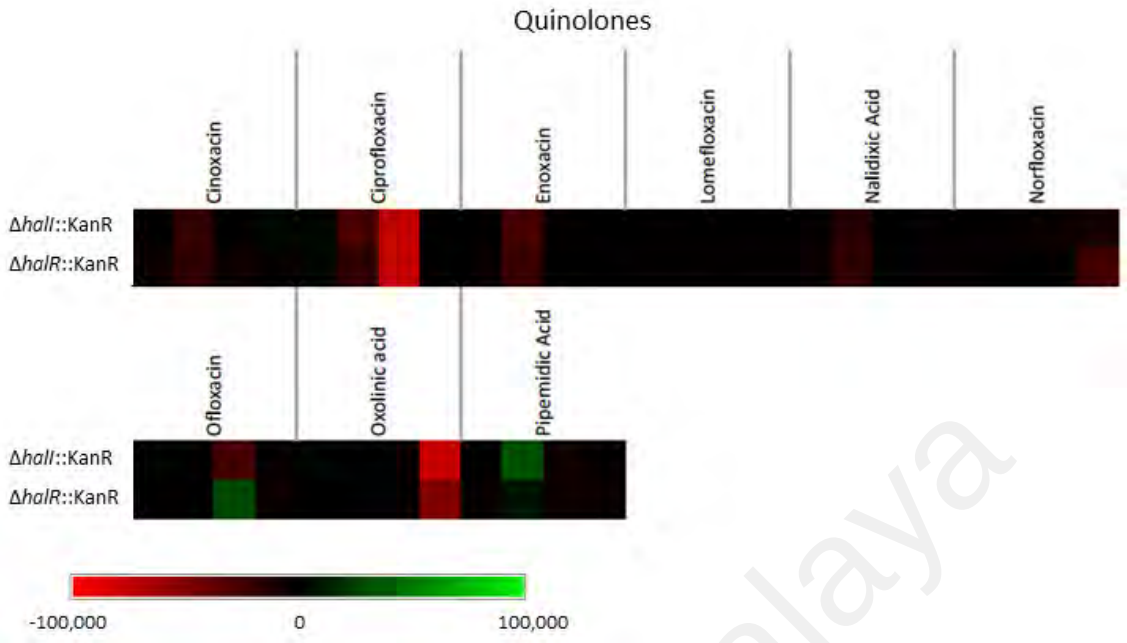

Figure 4.32, continued.

Table 4.12: Significant changes in resistance to antibiotics.

Class	Antibiotics	Change in Resistance		Mode of action
		Δ*halI*::KanR	Δ*halR*::KanR	
Aminoglycosides	Paromomycin	**98,123**	**93,573**	Protein synthesis inhibitor (30S ribosomal subunit)
	Tobramycin	7,506	**-69,942**	
Tetracyclines	Doxycycline	**-21,359**	-14,002	
	Demeclocyline	5,244	**-20,363**	
	Rolitetracycline	**-29,106**	**-43,507**	
Macrolides	Troleandomycin	**-27,930**	**-27,681**	Protein synthesis inhibitor (50S ribosomal subunit)
Amphenicols	Chloramphenicol	**-37,211**	7,506	
Lactams	Penicillin G	-474	**-88,514**	Inhibition of cell wall synthesis
	Carbenicillin	**23,348**	**-44,346**	
	Phenethicillin	-18,281	**-53,349**	
	Amoxicillin	-9,271	**-101,880**	
	Cefotaxime	**-42,410**	**-37,211**	
	Cefuroxime	19,817	**-66,031**	
	Cefsulodin	171	**-21,531**	
	Aztreonam	**-60,836**	-3,902	
Cyclic peptides	Colistin	881	**-22,292**	Membrane disruption
	Polymyxin B	2,936	**-49,666**	
Quinolones	Ofloxacin	**-25,675**	**29,447**	Inhibition of DNA synthesis (gyrase, topoisomerase)
	Norfloxacin	-8,696	**-24,126**	
	Ciprofloxacin	**-76,157**	**-76,041**	
	Enoxacin	**-25,620**	**-21,161**	
	Oxolinic acid	**-76,584**	**-49,842**	
	Pipemidic Acid	**32,867**	7,911	

Values above significant thresholds of 20,000 or below -20,000 were highlighted; Green: increased resistance; Red: decreased resistance

CHAPTER 5: DISCUSSION

5.1 Isolation and Identification of AHL-Producing Bacteria Isolated from Fish Paste Meatballs

Based on the subsequent identification results, these isolates consisted of seven species that belonged to the order *Enterobacteriales*. The selective medium (MacConkey agar) was used for the purpose of eliminating Gram-positive bacteria, as AHL is a form of signalling molecule that was produced exclusively by the phylum Proteobacteria. All seven species isolated from the samples, namely, *H. alvei*, *E. gergoviae*, *K. pneumoniae*, *R. ornithinolytica*, *P. vulgaris*, *P. mirabilis*, and *C. freundii*, have been reported on their recovery from food (Odenthal et al., 2016; Doulgeraki et al., 2011; Durlu-Özkaya et al., 2001; Stiles & Ng, 1981) and clinical association was reported for *K. pneumoniae* (Hiroi et al., 2012); *R. ornithinolytica* (Morais et al., 2009); *C. freundii* (Thurm & Gericke, 1994); and *P. mirabilis* (Wang et al., 2010).

The only AHL-producing isolate was preliminarily identified as *H. alvei* using MALDI-TOF MS platform. This proteome profiling method was superior to sequence-based typing in terms of speed and simplicity in sample processing, especially for Gram-negative bacteria, for which extraction is unnecessary under most conditions; and to biochemical method in terms of the more thorough representation of the profile pattern of gene products and metabolic functions (Singhal et al., 2015). Identification by MALDI-TOF MS has also been demonstrated to have high concordance with the microbial identification 'gold standard' 16S rDNA gene sequencing method (Suzuki et al., 2018; Timperio et al., 2017; Loucif et al., 2014). However, its accuracy in identifying an unknown isolate still relies heavily on the coverage of the reference database. Although customised libraries can be made, this method still has its limitation when it comes to characterisation of previously unencountered species. At the time when the experiment was performed, the local library did not include references for *H. paralvei* and *O. proteus*.

5.2 AHL Profile

A number of previous studies have reported on detection of AHL production in *H. alvei* (Viana et al., 2009; Pinto et al., 2007; Bruhn et al., 2004), and $3OC_6$-HSL seems to be the form of signalling molecule commonly produced throughout the species. Production of $3OC_8$-HSL by *H. alvei*, however, has not been documented. This AHL was, however, often detected and most intensively studied in plant-associated bacteria (Elasri et al., 2001; Cha et al., 1998; Zhu et al., 1998). Presence of this molecule has been linked to the virulence expression in *Pseudomonas aeruginosa*, an opportunistic human pathogen (Pearson et al., 1994), as well as *Yersinia ruckeri*, a fish pathogen (Kastbjerg et al., 2007). Whether $3OC_8$-HSL has a role in pathogenesis of *H. alvei* FB1, and does it contribute to the survival or colonisation of the strain in its environment of origin, remain questions to be solved in more in-depth studies.

5.3 Whole Genome Sequence (WGS) of *H. alvei* FB1

A complete genome offers various advantages over draft genomes, such as the possibility to accurately define gene coordination and distances within genome; reduced GC biased; ease in identifying paralogous genes; and detection of the presence of plasmids. In addition, methylation profiling of a certain genome is also possible with this technique. In this study, a complete genome of *H. alvei* FB1 was successfully generated by using PacBio SMRT technology.

The availability of whole genome sequence data of *H. alvei* FB1 served as a cornerstone to various downstream analyses that fulfilled the major objectives of this study. First, it allowed the identification of candidate genes involved in QS of *H. alvei* FB1 and subsequent mutagenesis work. In the later stage, the whole genome sequence also served as a reference for transcript annotation in RNA-Seq. Besides, several other analyses such as genome-based species circumscription, comparison with other genomes,

and phenotype-genotype association were made possible. Deposition of the genome sequence to a public database also contributed to forming a larger collection of genomic data of the species, which formed the basis of further studies accessible to a wider range of researchers.

5.3.1 Species Circumscription

A genome-based approach using ANI to determine the specific status of individual strains using the type strains of each species as references takes into account the diversity contained within genomic regions between closely related strains, which analysis on 16S rDNA gene sequences or individual genes fail to reflect (Appendix E). The results of ANI calculation between *H. alvei* FB1 and the type strains or type species within the family *Hafniaceae* not only confirmed the species identity of the strain, it also provided an insight into the species demarcation within the family *Hafniaceae*. One interesting finding in this study is, the type strain of *O. proteus*, DSM 2777^T, albeit with a different genus designation, shared a much larger ANI value (94.6%) with the type strain of *H. alvei* than that shared between the type strains of *H. alvei* and *H. paralvei* (82.6%). A high POCP shared between *O. proteus* DSM 2777^T with *H. alvei* ATCC 13337^T also supported the fact that it belonged to the genus *Hafnia*.

O. proteus has been reported to be closely related to *H. alvei*. Previously, '*O. proteus*' included microorganisms isolated from brewer's yeast, which could be divided into two biogroups by phenotypes and DDH (Priest et al., 1973). One of these biogroups was later transferred to the genus *Shimwellia*, whereas the remaining biogroup was reported to be related to *H. alvei* at a level as high as 75% renaturation in DDH by Priest and Barker (2010). However, the authors recommended that the name *O. proteus* be retained, as the similarity of multilocus sequence analysis (MLSA) comparison (95%) was found to be

above the mean similarity between species (92%), but still lower than the values that separated some other species involved in the study. Studies of *O. proteus* remain scarce.

5.3.2 Comparative Genomics Analysis

As ANI defined the species demarcation and demonstrated the relatedness between *H. alvei* FB1 with other closely or somewhat related genomes based solely on the nucleotide composition regardless of the functional aspect, comparison between the genomes were also carried out on the predicted proteomes. The values of average protein sequence identities reflected, roughly, the similarity between *H. alvei* FB1 and other genomes based on the putative orthologous genes that were shared between two genomes. When the genomic contents were sorted according to partitions with functional meaning instead of random nucleotide fragments, the results were somewhat in concordance with the ANI values.

For this analysis, the complete genome of *H. alvei* FB1 was used as a reference, and the CDSs from other genomes were mapped to their orthologues against it. Therefore, the results would not include the sequences that were not found in the reference genome. In order to provide an overview of the adaptation of *H. alvei* FB1, this analysis compared its genome with genomes of seven other strains confirmed to be *H. alvei*, one representative from each other species (type strains of *O. proteus* and *H. paralvei*) within the genus *Hafnia*, and the type strain of the type species of genus *Edwardsiella*, a fellow member of the family *Hafniaceae*, as a representative of the genus. It was found that the *H. alvei* FB1 genome contained only a handful of CDSs unique to itself, which were all annotated ambiguously.

From a brief overview on the circular map, it was obvious that phages and mobile elements, and the defense systems against which were the major contributors to the variation among the genomes. Unlike variation in some of the subsystem categories that

originated from a single genome of *E. tarda*, category Phages, Prophages, Transposable elements, Plasmids was shown to be the one that comprised most intra-species variation among *H. alvei* strains, and a majority of these CDSs were made up mainly of genetic elements of phage origins that had been integrated into bacterial genomes. As the most abundant life form on earth (Clokie et al., 2011), phages, the viruses that infect bacteria exist in all kinds of environments and have become a major driving force in bacterial evolution: the invasion of phages and the defence from their bacteria hosts drive the rapid co-evolution between both (Dy et al., 2014; Labrie, 2010; Samson et al., 2013). On the other hand, were also known as a form of vector for horizontal gene transfers (HGT), which contribute greatly to the genetic diversity in the bacterial populations (Ochman et al., 2000). Among the genomes involved in this analysis, it was found that not all genomes possessed CRISPR arrays or Cas genes, and the numbers of genes involved in restriction-modification vary. It is likely that the distribution of these genes was the results of selective forces from phage invasion actively at work at these regions. The frequent involvement in recombination events might also be a reason that the region containing the CRISPR-Cas systems particularly prone to mutations that led to the loss of gene functions or the genes entirely.

Type VI Secretion Systems (T6SS) were found within the regions showing low identities on the circular map. CDSs involved in this system were located on two separate loci in each of the *Hafnia* spp. genomes but not in *E. tarda* ATCC 15947^{T}. The presence of T6SS in other *E. tarda* strain has been studied extensively in the past decades (Chakraborty et al., 2011; Zheng & Leung, 2007; Rao et al., 2004). A brief search using the Protein Families feature on PATRIC (https://www.patricbrc.org/) revealed that T6SS was present in only some of the *Edwardsiella* strains. Some of the T6SS genes in *Hafnia* spp., when searched against the GenBank database using the BLAST feature, found closer matches in organisms more distantly related than *Edwardsiella* spp., such as *E. coli* and

Pseudomonas, suggesting possible events of HGT, of which the involvement with T6SS has been demonstrated experimentally by Thomas et al. (2017). Replacement of genes encoding the effectors/toxins through HGT has also been reported recently (Kirchberger et al., 2017). T6SS is known to be a toxin secretion system that can target both prokaryotic and eukaryotic cells, which has been reported to play a role in either virulence in host organisms (Burtnick et al., 2011; Ma & Mekalanos, 2010) or inter- or intraspecies competition (Jiang et al., 2014; Weyrich et al., 2012). T6SS has also been reported to be under regulation of QS in several microorganisms, such as *Vibrio* spp. (Sheng et al., 2012; Ishikawa et al., 2009; Enos-Berlage et al., 2005), *P. aeruginosa* (Lesic et al., 2009), and *Yersinia pseudotuberculosis* (Zhang et al., 2011).

It is worth noting that, of all *H. alvei* genomes involved in the comparison, genes responsible for urease activity, which were shown to be negative in *H. alvei* FB1 but positive in ATCC 13337^{T} according to the API Biochemical Assays, were found present only in ATCC 13337^{T} and FDAARGOS_350. On the other hand, genes responsible for amygdalin degradation were not specifically identified in the genome annotations. Urease, being known to have a well-established role in virulence of some pathogens (Mobley & Hausinger, 1989), also contributed to the acclimatisation of bacteria like *H. pylori* in the acidic gastric environment (Weeks et al., 2000). The presence in only part of the *H. alvei* genome could be an indication of the role of these genes in adaptation and colonisation. More intensive study would be required to support the speculation.

Comparison between *Hafnia* spp. genomes and the representative genome of the genus *Edwardsiella* revealed a number of subsystems that were present in *Hafnia* spp. but not their most closely related genus. Interestingly, some of these genes were found to be present in some of the more distantly related members of the family Enterobacteriaceae, some included species of known pathogens, such as *E. coli*, *Salmonella*, and *Klebsiella*.

These findings point to the occurrence of events of gene gains and losses along the divergence of the two genera, which could be linked to the adaptation to the environments.

From the brief comparison between *Hafnia* spp. and the type strain of *E. tarda*, it was shown that the major difference was represented by the lack of 527 CDSs in the latter. Most of these sequences were assigned to subsystems that were found to be involved in utilisation of certain sources of nutrients, such as xylose, rhamnose, and arabinose, indicating significance in adaptation. *E. tarda* ATCC 15947^{T}, as some of the *Hafnia* spp. involved in the analysis was isolated from human faeces. This lack of these genes possibly reflected the preference in nutrient uptake in a similar environment setting.

5.4 QS System in *H. alvei* FB1

Having examined *in silico* the characteristics of the candidates of QS genes in *H. alvei* FB1, the strain, unlike some other members of Proteobacteria, possessed only a single pair of *luxI-luxR* homologues. Throughout the genus *Hafnia*, only one *H. paralvei* strain, bta3-1 (CP004083.1), possessed an extra orphan *luxR* homologue. The observation of the presence of conserved domains and amino acid sites that are signature to the group of proteins, along with the orientation of the genes were strong evidence of the identity of the QS genes candidates. The clone of *halI* gene, when expressed in a non-AHL-producing host, produced the same forms of signalling molecules in the transformants, indicating that the candidate of *halI* gene indeed carried the function of AHL-synthase. In the subsequent step of mutant construction, it was shown that the removal of *halI* abolished the ability of AHL production in *H. alvei* FB1. Therefore, it is confirmed that the above mentioned *halI* gene was the one responsible in producing both $3OC_6$-HSL and $3OC_8$-HSL in *H. alvei* FB1.

The figure displaying the coding regions flanking the *luxI-luxR* homologues in closely related strains aligned according to a whole genome phylogenetic tree showed a relatively high degree of synteny within species *H. alvei* and the type strain of *O. proteus* but not *H. paralvei*. The presence of 'blocks' that varied within the species indicated recent events of gene gain/loss. The total lack of synteny between *H. alvei* and *H. paralvei* also suggested that the region could be prone to genome re-shuffling.

Phylogenetic trees constructed using choices of sequences included in the analyses adapted from a review by Tsai and Winans (2010) revealed that the amino acid sequences of HalR proteins from genus *Hafnia* fell into the monophyletic clade with other EsaR-like proteins. This, along with other traits, such as a convergent orientation with overlapping 3'-ends and responding to $3OC_6$-HSL, suggested the possibility that HalR might establish the similar quorum-hindered behaviour. Intermingling pattern between sequences originated from genomes that belonged to different classes of Proteobacteria was observed in one of the major clusters in both phylogenetic trees. This observation, along with the distant phylogenetic relationship between the orphan LuxR homologue with HalR, reflected the occurrence of HGT in the past, which has been reported in previous studies (Hao et al., 2010; Gray & Garey, 2001)

5.5 Genes under Regulation of QS

5.5.1 Distribution of Differentially Expressed Genes (DEGs)

According to the results of transcriptomic study, Δ*halI*::KanR and Δ*halR*::KanR mutants showed difference in functional distribution patterns of DEGs, which supports the postulation that HalR proteins belong to the quorum-hindered group. At early exponential phase, no significant DEG was observed in Δ*halI*::KanR, whereas a large number of DEGs were found in Δ*halR*::KanR. It is postulated that, at OD_{600} of 0.5, the concentration of AHLs within the culture environment was still too low to affect the

expression of any gene. Therefore, the mutant lacking AHL-synthase established a gene expression profile similar to the WT strain. The observation that removal of *halR* gene resulted in a very different expression profile pointed to the possibility that there were HalR proteins binding at the promoter regions of certain genes at such early stage and having a regulatory role in the absence of sufficient QS signals. A much larger number of up-regulated genes were observed in the Δ*halR*::KanR mutant compared with the down-regulated ones, indicating that the major role of HalR protein at this stage could be repression of certain functions in an early growth phase.

Later in the mid-exponential phase, the gene expression profiles in the two mutants changed. As the PCA plot implied, the triplicates of Δ*halR*::KanR mutant were now the ones clustered closer to the WT strain, implying that, with the increasing concentration of AHL molecules over time, the HalR proteins in FB1 WT were then released from their binding sites and the expression levels of the previously repressed genes became similar to the unrepressed ones in Δ*halR*::KanR. At this stage, DEGs could also be observed in Δ*halI*::KanR mutant. More than half of these genes showed changes in the same directions in both mutants, which reflected a scenario not as simple as the classical examples of 'quorum-hindered apo-proteins', in which the changes in both mutants were expected to be in opposite manners, suggesting a more complicated regulatory mechanism could be involved in the QS system in *H. alvei*.

5.5.2 Functional Distribution of QS-Regulated Genes

The enrichment analyses revealed that, in the early exponential phase, a number of traits related to dormancy and survival under stressful condition were found to be affected by the removal of the *halR* gene. The four GO terms most significantly enriched for up-regulated genes in exponential phase (cytoplasm, RNA binding, ATP binding, and tRNA binding) contained DEGs that could be roughly put into three categories: DNA replication

(helicases, gyrase, and topoisomerase), mismatch repair (*mutS*), and protein biosynthesis (rRNA and tRNA methyltransferases, aminoacyl-tRNA synthetases), which corresponded to the enriched KEGG pathways (Aminoacyl-tRNA biosynthesis, DNA replication, Mismatch repair, and Protein export). Genes involved in metabolism of ribose, an important building block of DNA and RNA backbones, was observed to be among the genes with the highest FCs. This up-regulation that occurred in the absence of HalR indicated that metabolism of nucleic acids was highly repressed in WT cells. Besides, fatty acid biosynthesis was also among the up-regulated functions in both analysis, suggesting that the cell membrane biosynthesis was also repressed. Regulation of chromosomal replication and cell division by QS has been reported in *E. coli* (DeLisa et al., 2001; Withers & Nordström, 1998) and *P. aeruginosa* (Wagner et al., 2003).

On the other hand, genes involved in stress response and sugar uptake showed decrease in expression in the Δ*halR*::KanR mutant, which could be reflected in the down-regulation of two biological process terms (stress response and phosphoenolpyruvate-dependent sugar phosphotransferase system) and five pathways (Phosphotransferase systems, carbon metabolism, Microbial metabolism in diverse environments, Fructose and mannose metabolism, and Citrate cycle). Several genes involved in PTS with specificity towards mannitol and ascorbate, along with a number of other sugar permeases and transporters, such as maltose, fructose, and galactose, were found among the genes with significant FC.

In the mid-exponential phase, many pathways involved in amino acid and fatty acid metabolism were down-regulated. In other words, these pathways were expressed at a higher level in the WT strain compared with the mutants. indicating that quorum played a significant role in promoting the metabolic activities in *H. alvei* FB1. Interestingly, the results of GO enrichment analysis implied that phosphotransferase systems that were activated in WT earlier were now repressed, suggesting that the importance of these

functions lied in an early growth phase but not in the mid-exponential phase. PTS is known to work not only as carbohydrate transport and modification systems in all phyla of bacteria, but also have regulatory roles in numerous cellular functions (Galinier & Deutscher, 2017). In *E. coli*, glucose-specific PTS was found to inhibit other non-PTS sugar permeases in the availability of glucose via dephosphorylation of the EIIA subunit (Kotrba et al., 2001). This phenomenon, termed "catabolite repression", contributes to the establishment of a hierarchy of sugar utilisation, which allows bacteria to utilise energy sources in an economical manner, as well as a regulatory circuit that acts according to nutrient availability (Brückner & Titgemeyer, 2002).

An overall picture gained from this observation is that QS seemed to be involved in repressing the functions involved in cell growth in an early growth phase, in which the cells were still in the process of recovery from the stationary phase stress, in a typical 'quorum-hindered apo-protein' manner. The repressed gene could be activated at a later stage when the DNA-bound apo-proteins were then 'hindered' by the presence of AHL molecules when cells were abundant. Apo-HalR, on the other hand, could be positively regulating the stress response and sugar uptake functions in the early exponential phase. PTS and various sugar transport systems that were kept activated at a low cell density could be a mechanism for detection of nutrient availability and management of energy consumption. Whether these events of repression and activation are interdependent or under separate regulatory circuit is a question remained to be solved in further studies.

The interesting fact that both mutants now shared more than half of their enriched pathways strongly suggests that in mid-exponential phase QS regulation worked in a manner different from the early exponential phase. In contrast with what would be expected in a 'quorum-hindered apo-protein' model, very few DEGs showed contradicting expression level between two mutants at this stage. However, currently

available data is still insufficient in providing a strong enough basis for the regulatory mechanism of HalR protein.

5.6 Phenotypic Changes with the Removal of QS Genes

5.6.1 Carbon Source Utilisation

Galactose is a monosaccharide that is commonly present in human diet, which is found in dairy products, avocados and sugar beets. It is also synthesised in human body in the form of glycoconjugates, which is found to be abundant in the gastric mucosa (Hynes et al., 2003). According to the SEED annotation, *H. alvei* FB1 possessed the complete apparatus that catabolised the conversion of galactose to UDP-glucose, namely, galactokinase, GalK (AT03_RS15760), and galactose-1-phosphate uridylyltransferase, GalT (AT03_RS15755). No significant changes in expression levels were observed in both genes in both mutants. Significant decrease was observed, however, in galactose ABC transporter substrate binding protein (AT03_RS07475) in Δ*halR*::KanR mutant in both early and mid-exponential phases (log_2FC = -2.720 and -2.744, respectively). This observation implied that the regulation of galactose uptake and utilisation by QS in *H. alvei* FB1 acted on the transport of the substrate into the cell.

Trehalose is a natural disaccharide that acts as a stress protectant in plants, fungi, prokaryotes, and invertebrates, but not produced in mammals (Tournu et al., 2013). It is also a common form of carbohydrate storage and blood sugar in insects like bees (Kunieda et al., 2006; Wyatt & Kale, 1957). Although not naturally synthesised in the human body, trehalose is a common presence in the human diet, such as in honey, bread, mushrooms, beer, and wine. The properties of trehalose as a non-reducing sugar with a relatively stable glycosidic bond and its non-involvement in the food browning process also make it an attractive candidate as a food additive (Iturriaga et al., 2009). The ability of *H. alvei* to utilise trehalose as a sole source of carbon could contribute in its survival

in food and likely to cause spoilage. In Gram-negative bacteria, trehalose is transported across the outer membrane through maltoporin (LamB), prior to its transportation into the cytoplasm via a trehalose-specific PTS transporter. The resulting trehalose-6-phosphate (T6P) is then hydrolysed into a glucose-6-phosphate (G6P) molecule and a glucose molecule by T6P hydrolase (Tournu et al., 2013). In *H. alvei* FB1, a negative change was observed in the expression level of *lamB* (AT03_RS02545, $\log_2$FC = -2.481) in Δ*halR*::KanR in the early exponential phase, while the other two showed no significant difference compared with WT, suggesting that the influence of QS on this phenotype was on the maltoporin gene.

Acetic acid, in the form of acetate, is among the short-chain fatty acids that are present in abundance in human colon, which has a role in the complicated network of metabolic cross-feeding among the colonic microbiota (den Besten et al., 2013; Venema, 2010; Duncan et al., 2004). The result of this study showed that removal of the QS genes lowered the efficiency in acetic acid utilisation in *H. alvei* FB1, which could affect its fitness in survival in a well-balanced intestinal environment. A previously reported example of QS affecting the utilisation of acetate was the AinS-induced acetate switch in *A*. *fischeri*, which played an important role in the symbiotic relationship between the bacteria and the squid (Studer et al., 2008). However, acetate kinase (Acs), the key enzyme under the regulation of AinS in the case of *A. fischeri*, did not show any significant changes in any of the mutants in each growth phase that was studied in *H. alvei* FB1. Instead, significant changes in the expression level of a cation acetate symporter (AT03_RS02360) were observed in both mutants in mid-exponential phase (-3.208 in Δ*hall*::KanR and -5.066 in Δ*halR*::KanR), indicating that the regulation on uptake and utilisation of acetate, albeit being present in both microorganisms, were done through different mechanisms.

5.6.2 Antibiotics Resistance

Among the 23 antibiotic resistance genes identified in *H. alvei* FB1 with PATRIC, three were observed to show reduced FC in the mid-exponential phase in both mutants, which could play a role in changes in resistance towards some of the antibiotics tested. Two of these were genes involved in a multidrug efflux system EmrAB-OMF (AT03_RS05530 and AT03_RS05535), whereas the other one was a Class C β-lactamase (AT03_RS21090).

It is well known that Gram-negative bacteria are more recalcitrant towards drug treatments due to the sophisticated structure of the cell envelope that is made up of an outer membrane (OM) that effectively limits the uptake of molecules from the environment (Delcour, 2009) and the presence of various efflux pumps that actively remove toxic molecules from the cytosol (Sun et al., 2014). EmrAB efflux system belongs to the major facilitator superfamily (MFS) efflux pump. It was demonstrated in *Erwinia chrysanthemi* that mutations in *emr* genes increased the sensitivity of strains towards a wide range of antimicrobial compounds, including carbenicillin, chloramphenicol, tetracycline, oleic acid, norfloxacin, oxacillin, and novobiocin (Maggiorani Valecillos et al., 2006). Both components of ErmAB-OMF were found to be down-regulated for two to three folds in both mutants in the mid-exponential phase. Therefore, it is likely that they had a role in the reduced resistance of mutants against some of the antibiotics.

Class C β-lactamases, also known as Group 1 cephalosporinases, are commonly found in the chromosomes of many *Enterobacteriales* (Bush & Jacoby, 2010). β-lactamases of this category are active on cephalosporins and may confer resistance against carbapenems under certain conditions, such as when produced in large amounts in hosts with low β-lactam accumulation due to porin mutations (Mammeri et al., 2008; Jacoby et al., 2004). The Class C β-lactamase gene in *H. alvei* FB1 was observed to be down-regulated at a $\log_2$FC of -1.379 in *hall*::KanR mutant in the mid-exponential phase. Difference in the

expression of this gene was not significant enough between *halR*::KanR and WT. However, results of Biolog PMs showed the opposite, in which *halR*::KanR, but not *halI*::KanR, showed reduced resistance towards a number of lactam antibiotics. These findings indicated that the changes in resistance towards lactam antibiotics in this experiment might not be directly related to the β-lactamase gene, and the possibility of this trait being a result of a different mechanism.

At current stage, no defined pattern was observed between the changes in antibiotic resistance of the QS mutants and the modes of action of the drugs, except that the increase in resistance towards some of the aminoglycosides (Paromomycin and Tobramycin) observed in the mutants could be due to the insertion of aminoglycoside phosphotransferase encoding gene that replaced the QS genes when the mutants were constructed. More work needs to be done in order to confirm these mechanisms.

5.7 Future Work

This study fulfilled its objective to investigate the influence of QS on the global gene expression by listing hundreds of candidates that could be under direct or indirect regulation of HalR. Consequently, a number of new questions arise, as the global expression profiles are in fact resulted from cascades of interactions between different pathways, under the influence of two AHLs of different carbon chain lengths. The questions, for instance, include: Whether the two different AHLs have separate effects on different subsets of genes; the modes of regulation of HalR with or without the presence of AHL; which genes are under direct regulation of QS; and the nature of the mechanisms that led to the phenotypic changes.

A few experiments can be done as continuation and complementation of this work. To study the regulatory role of each AHL in *H. alvei* FB1, transcriptomic profiling via RNA-Seq can be performed with Δ*halI*::KanR mutant complemented with different AHLs with

varying concentrations. To identify the genes that are under direct regulation of HalR and the modes of regulation, the protein-DNA interaction will be explored via ChIP-Seq. ChIP-Seq combines chromatin immunoprecipitation (ChIP) with massively parallel DNA sequencing to identify the binding sites of DNA-associated proteins. Transcriptomic study can also be carried out by harvesting RNA samples under various controlled growth conditions, based on the traits of interest.

CHAPTER 6: CONCLUSION

With the aim to study the QS system of *H. alvei* FB1, a food associated opportunistic pathogen that produces AHLs, this work covered all the objectives from isolation, characterisation of *H. alvei* FB1 AHL profile, locating and the subsequent deletion of its QS genes, to identification of a series of genes and phenotypes under the influence of QS. *H. alvei* FB1 was found to produce two types of signalling molecules, namely $3OC_6$-HSL and $3OC_8$-HSL, of which the production of the latter by *H. alvei* FB1 has not be reported previously. Using whole genome sequence analysis, a single pair of *luxI-luxR* homologues (*halI* and *halR*) was identified as the genes responsible for the AHL production and downstream regulation, further confirmed by mass spectrometry and mutagenesis analyses. This is also the first work reporting on the global transcriptomic profiles of QS gene knockout mutants of species *H. alvei*, which revealed not only a typical pattern of "quorum-hindered apo-protein", but also a complicated pattern of shifting in gene expression from early to mid-exponential growth phase. Hundreds of genes were observed to be affected by the removal of each of the two major components of the QS system, hence shortlisting the candidates to be focused on in the future study. In *H. alvei* FB1, removal of the QS system affected the utilisation of sugars, such as galactose, trehalose, and acetic acid, possibly through the transport mechanisms into the cells. Changes in resistance to a number of antibiotics were also observed. Some of the phenotypic changes could not be linked to the corresponding genes, possibly due to the different nature of the experiments. Our transcriptomic data captures only the expression profiles of the microorganisms at a fixed time point under a certain growth condition. Therefore, the gap between phenotypic and transcriptomic observation could very likely to be filled with the availability of datasets that cover multiple time points and growth conditions. Although with its limitations, this study has nevertheless fulfilled its role in a preliminary fundamental study, which could serve as a basis of more in depth study and

application in the future. It is hoped that these findings could serve as a cornerstone to provide an insight into further characterisation of the role of *H. alvei* in food industry and clinical studies.

REFERENCES

Adams, M. D., Kelley, J. M., Gocayne, J. D., Dubnick, M., Polymeropoulos, M. H., Xiao, H., . . . Moreno, R. F. (1991). Complementary DNA sequencing: Expressed sequence tags and human genome project. *Science, 252*(5013), 1651-1656.

Adeolu, M., Alnajar, S., Naushad, S., & S Gupta, R. (2016). Genome-based phylogeny and taxonomy of the 'Enterobacteriales': proposal for Enterobacterales ord. nov. divided into the families Enterobacteriaceae, Erwiniaceae fam. nov., Pectobacteriaceae fam. nov., Yersiniaceae fam. nov., Hafniaceae fam. nov., Morganellaceae fam. nov., and Budviciaceae fam. nov. *International Journal of Systematic and Evolutionary Microbiology, 66*(12), 5575-5599.

Altschul, S. F., Madden, T. L., Schäffer, A. A., Zhang, J., Zhang, Z., Miller, W., & Lipman, D. J. (1997). Gapped BLAST and PSI-BLAST: A new generation of protein database search programs. *Nucleic Acids Research, 25*(17), 3389-3402.

Andersen, J. B., Heydorn, A., Hentzer, M., Eberl, L., Geisenberger, O., Christensen, B. B., . . . Givskov, M. (2001). gfp-based *N*-acyl homoserine-lactone sensor systems for detection of bacterial communication. *Applied Environmental Microbiology, 67*(2), 575-585.

Andersson, R. A., Eriksson, A. R., Heikinheimo, R., Mäe, A., Pirhonen, M., Kõiv, V., . . . Palva, E. T. (2000). Quorum sensing in the plant pathogen *Erwinia carotovora* subsp. *carotovora*: the role of expR(Ecc). *Molecular Plant-Microbe Interactions, 13*(4), 384-393.

Andrews, S. (2010). FastQC: A quality control tool for high throughput sequence data. Retrieved on July 5, 2017 from http://www.bioinformatics.babraham.ac.uk/ projects/fastqc/

Angiuoli, S. V., Gussman, A., Klimke, W., Cochrane, G., Field, D., Garrity, G., . . . White, O. (2008). Toward an online repository of Standard Operating Procedures (SOPs) for (meta)genomic annotation. *OMICS: A Journal of Integrative Biology, 12*(2), 137-141.

Atkinson, S., Chang, C. Y., Sockett, R. E., Cámara, M., & Williams, P. (2006). Quorum sensing in *Yersinia enterocolitica* controls swimming and swarming motility. *Journal of Bacteriology, 188*(4), 1451-1461.

Aziz, R. K., Bartels, D., Best, A. A., DeJongh, M., Disz, T., Edwards, R. A., . . . Zagnitko, O. (2008). The RAST Server: Rapid annotations using subsystems technology. *BMC Genomics, 9*, 75.

Aziz, R. K., Devoid, S., Disz, T., Edwards, R. A., Henry, C. S., Olsen, G. J., . . . Xia, F. (2012). SEED servers: High-performance access to the SEED genomes, annotations, and metabolic models. *PLoS ONE, 7*(10).

Bainton, N. J., Bycroft, B. W., Chhabra, S. R., Stead, P., Gledhill, L., Hill, P. J., . . . Stewart, G. S. (1992). A general role for the *lux* autoinducer in bacterial cell signalling: control of antibiotic biosynthesis in *Erwinia*. *Gene, 116*(1), 87-91.

Bainton, N. J., Stead, P., Chhabra, S. R., Bycroft, B. W., Salmond, G. P., Stewart, G. S., & Williams, P. (1992). *N*-(3-oxohexanoyl)-L-homoserine lactone regulates carbapenem antibiotic production in *Erwinia carotovora*. *Biochemical Journal, 288 (Pt 3)*, 997-1004.

Barnard, A. M., Bowden, S. D., Burr, T., Coulthurst, S. J., Monson, R. E., & Salmond, G. P. (2007). Quorum sensing, virulence and secondary metabolite production in plant soft-rotting bacteria. *Philosophical transactions of the Royal Society of London. Series B, Biological sciences Royal Society (Great Britain), 362*(1483), 1165-1183.

Bassler, B. L., Wright, M., Showalter, R. E., & Silverman, M. R. (1993). Intercellular signalling in *Vibrio harveyi*: Sequence and function of genes regulating expression of luminescence. *Mole cular Microbiology, 9*(4), 773-786.

Blana, V. A., & Nychas, G. J. (2014). Presence of quorum sensing signal molecules in minced beef stored under various temperature and packaging conditions. *The International Journal of Food Microbiology, 173*, 1-8.

Bochner, B. R., Gadzinski, P., & Panomitros, E. (2001). Phenotype microarrays for high-throughput phenotypic testing and assay of gene function. *Genome Research, 11*(7), 1246-1255.

Brenner, D. J., & Farmer, J. J. (2005). Order XIII."Enterobacteriales". In D. J. Brenner, N. R. Krieg & J. T. Staley (Eds.), *Bergey's manual of systematic bacteriology* (2nd ed., pp. 587 – 849). Boston, MA: Springer.

Brenner, D. J., Fanning, G. R., Rake, A. V., & Johnson, K. E. (1969). Batch procedure for thermal elution of DNA from hydroxyapatite. *Analytical Biochemistry, 28*(1), 447-459.

Bruhn, J. B., Christensen, A. B., Flodgaard, L. R., Nielsen, K. F., Larsen, T. O., Givskov, M., & Gram, L. (2004). Presence of acylated homoserine lactones (AHLs) and AHL-producing bacteria in meat and potential role of AHL in spoilage of meat. *Applied Environmental Microbiology, 70*(7), 4293-4302.

Brückner, R., & Titgemeyer, F. (2002). Carbon catabolite repression in bacteria: Choice of the carbon source and autoregulatory limitation of sugar utilization. *FEMS Microbiology Letters, 209*(2), 141-148.

Burke, A. K., Duong, D. A., Jensen, R. V., & Stevens, A. M. (2015). Analyzing the transcriptomes of two quorum-sensing controlled transcription factors, RcsA and LrhA, important for *Pantoea stewartii* virulence. *PLoS ONE, 10*(12).

Burtnick, M. N., Brett, P. J., Harding, S. V., Ngugi, S. A., Ribot, W. J., Chantratita, N., . . . Deshazer, D. (2011). The cluster 1 type VI secretion system is a major virulence determinant in *Burkholderia pseudomallei*. *Infection and Immunity, 79*(4), 1512-1525.

Burton, E. O., Read, H. W., Pellitteri, M. C., & Hickey, W. J. (2005). Identification of acyl-homoserine lactone signal molecules produced by *Nitrosomonas europaea* strain Schmidt. *Applied Environmental Microbiology, 71*(8), 4906-4909.

Bush, K., & Jacoby, G. A. (2010). Updated functional classification of beta-lactamases. *Antimicrobial Agents and Chemotherapy, 54*(3), 969-976.

Case, R. J., Labbate, M., & Kjelleberg, S. (2008). AHL-driven quorum-sensing circuits: Their frequency and function among the Proteobacteria. *The ISME Journal, 2*(4), 345-349.

Cha, C., Gao, P., Chen, Y. C., Shaw, P. D., & Farrand, S. K. (1998). Production of acyl-homoserine lactone quorum-sensing signals by gram-negative plant-associated bacteria. *Molecular Plant-Microbe Interactions, 11*(11), 1119-1129.

Chhabra, S. R., Philipp, B., Eberl, L., Givskov, M., Williams, P., & Cámara, M. (2005). Extracellular communication in bacteria. In S. Schulz (Ed.), *The chemistry of pheromones and other semiochemicals II* (pp. 279-315). Berlin, Heidelberg: Springer Berlin Heidelberg.

Chakraborty, S., Sivaraman, J., Leung, K. Y., & Mok, Y. K. (2011). Two-component PhoB-PhoR regulatory system and ferric uptake regulator sense phosphate and iron to control virulence genes in type III and VI secretion systems of *Edwardsiella tarda*. *Journal of Biological Chemistry, 286*(45), 39417-39430.

Chandler, J. R., Duerkop, B. A., Hinz, A., West, T. E., Herman, J. P., Churchill, M. E., . . . Greenberg, E. P. (2009). Mutational analysis of *Burkholderia thailandensis* quorum sensing and self-aggregation. *Journal Bacteriology, 191*(19), 5901-5909.

Chin, C. S., Alexander, D. H., Marks, P., Klammer, A. A., Drake, J., Heiner, C., . . . Korlach, J. (2013). Nonhybrid, finished microbial genome assemblies from long-read SMRT sequencing data. *Nature Methods, 10*(6), 563-569.

Choi, S. H., & Greenberg, E. P. (1991). The C-terminal region of the *Vibrio fischeri* LuxR protein contains an inducer-independent *lux* gene activating domain. *Proceedings of the National Academy of Sciences of the United States of America, 88*(24), 11115-11119.

Christensen, A. B., Riedel, K., Eberl, L., Flodgaard, L. R., Molin, S., Gram, L., & Givskov, M. (2003). Quorum-sensing-directed protein expression in *Serratia proteamaculans* B5a. *Microbiology, 149*(2), 471-483.

Clokie, M. R., Millard, A. D., Letarov, A. V., & Heaphy, S. (2011). Phages in nature. *Bacteriophage, 1*(1), 31-45.

Coulthurst, S. J., Williamson, N. R., Harris, A. K., Spring, D. R., & Salmond, G. P. (2006). Metabolic and regulatory engineering of Serratia marcescens: mimicking phage-mediated horizontal acquisition of antibiotic biosynthesis and quorum-sensing capacities. *Microbiology, 152*(7), 1899-1911.

Danino, V. E., Wilkinson, A., Edwards, A., & Downie, J. A. (2003). Recipient-induced transfer of the symbiotic plasmid pRL1JI in *Rhizobium leguminosarum* bv. *viciae* is regulated by a quorum-sensing relay. *Molecular Microbiology, 50*(2), 511-525.

Datta, S., Costantino, N., & Court, D. L. (2006). A set of recombineering plasmids for gram-negative bacteria. *Gene, 379*, 109-115.

Davies, D. G., Parsek, M. R., Pearson, J. P., Iglewski, B. H., Costerton, J. W., & Greenberg, E. P. (1998). The involvement of cell-to-cell signals in the development of a bacterial biofilm. *Science, 280*(5361), 295-298.

de Oca-Mejía, M. M., Castillo-Juárez, I., Martínez-Vázquez, M., Soto-Hernandez, M., & García-Contreras, R. (2015). Influence of quorum sensing in multiple phenotypes of the bacterial pathogen *Chromobacterium violaceum*. *Pathogens and Disease, 73*(2), 1-4.

Delcour, A. H. (2009). Outer membrane permeability and antibiotic resistance. *Biochimica et Biophysica Acta, 1794*(5), 808-816.

DeLisa, M. P., Wu, C. F., Wang, L., Valdes, J. J., & Bentley, W. E. (2001). DNA microarray-based identification of genes controlled by autoinducer 2-stimulated quorum sensing in *Escherichia coli*. *Journal of Bacteriology, 183*(18), 5239-5247.

den Besten, G., van Eunen, K., Groen, A. K., Venema, K., Reijngoud, D. J., & Bakker, B. M. (2013). The role of short-chain fatty acids in the interplay between diet, gut microbiota, and host energy metabolism. *The Journal of Lipid Research, 54*(9), 2325-2340.

Devine, J. H., Shadel, G. S., & Baldwin, T. O. (1989). Identification of the operator of the *lux* regulon from the *Vibrio fischeri* strain ATCC7744. *Proceedings of the National Academy of Sciences of the United States of America, 86*(15), 5688-5692.

Dewhirst, F. E., Tamer, M. A., Ericson, R. E., Lau, C. N., Levanos, V. A., Boches, S. K., . . . Paster, B. J. (2000). The diversity of periodontal spirochetes by 16S rRNA analysis. *Oral Microbiology and Immunology, 15*(3), 196-202.

Dong, Y. H., Zhang, X. F., Soo, H. M., Greenberg, E. P., & Zhang, L. H. (2005). The two-component response regulator PprB modulates quorum-sensing signal production and global gene expression in *Pseudomonas aeruginosa*. *Molecular Microbiology, 56*(5), 1287-1301.

Doulgeraki, A. I., Ercolini, D., Villani, F., & Nychas, G. J. (2012). Spoilage microbiota associated to the storage of raw meat in different conditions. *International Journal of Food Microbiology, 157*(2), 130-141.

Doulgeraki, A. I., Paramithiotis, S., & Nychas, G. J. (2011). Characterization of the *Enterobacteriaceae* community that developed during storage of minced beef under aerobic or modified atmosphere packaging conditions. *International Journal of Food Microbiology, 145*(1), 77-83.

Duerkop, B. A., Ulrich, R. L., & Greenberg, E. P. (2007). Octanoyl-homoserine lactone is the cognate signal for *Burkholderia mallei* BmaR1-BmaI1 quorum sensing. *Journal of Bacteriology, 189*(14), 5034-5040.

Dumenyo, C. K., Mukherjee, A., Chun, W., & Chatterjee, A. K. (1998). Genetic and physiological evidence for the production of *N*-acyl homoserine lactones by *Pseudomonas syringae* pv. *syringae* and other fluorescent plant pathogenic *Pseudomonas* species. *European Journal of Plant Pathology, 104*(6), 569-582.

Duncan, S. H., Holtrop, G., Lobley, G. E., Calder, A. G., Stewart, C. S., & Flint, H. J. (2004). Contribution of acetate to butyrate formation by human faecal bacteria. *British Journal of Nutrition, 91*(6), 915-923.

Durlu-Özkaya, F., Ayhan, K., & Vural, N. (2001). Biogenic amines produced by Enterobacteriaceae isolated from meat products. *Meat Science, 58*(2), 163-166.

Dy, R. L., Richter, C., Salmond, G. P., & Fineran, P. C. (2014). Remarkable mechanisms in microbes to resist phage infections. *Annual Review of Virology, 1*(1), 307-331.

Eberl, L., Christiansen, G., Molin, S., & Givskov, M. (1996). Differentiation of *Serratia liquefaciens* into swarm cells is controlled by the expression of the *flhD* master operon. *Journal of Bacteriology, 178*(2), 554-559.

Eberl, L., Molin, S., & Givskov, M. (1999). Surface motility of *Serratia liquefaciens* MG1. *Journal of Bacteriology, 181*(6), 1703-1712.

Edwards, A., Frederix, M., Wisniewski-Dyé, F., Jones, J., Zorreguieta, A., & Downie, J. A. (2009). The *cin* and *rai* quorum-sensing regulatory systems in *Rhizobium leguminosarum* are coordinated by ExpR and CinS, a small regulatory protein coexpressed with CinI. *Journal of Bacteriology, 191*(9), 3059-3067.

Elasri, M., Delorme, S., Lemanceau, P., Stewart, G., Laue, B., Glickmann, E., . . . Dessaux, Y. (2001). Acyl-homoserine lactone production is more common among plant-associated *Pseudomonas* spp. than among soilborne *Pseudomonas* spp. *Applied Environmental Microbiology, 67*(3), 1198-1209.

Ellis, H. M., Yu, D., DiTizio, T., & Court, D. L. (2001). High efficiency mutagenesis, repair, and engineering of chromosomal DNA using single-stranded oligonucleotides. *Proceedings of the National Academy of Sciences of the United States of America, 98*(12), 6742-6746.

Engebrecht, J., Nealson, K., & Silverman, M. (1983). Bacterial bioluminescence: Isolation and genetic analysis of functions from *Vibrio fischeri*. *Cell, 32*(3), 773-781.

Engebrecht, J., & Silverman, M. (1984). Identification of genes and gene products necessary for bacterial bioluminescence. *Proceedings of the National Academy of Sciences of the United States of America, 81*(13), 4154-4158.

Engebrecht, J., & Silverman, M. (1987). Nucleotide sequence of the regulatory locus controlling expression of bacterial genes for bioluminescence. *Nucleic Acids Research, 15*(24), 10455-10467.

Engering, A., Hogerwerf, L., & Slingenbergh, J. (2013). Pathogen-host-environment interplay and disease emergence. *Emerging Microbes and Infections, 2*(2), e5.

Enos-Berlage, J. L., Guvener, Z. T., Keenan, C. E., & McCarter, L. L. (2005). Genetic determinants of biofilm development of opaque and translucent *Vibrio parahaemolyticus*. *Molecular Microbiology, 55*(4), 1160-1182.

Farmer, J. J., III. (2003). *Enterobacteriaceae* : Introduction and identification. In P. R. Murray, E. J. Baron, J. H. Jorgensen, M. A. Pfaller, & R. H. Tolken (Eds.), *Manual of clinical microbiology* (8th ed., pp. 636-653). Washington, D.C.: American Society of Microbiology Press.

Farrand, S. K., Qin, Y., & Oger, P. (2002). Quorum-sensing system of *Agrobacterium* plasmids: analysis and utility. *Methods in Enzymology, 358*, 452-484.

Fleischmann, R. D., Adams, M. D., White, O., Clayton, R. A., Kirkness, E. F., Kerlavage, A. R., . . . Merrick, J. M. (1995). Whole-genome random sequencing and assembly of *Haemophilus influenzae* Rd. *Science, 269*(5223), 496-512.

Fuqua, W. C., & Greenberg, E. P. (2002). Listening in on bacteria: Acyl-homoserine lactone signalling. *Nature Reviews Molecular Cell Biology, 3*(9), 685-695.

Fuqua, W. C., Winans, S. C., & Greenberg, E. P. (1994). Quorum sensing in bacteria: The LuxR-LuxI family of cell density-responsive transcriptional regulators. *Journal of Bacteriology, 176*(2), 269-275.

Galinier, A., & Deutscher, J. (2017). Sophisticated regulation of transcriptional factors by the bacterial phosphoenolpyruvate: Sugar phosphotransferase system. *Journal of Molecular Biology, 429*(6), 773-789.

Gao, R., Krysciak, D., Petersen, K., Utpatel, C., Knapp, A., Schmeisser, C., . . . Streit, W. R. (2015). Genome-wide RNA sequencing analysis of quorum sensing-controlled regulons in the plant-associated *Burkholderia glumae* PG1 strain. *Applied Environmental Microbiology, 81*(23), 7993-8007.

García-Contreras, R., Nuñez-López, L., Jasso-Chávez, R., Kwan, B. W., Belmont, J. A., Rangel-Vega, A., . . . Wood, T. K. (2015). Quorum sensing enhancement of the stress response promotes resistance to quorum quenching and prevents social cheating. *The ISME Journal, 9*(1), 115-125.

Goo, E., Majerczyk, C. D., An, J. H., Chandler, J. R., Seo, Y. S., Ham, H., . . . Hwang, I. (2012). Bacterial quorum sensing, cooperativity, and anticipation of stationary-phase stress. *Proceedings of the National Academy of Sciences of the United States of America, 109*(48), 19775-19780.

Goris, J., Konstantinidis, K. T., Klappenbach, J. A., Coenye, T., Vandamme, P., & Tiedje, J. M. (2007). DNA-DNA hybridization values and their relationship to whole-genome sequence similarities. *International Journal of Systematic Evolutionary Microbiology, 57*(1), 81-91.

Gram, L., Christensen, A. B., Ravn, L., Molin, S., & Givskov, M. (1999). Production of acylated homoserine lactones by psychrotrophic members of the Enterobacteriaceae isolated from foods. *Applied Environmental Microbiology, 65*(8), 3458-3463.

Grant, J. R., & Stothard, P. (2008). The CGView Server: A comparative genomics tool for circular genomes. *Nucleic Acids Research, 36*(Web Server issue), W181-184.

Gray, K. M., & Garey, J. R. (2001). The evolution of bacterial LuxI and LuxR quorum sensing regulators. *Microbiology, 147*(8), 2379-2387.

Gu, Z., Liu, Y., Shen, L., Liu, X., Xiao, N., Jiao, N., . . . Zhang, S. (2015). *Hafnia psychrotolerans* sp. nov., isolated from lake water. *International Journal of Systematic Evolutionary Microbiology, 65*(3), 971-974.

Hanzelka, B. L., & Greenberg, E. P. (1995). Evidence that the N-terminal region of the *Vibrio fischeri* LuxR protein constitutes an autoinducer-binding domain. *Journal of Bacteriology, 177*(3), 815-817.

Hanzelka, B. L., & Greenberg, E. P. (1996). Quorum sensing in *Vibrio fischeri*: Evidence that *S*-adenosylmethionine is the amino acid substrate for autoinducer synthesis. *Journal of Bacteriology, 178*(17), 5291-5294.

Hao, G., & Burr, T. J. (2006). Regulation of long-chain *N*-acyl-homoserine lactones in *Agrobacterium vitis*. *Journal of Bacteriology, 188*(6), 2173-2183.

Hao, Y., Winans, S. C., Glick, B. R., & Charles, T. C. (2010). Identification and characterization of new LuxR/LuxI-type quorum sensing systems from metagenomic libraries. *Environmental Microbiology, 12*(1), 105-117.

Heller, M. J. (2002). DNA microarray technology: Devices, systems, and applications. *Annual Review of Biomedical Engineering. 4*, 129-153.

Hiroi, M., Yamazaki, F., Harada, T., Takahashi, N., Iida, N., Noda, Y., . . . Ohashi, N. (2012). Prevalence of extended-spectrum β-lactamase-producing *Escherichia coli* and *Klebsiella pneumoniae* in food-producing animals. *Journal of Veterinary Medical Science, 74*(2), 189-195.

Holden, M. T., Seth-Smith, H. M., Crossman, L. C., Sebaihia, M., Bentley, S. D., Cerdeño-Tárraga, A. M., . . . Parkhill, J. (2009). The genome of *Burkholderia cenocepacia* J2315, an epidemic pathogen of cystic fibrosis patients. *Journal of Bacteriology, 191*(1), 261-277.

Holt, R. A., & Jones, S. J. (2008). The new paradigm of flow cell sequencing. *Genome Research, 18*(6), 839-846.

Horng, Y. T., Deng, S. C., Daykin, M., Soo, P. C., Wei, J. R., Luh, K. T., . . . Williams, P. (2002). The LuxR family protein SpnR functions as a negative regulator of *N*-acylhomoserine lactone-dependent quorum sensing in *Serratia marcescens*. *Molecular Microbiology, 45*(6), 1655-1671.

Hou, H. M., Zhu, Y. L., Wang, J. Y., Jiang, F., Qu, W. Y., Zhang, G. L., & Hao, H. S. (2017). Characteristics of *N*-acylhomoserine lactones produced by *Hafnia alvei* H4 isolated from spoiled instant sea cucumber. *Sensors*, *17*(4), 772.

Huang, d. W., Sherman, B. T., & Lempicki, R. A. (2009). Bioinformatics enrichment tools: Paths toward the comprehensive functional analysis of large gene lists. *Nucleic Acids Research, 37*(1), 1-13.

Huang, d. W., Sherman, B. T., & Lempicki, R. A. (2009). Systematic and integrative analysis of large gene lists using DAVID bioinformatics resources. *Nature Protocols, 4*(1), 44-57.

Huber, B., Riedel, K., Hentzer, M., Heydorn, A., Gotschlich, A., Givskov, M., . . . Eberl, L. (2001). The *cep* quorum-sensing system of *Burkholderia cepacia* H111 controls biofilm formation and swarming motility. *Microbiology, 147*(9), 2517-2528.

Hussain, M. B., Zhang, H. B., Xu, J. L., Liu, Q., Jiang, Z., & Zhang, L. H. (2008). The acyl-homoserine lactone-type quorum-sensing system modulates cell motility and virulence of *Erwinia chrysanthemi* pv. *zeae*. *Journal of Bacteriology, 190*(3), 1045-1053.

Huys, G., Cnockaert, M., Abbott, S. L., Janda, J. M., & Vandamme, P. (2010). *Hafnia paralvei* sp. nov., formerly known as *Hafnia alvei* hybridization group 2. *International Journal of Systematic Evolutionary Microbiology, 60*(8), 1725-1728.

Huys, G., Cnockaert, M., Janda, J. M., & Swings, J. (2003). *Escherichia albertii* sp. nov., a diarrhoeagenic species isolated from stool specimens of Bangladeshi children. *International Journal of Systematic Evolutionary Microbiology, 53*(3), 807-810.

Hynes, S. O., Teneberg, S., Roche, N., & Wadström, T. (2003). Glycoconjugate binding of gastric and enterohepatic *Helicobacter* spp. *Infection and Immunity, 71*(5), 2976-2980.

Höll, L., Behr, J., & Vogel, R. F. (2016). Identification and growth dynamics of meat spoilage microorganisms in modified atmosphere packaged poultry meat by MALDI-TOF MS. *Food Microbiology, 60*, 84-91.

Ishikawa, T., Rompikuntal, P. K., Lindmark, B., Milton, D. L., & Wai, S. N. (2009). Quorum sensing regulation of the two *hcp* alleles in *Vibrio cholerae* O1 strains. *PLoS ONE, 4*(8), e6734.

Iturriaga, G., Suárez, R., & Nova-Franco, B. (2009). Trehalose metabolism: from osmoprotection to signaling. *International Journal of Molecular Sciences, 10*(9), 3793-3810.

Jacoby, G. A., Mills, D. M., & Chow, N. (2004). Role of beta-lactamases and porins in resistance to ertapenem and other beta-lactams in *Klebsiella pneumoniae*. *Antimicrobial Agents and Chemotherapy, 48*(8), 3203-3206.

Janda, J. M., & Abbott, S. L. (2002). Bacterial identification for publication: when is enough enough? *Journal of Clinical Microbiology, 40*(6), 1887-1891.

Janda, J. M., & Abbott, S. L. (2006). The genus *Hafnia*: From soup to nuts. *Clinical Microbiology Reviews, 19*(1), 12-18.

Jiang, F., Waterfield, N. R., Yang, J., Yang, G., & Jin, Q. (2014). A *Pseudomonas aeruginosa* type VI secretion phospholipase D effector targets both prokaryotic and eukaryotic cells. *Cell Host & Microbe, 15*(5), 600-610.

Jones, P., Binns, D., Chang, H. Y., Fraser, M., Li, W., McAnulla, C., . . . Hunter, S. (2014). InterProScan 5: Genome-scale protein function classification. *Bioinformatics, 30*(9), 1236-1240.

Kastbjerg, V. G., Nielsen, K. F., Dalsgaard, I., Rasch, M., Bruhn, J. B., Givskov, M., & Gram, L. (2007). Profiling acylated homoserine lactones in *Yersinia ruckeri* and influence of exogenous acyl homoserine lactones and known quorum-sensing inhibitors on protease production. *Journal of Applied Microbiology, 102*(2), 363-374.

Khan, S. R., Mavrodi, D. V., Jog, G. J., Suga, H., Thomashow, L. S., & Farrand, S. K. (2005). Activation of the *phz* operon of *Pseudomonas fluorescens* 2-79 requires the LuxR homolog PhzR, *N*-(3-OH-Hexanoyl)-L-homoserine lactone produced by the LuxI homolog PhzI, and a *cis*-acting *phz* box. *Journal of Bacteriology, 187*(18), 6517-6527.

Kim, S., Park, J., Choi, O., Kim, J., & Seo, Y. S. (2014). Investigation of quorum sensing-dependent gene expression in *Burkholderia gladioli* BSR3 through RNA-seq analyses. *Journal of Microbiology and Biotechnology, 24*(12), 1609-1621.

Kimura, M. (1983). The neutral theory of molecular evolution. Cambridge, UK: Cambridge University Press.

Kirchberger, P. C., Unterweger, D., Provenzano, D., Pukatzki, S., & Boucher, Y. (2017). Sequential displacement of Type VI Secretion System effector genes leads to evolution of diverse immunity gene arrays in *Vibrio cholerae*. *Scientific Reports, 7*, 45133.

Koonin, E. V., & Galperin, M. (2013). Sequence—evolution—function: Computational approaches in comparative genomics. Berlin, Germany: Springer Science & Business Media.

Kotrba, P., Inui, M., & Yukawa, H. (2001). Bacterial phosphotransferase system (PTS) in carbohydrate uptake and control of carbon metabolism. *Journal of Bioscience and Bioengineering, 92*(6), 502-517.

Krumsiek, J., Arnold, R., & Rattei, T. (2007). Gepard: A rapid and sensitive tool for creating dotplots on genome scale. *Bioinformatics, 23*(8), 1026-1028.

Kumar, S., Stecher, G., & Tamura, K. (2016). MEGA7: Molecular Evolutionary Genetics Analysis version 7.0 for bigger datasets. *Molecular Biology and Evolution, 33*(7), 1870-1874.

Kunieda, T., Fujiyuki, T., Kucharski, R., Foret, S., Ament, S. A., Toth, A. L., . . . Maleszka, R. (2006). Carbohydrate metabolism genes and pathways in insects: Insights from the honey bee genome. *Insect Molecular Biology, 15*(5), 563-576.

Labbate, M., Queck, S. Y., Koh, K. S., Rice, S. A., Givskov, M., & Kjelleberg, S. (2004). Quorum sensing-controlled biofilm development in *Serratia liquefaciens* MG1. *Journal of Bacteriology, 186*(3), 692-698.

Labrie, S. J., Samson, J. E., & Moineau, S. (2010). Bacteriophage resistance mechanisms. *Nature Reviews Microbiology, 8*(5), 317-327.

Lane, D. J. (1991). 16S/23S rRNA sequencing. In E. Stackebrandt & M. Goodfellow (Eds.), *Nucleic acid techniques in bacterial systematics* (pp. 115-175). Chichester, UK: John Wiley and Sons.

Laue, B. E., Jiang, Y., Chhabra, S. R., Jacob, S., Stewart, G. S., Hardman, A., . . . Williams, P. (2000). The biocontrol strain *Pseudomonas fluorescens* F113 produces the *Rhizobium* small bacteriocin, *N*-(3-hydroxy-7-*cis*-tetradecenoyl)homoserine lactone, via HdtS, a putative novel *N*-acylhomoserine lactone synthase. *Microbiology, 146*(10), 2469-2480.

Lee, I., Ouk Kim, Y., Park, S. C., & Chun, J. (2016). OrthoANI: An improved algorithm and software for calculating average nucleotide identity. *International Journal of Systematic Evolutionary Microbiology, 66*(2), 1100-1103.

Lesic, B., Starkey, M., He, J., Hazan, R., & Rahme, L. G. (2009). Quorum sensing differentially regulates *Pseudomonas aeruginosa* type VI secretion locus I and homologous loci II and III, which are required for pathogenesis. *Microbiology, 155*(9), 2845-2855.

Lewenza, S., Conway, B., Greenberg, E. P., & Sokol, P. A. (1999). Quorum sensing in *Burkholderia cepacia*: Identification of the LuxRI homologs CepRI. *Journal of Bacteriology, 181*(3), 748-756.

Lindemann, A., Pessi, G., Schaefer, A. L., Mattmann, M. E., Christensen, Q. H., Kessler, A., . . . Harwood, C. S. (2011). Isovaleryl-homoserine lactone, an unusual branched-chain quorum-sensing signal from the soybean symbiont *Bradyrhizobium japonicum*. *Proceedings of the National Academy of Sciences of the United States of America, 108*(40), 16765-16770.

Lindsay, A., & Ahmer, B. M. (2005). Effect of *sdiA* on biosensors of *N*-acylhomoserine lactones. *Journal of Bacteriology, 187*(14), 5054-5058.

Lithgow, J. K., Wilkinson, A., Hardman, A., Rodelas, B., Wisniewski-Dyé, F., Williams, P., & Downie, J. A. (2000). The regulatory locus *cinRI* in *Rhizobium leguminosarum* controls a network of quorum-sensing loci. *Molecular Microbiology, 37*(1), 81-97.

Liu, C. H., Lin, W. J., Wang, C. C., Lee, K. L., & Tsai, M. C. (2007). Young-infant sepsis combined with urinary tract infection due to *Hafnia alvei*. *Journal of the Formosan Medical Association, 106*(3), S39-43.

Liu, M., Wang, H., & Griffiths, M. W. (2007). Regulation of alkaline metalloprotease promoter by *N*-acyl homoserine lactone quorum sensing in *Pseudomonas fluorescens*. *Journal of Applied Microbiology, 103*(6), 2174-2184.

Llamas, I., Keshavan, N., & González, J. E. (2004). Use of *Sinorhizobium meliloti* as an indicator for specific detection of long-chain *N*-acyl homoserine lactones. *Applied Environmental Microbiology, 70*(6), 3715-3723.

Loucif, L., Bendjama, E., Gacemi-Kirane, D., & Rolain, J. M. (2014). Rapid identification of Streptomyces isolates by MALDI-TOF MS. *Microbiological Research, 169*(12), 940-947.

Love, M. I., Huber, W., & Anders, S. (2014). Moderated estimation of fold change and dispersion for RNA-seq data with DESeq2. *Genome Biology, 15*(12), 550.

Lynch, M. J., Swift, S., Kirke, D. F., Keevil, C. W., Dodd, C. E., & Williams, P. (2002). The regulation of biofilm development by quorum sensing in *Aeromonas hydrophila*. *Environmental Microbiology, 4*(1), 18-28.

Ma, A. T., & Mekalanos, J. J. (2010). *In vivo* actin cross-linking induced by *Vibrio cholerae* type VI secretion system is associated with intestinal inflammation. *Proceedings of the National Academy of Sciences of the United States of America, 107*(9), 4365-4370.

Maggiorani, V. A., Rodríguez Palenzuela, P., & López-Solanilla, E. (2006). The role of several multidrug resistance systems in *Erwinia chrysanthemi* pathogenesis. *Molecular Plant-Microbe Interactions, 19*(6), 607-613.

Majerczyk, C., Brittnacher, M., Jacobs, M., Armour, C. D., Radey, M., Schneider, E., . . . Greenberg, E. P. (2014). Global analysis of the *Burkholderia thailandensis* quorum sensing-controlled regulon. *Journal of Bacteriology, 196*(7), 1412-1424.

Mammeri, H., Nordmann, P., Berkani, A., & Eb, F. (2008). Contribution of extended-spectrum AmpC (ESAC) beta-lactamases to carbapenem resistance in *Escherichia coli*. *FEMS Microbiology Letters, 282*(2), 238-240.

Marchler-Bauer, A., Bo, Y., Han, L., He, J., Lanczycki, C. J., Lu, S., . . . Bryant, S. H. (2017). CDD/SPARCLE: Functional classification of proteins via subfamily domain architectures. *Nucleic Acids Research, 45*(D1), D200-D203.

McClean, K. H., Winson, M. K., Fish, L., Taylor, A., Chhabra, S. R., Camara, M., . . . Williams, P. (1997). Quorum sensing and *Chromobacterium violaceum*: exploitation of violacein production and inhibition for the detection of *N*-acylhomoserine lactones. *Microbiology, 143*(12), 3703-3711.

McClure, R., Tjaden, B., & Genco, C. (2014). Identification of sRNAs expressed by the human pathogen *Neisseria gonorrhoeae* under disparate growth conditions. *Frontiers in Microbiology, 5*, 456.

McGowan, S., Sebaihia, M., Jones, S., Yu, B., Bainton, N., Chan, P. F., . . . Salmond, G. P. (1995). Carbapenem antibiotic production in *Erwinia carotovora* is regulated by CarR, a homologue of the LuxR transcriptional activator. *Microbiology, 141*(3), 541-550.

McNally, A., Thomson, N. R., Reuter, S., & Wren, B. W. (2016). 'Add, stir and reduce': *Yersinia* spp. as model bacteria for pathogen evolution. *Nature Reviews Microbiology, 14*(3), 177-190.

Miller, M. B., & Bassler, B. L. (2001). Quorum sensing in bacteria. *Annual Review of Microbiology, 55*, 165-199.

Minogue, T. D., Carlier, A. L., Koutsoudis, M. D., & von Bodman, S. B. (2005). The cell density-dependent expression of stewartan exopolysaccharide in *Pantoea stewartii* ssp. *stewartii* is a function of EsaR-mediated repression of the *rcsA* gene. *Molecular Microbiology, 56*(1), 189-203

Morais, V. P., Daporta, M. T., Bao, A. F., Campello, M. G., & Andrés, G. Q. (2009). Enteric fever-like syndrome caused by *Raoultella ornithinolytica* (*Klebsiella ornithinolytica*). *Journal of Clinical Microbiology, 47*(3), 868-869.

Moreno, C., Troncoso, M., Coria De La, P., Ledermann, W., Del Valle, G., Nuñez, C., . . . Fernández, A. (2010). Report of four clinical cases of *Hafnia alvei* bacteremia in a pediatric cardiac surgery unit. *Revista chilena de infectología, 27*(1), 40-44.

Moré, M. I., Finger, L. D., Stryker, J. L., Fuqua, C., Eberhard, A., & Winans, S. C. (1996). Enzymatic synthesis of a quorum-sensing autoinducer through use of defined substrates. *Science, 272*(5268), 1655-1658.

Møller, V. (1954). Distribution of amino acid decarboxylases in *Enterobacteriaceae*. *Acta Pathologica et Microbiologica Scandinavica 35*(3), 259-277.

Nieto Penalver, C. G., Morin, D., Cantet, F., Saurel, O., Milon, A., & Vorholt, J. A. (2006). *Methylobacterium extorquens* AM1 produces a novel type of acyl-homoserine lactone with a double unsaturated side chain under methylotrophic growth conditions. *FEBS Letters, 580*(2), 561-567.

Ochman, H., Lawrence, J. G., & Groisman, E. A. (2000). Lateral gene transfer and the nature of bacterial innovation. *Nature, 405*(6784), 299-304.

Odenthal, S., Akineden, Ö., & Usleber, E. (2016). Extended-spectrum β-lactamase producing *Enterobacteriaceae* in bulk tank milk from German dairy farms. *International Journal of Food Microbiology, 238*, 72-78.

Ortori, C. A., Dubern, J. F., Chhabra, S. R., Cámara, M., Hardie, K., Williams, P., & Barrett, D. A. (2011). Simultaneous quantitative profiling of *N*-acyl-L-homoserine lactone and 2-alkyl-4(*1H*)-quinolone families of quorum-sensing signaling molecules using LC-MS/MS. *Analytical and Bioanalytical Chemistry, 399*(2), 839-850.

Osuka, H., Hitomi, S., Koganemaru, H., & Kaneko, T. (2011). A case of bacteremia caused by *Hafnia paralvei*. *Journal of Infection and Chemotherapy, 17*(6), 855-857.

Papadopoulou, C., Economou, E., Zakas, G., Salamoura, C., Dontorou, C., & Apostolou, J. (2007). Microbiological and pathogenic contaminants of seafood in Greece. *Journal of Food Quality, 30*(1), 28-42.

Parsek, M. R., & Greenberg, E. P. (2000). Acyl-homoserine lactone quorum sensing in Gram-negative bacteria: A signaling mechanism involved in associations with higher organisms. *Proceedings of the National Academy of Sciences of the United States of America , 97*(16), 8789-8793.

Passador, L., Cook, J. M., Gambello, M. J., Rust, L., & Iglewski, B. H. (1993). Expression of *Pseudomonas aeruginosa* virulence genes requires cell-to-cell communication. *Science, 260*(5111), 1127-1130.

Pearson, J. P., Feldman, M., Iglewski, B. H., & Prince, A. (2000). *Pseudomonas aeruginosa* cell-to-cell signaling is required for virulence in a model of acute pulmonary infection. *Infection and Immunity, 68*(7), 4331-4334.

Pearson, J. P., Gray, K. M., Passador, L., Tucker, K. D., Eberhard, A., Iglewski, B. H., & Greenberg, E. P. (1994). Structure of the autoinducer required for expression of *Pseudomonas aeruginosa* virulence genes. *Proceedings of the National Academy of Sciences of the United States of America, 91*(1), 197-201.

Pearson, J. P., Van Delden, C., & Iglewski, B. H. (1999). Active efflux and diffusion are involved in transport of *Pseudomonas aeruginosa* cell-to-cell signals. *Journal of Bacteriology, 181*(4), 1203-1210.

Pesci, E. C., Pearson, J. P., Seed, P. C., & Iglewski, B. H. (1997). Regulation of *las* and *rhl* quorum sensing in *Pseudomonas aeruginosa*. *Journal of Bacteriology, 179*(10), 3127-3132.

Pierson, L. S., Gaffney, T., Lam, S., & Gong, F. (1995). Molecular analysis of genes encoding phenazine biosynthesis in the biological control bacterium. *Pseudomonas aureofaciens* 30-84. *FEMS Microbiology Letters, 134*(2-3), 299-307.

Pinto, U. M., de Souza Viana, E., Martins, M. L., & Vanetti, M. C. D. (2007). Detection of acylated homoserine lactones in gram-negative proteolytic psychrotrophic bacteria isolated from cooled raw milk. *Food Control, 18*(10), 1322-1327.

Piper, K. R., von Bodman, S. B., Hwang, I., & Farrand, S. K. (1999). Hierarchical gene regulatory systems arising from fortuitous gene associations: Controlling quorum sensing by the opine regulon in *Agrobacterium*. *Molecular Microbiology, 32*(5), 1077-1089.

Pirhonen, M., Flego, D., Heikinheimo, R., & Palva, E. T. (1993). A small diffusible signal molecule is responsible for the global control of virulence and exoenzyme production in the plant pathogen *Erwinia carotovora*. *The EMBO Journal, 12*(6), 2467-2476.

Priest, F. G., & Barker, M. (2010). Gram-negative bacteria associated with brewery yeasts: Reclassification of *Obesumbacterium proteus* biogroup 2 as *Shimwellia pseudoproteus* gen. nov., sp. nov., and transfer of *Escherichia blattae* to *Shimwellia blattae* comb. nov. *International Journal of Systematic Evolutionary Microbiology, 60*(4), 828-833.

Priest, F. G., Somerville, H. J., Cole, J. A., & Hough, J. S. (1973). The taxonomic position of *Obesumbacterium proteus*, a common brewery contaminant. *Journal of general microbiology, 75*(2), 295-307.

Puskas, A., Greenberg, E. P., Kaplan, S., & Schaefer, A. L. (1997). A quorum-sensing system in the free-living photosynthetic bacterium *Rhodobacter sphaeroides*. *Journal of Bacteriology, 179*(23), 7530-7537.

Qin, Q. L., Xie, B. B., Zhang, X. Y., Chen, X. L., Zhou, B. C., Zhou, J., . . . Zhang, Y. Z. (2014). A proposed genus boundary for the prokaryotes based on genomic insights. *Journal of Bacteriology, 196*(12), 2210-2215.

Quiñones, B., Pujol, C. J., & Lindow, S. E. (2004). Regulation of AHL production and its contribution to epiphytic fitness in *Pseudomonas syringae*. *Molecular Plant-Microbe Interactions, 17*(5), 521-531.

Rahman, S. R., Ahmed, M. F., & Begum, A. (2014). Occurrence of urinary tract infection in adolescent and adult women of shanty town in Dhaka City, Bangladesh. *Ethiopian Journal of Health Sciences, 24*(2), 145-152.

Ramachandran, R., Burke, A. K., Cormier, G., Jensen, R. V., & Stevens, A. M. (2014). Transcriptome-based analysis of the *Pantoea stewartii* quorum-sensing regulon and identification of EsaR direct targets. *Applied Environmental Microbiology, 80*(18), 5790-5800.

Ramos, A., & Dámaso, D. (2000). Extraintestinal infection due to *Hafnia alvei*. *European Journal of Clinical Microbiology & Infectious Diseases, 19*(9), 708-710.

Rao, P. S., Yamada, Y., Tan, Y. P., & Leung, K. Y. (2004). Use of proteomics to identify novel virulence determinants that are required for *Edwardsiella tarda* pathogenesis. *Molecular Microbiology, 53*(2), 573-586.

Redfield, R. J. (2002). Is quorum sensing a side effect of diffusion sensing? *Trends in Microbiology, 10*(8), 365-370.

Redondo, J., Maseda, E., Riquelme, A., Alday, E., Uña, R., & Criado, A. (2005). *Hafnia alvei* in a rare case of severe pneumonia in a postanesthesia recovery unit. *Revista Española de Anestesiología y Reanimación, 52*(6), 359-362.

Richter, M., & Rosselló-Móra, R. (2009). Shifting the genomic gold standard for the prokaryotic species definition. *Proceedings of the National Academy of Sciences of the United States of America, 106*(45), 19126-19131.

Ridell, J., & Korkeala, H. (1997). Minimum growth temperatures of *Hafnia alvei* and other *Enterobacteriaceae* isolated from refrigerated meat determined with a temperature gradient incubator. *International Journal Food Microbiology, 35*(3), 287-292.

Ridell, J., Siitonen, A., Paulin, L., Lindroos, O., Korkeala, H., & Albert, M. J. (1995). Characterization of *Hafnia alvei* by biochemical tests, random amplified polymorphic DNA PCR, and partial sequencing of 16S rRNA gene. *Journal of Clinical Microbiology, 33*(9), 2372-2376.

Ridell, J., Siitonen, A., Paulin, L., Mattila, L., Korkeala, H., & Albert, M. J. (1994). *Hafnia alvei* in stool specimens from patients with diarrhea and healthy controls. *Journal of Clinical Microbiology, 32*(9), 2335-2337.

Riedel, K., Hentzer, M., Geisenberger, O., Huber, B., Steidle, A., Wu, H., . . . Eberl, L. (2001). *N*-acylhomoserine-lactone-mediated communication between *Pseudomonas aeruginosa* and *Burkholderia cepacia* in mixed biofilms. *Microbiology, 147*(12), 3249-3262.

Rivas, M., Seeger, M., Jedlicki, E., & Holmes, D. S. (2007). Second acyl homoserine lactone production system in the extreme acidophile *Acidithiobacillus ferrooxidans*. *Applied Environmental Microbiology, 73*(10), 3225-3231.

Rodelas, B., Lithgow, J. K., Wisniewski-Dye, F., Hardman, A., Wilkinson, A., Economou, A., . . . Downie, J. A. (1999). Analysis of quorum-sensing-dependent control of rhizosphere-expressed (*rhi*) genes in *Rhizobium leguminosarum* bv. *viciae*. *Journal of Bacteriology, 181*(12), 3816-3823.

Rodríguez-Guardado, A., Boga, J. A., de Diego, I., & Pérez, F. (2006). Bacteremia caused by *Hafnia alvei* in an intensive care neonatal unit. *Medicina Clínica, 126*(9), 355-356.

Rosselló-Mora, R., & Amann, R. (2001). The species concept for prokaryotes. *FEMS Microbiology Reviews, 25*(1), 39-67.

Saitou, N., & Nei, M. (1987). The neighbor-joining method: A new method for reconstructing phylogenetic trees. *Molecular Biology and Evolution, 4*(4), 406-425.

Samson, J. E., Magadán, A. H., Sabri, M., & Moineau, S. (2013). Revenge of the phages: Defeating bacterial defences. *Nature Reviews Microbiology, 11*(10), 675-687.

Savini, V., Di Bartolomeo, E., Catavitello, C., Talia, M., Manna, A., Febbo, F., . . . D'Antonio, D. (2008). Graft versus host disease-related *Hafnia alvei* colonization and probable infection. *Journal of Medical Microbiology, 57*(9), 1167-1169.

Schu, D. J., Carlier, A. L., Jamison, K. P., von Bodman, S., & Stevens, A. M. (2009). Structure/function analysis of the *Pantoea stewartii* quorum-sensing regulator EsaR as an activator of transcription. *Journal of Bacteriology, 191*(24), 7402-7409.

See-Too, W. S., Ee, R., Madhaiyan, M., Kwon, S. W., Tan, J. Y., Lim, Y. L., . . . Chan, K. G. (2016). *Planococcus versutus* sp. nov., Isolated from soil. *International Journal of Systematic Evolutionary Microbiology*. *67, 944-95*.

Seemann, T. (2014). Prokka: Rapid prokaryotic genome annotation. *Bioinformatics, 30*(14), 2068-2069.

Seng, P., Drancourt, M., Gouriet, F., La Scola, B., Fournier, P. E., Rolain, J. M., & Raoult, D. (2009). Ongoing revolution in bacteriology: Routine identification of bacteria by matrix-assisted laser desorption ionization time-of-flight mass spectrometry. *Clinical Infectious Diseases, 49*(4), 543-551.

Sharan, S. K., Thomason, L. C., Kuznetsov, S. G., & Court, D. L. (2009). Recombineering: A homologous recombination-based method of genetic engineering. *Nature Protocols, 4*(2), 206-223.

Sheng, L., Gu, D., Wang, Q., Liu, Q., & Zhang, Y. (2012). Quorum sensing and alternative sigma factor RpoN regulate type VI secretion system I (T6SSVA1) in fish pathogen *Vibrio alginolyticus*. *Archives of Microbiology, 194*(5), 379-390.

Singhal, N., Kumar, M., Kanaujia, P. K., & Virdi, J. S. (2015). MALDI-TOF mass spectrometry: An emerging technology for microbial identification and diagnosis. *Frontiers in Microbiology, 6*, 791.

Stauff, D. L., & Bassler, B. L. (2011). Quorum sensing in *Chromobacterium violaceum*: DNA recognition and gene regulation by the CviR receptor. *Journal of Bacteriology, 193*(15), 3871-3878.

Steindler, L., & Venturi, V. (2007). Detection of quorum-sensing *N*-acyl homoserine lactone signal molecules by bacterial biosensors. *FEMS Microbiology Letters, 266*(1), 1-9.

Stiles, M. E., & Ng, L. K. (1981). Biochemical characteristics and identification of *Enterobacteriaceae* isolated from meats. *Applied Environmental Microbiology, 41*(3), 639-645.

Studer, S. V., Mandel, M. J., & Ruby, E. G. (2008). AinS quorum sensing regulates the *Vibrio fischeri* acetate switch. *Journal of Bacteriology, 190*(17), 5915-5923.

Sturme, M. H., Kleerebezem, M., Nakayama, J., Akkermans, A. D., Vaugha, E. E., & de Vos, W. M. (2002). Cell to cell communication by autoinducing peptides in gram-positive bacteria. *Antonie Van Leeuwenhoek, 81*(1-4), 233-243.

Su, Z., Fang, H., Hong, H., Shi, L., Zhang, W., Zhang, Y., . . . Tong, W. (2014). An investigation of biomarkers derived from legacy microarray data for their utility in the RNA-seq era. *Genome Biology, 15*(12), 523.

Subramoni, S., Florez Salcedo, D. V., & Suarez-Moreno, Z. R. (2015). A bioinformatic survey of distribution, conservation, and probable functions of LuxR solo regulators in bacteria. *Frontiers in Cellular and Infection Microbiology, 5*, 16.

Sun, J., Deng, Z., & Yan, A. (2014). Bacterial multidrug efflux pumps: Mechanisms, physiology and pharmacological exploitations. *Biochemical and Biophysical Research Communications, 453*(2), 254-267.

Suzuki, Y., Niina, K., Matsuwaki, T., Nukazawa, K., & Iguchi, A. (2018). Bacterial flora analysis of coliforms in sewage, river water, and ground water using MALDI-TOF mass spectrometry. *Journal of Environmental Science and Health, Part A: Toxic/Hazardous Substances and Environmental Engineering, 53*(2), 160-173.

Swift, S., Karlyshev, A. V., Fish, L., Durant, E. L., Winson, M. K., Chhabra, S. R., . . . Stewart, G. S. (1997). Quorum sensing in *Aeromonas hydrophila* and *Aeromonas salmonicida*: Identification of the LuxRI homologs AhyRI and AsaRI and their cognate *N*-acylhomoserine lactone signal molecules. *Journal of Bacteriology, 179*(17), 5271-5281.

Thomas, J., Watve, S. S., Ratcliff, W. C., & Hammer, B. K. (2017). Horizontal gene transfer of functional type VI killing genes by natural transformation. *MBio, 8*(4).

Thurm, V., & Gericke, B. (1994). Identification of infant food as a vehicle in a nosocomial outbreak of *Citrobacter freundii*: Epidemiological subtyping by allozyme, whole-cell protein and antibiotic resistance. *Journal of Applied Bacteriology, 76*(6), 553-558.

Timperio, A. M., Gorrasi, S., Zolla, L., & Fenice, M. (2017). Evaluation of MALDI-TOF mass spectrometry and MALDI BioTyper in comparison to 16S rDNA sequencing for the identification of bacteria isolated from Arctic sea water. *PLoS ONE, 12*(7).

Tjaden, B. (2015). De novo assembly of bacterial transcriptomes from RNA-seq data. *Genome Biology, 16*, 1.

TomLin, K. L., Malott, R. J., Ramage, G., Storey, D. G., Sokol, P. A., & Ceri, H. (2005). Quorum-sensing mutations affect attachment and stability of *Burkholderia cenocepacia* biofilms. *Applied Environmental Microbiology, 71*(9), 5208-5218.

Tournu, H., Fiori, A., & Van Dijck, P. (2013). Relevance of trehalose in pathogenicity: Some general rules, yet many exceptions. *PLoS Pathogens, 9*(8).

Trmčić, A., Chauhan, K., Kent, D. J., Ralyea, R. D., Martin, N. H., Boor, K. J., & Wiedmann, M. (2016). Coliform detection in cheese is associated with specific cheese characteristics, but no association was found with pathogen detection. *Journal of Dairy Science, 99*(8), 6105-6120.

Tsai, C. S., & Winans, S. C. (2010). LuxR-type quorum-sensing regulators that are detached from common scents. *Molecular Microbiology, 77*(5), 1072-1082.

Tsai, C. S., & Winans, S. C. (2011). The quorum-hindered transcription factor YenR of *Yersinia enterocolitica* inhibits pheromone production and promotes motility via a small non-coding RNA. *Molecular Microbiology, 80*(2), 556-571.

Urbanowski, M. L., Lostroh, C. P., & Greenberg, E. P. (2004). Reversible acyl-homoserine lactone binding to purified *Vibrio fischeri* LuxR protein. *Journal of Bacteriology, 186*(3), 631-637.

Van Domselaar, G. H., Stothard, P., Shrivastava, S., Cruz, J. A., Guo, A., Dong, X., . . . Wishart, D. S. (2005). BASys: A web server for automated bacterial genome annotation. *Nucleic Acids Research*, *33*(Web Server issue), W455-459.

Vandamme, P., & Dawyndt, P. (2011). Classification and identification of the *Burkholderia cepacia* complex: Past, present and future. *Systematic Applied Microbiology, 34*(2), 87-95.

Venema, K. (2010). Role of gut microbiota in the control of energy and carbohydrate metabolism. *Current Opinion in Clinical Nutrition & Metabolic Care, 13*(4), 432-438.

Venter, J. C., Smith, H. O., & Hood, L. (1996). A new strategy for genome sequencing. *Nature, 381*(6581), 364-366.

Viana, E. S., Campos, M. E., Ponce, A. R., Mantovani, H. C., & Vanetti, M. C. (2009). Biofilm formation and acyl homoserine lactone production in *Hafnia alvei* isolated from raw milk. *Biological Research, 42*(4), 427-436.

Vieira Colombo, A. P., Magalhães, C. B., Hartenbach, F. A., Martins do Souto, R., & Maciel da Silva-Boghossian, C. (2016). Periodontal-disease-associated biofilm: A reservoir for pathogens of medical importance. *Microbial Pathogenesis, 94*, 27-34.

von Bodman, S. B., & Farrand, S. K. (1995). Capsular polysaccharide biosynthesis and pathogenicity in *Erwinia stewartii* require induction by an *N*-acylhomoserine lactone autoinducer. *Journal of Bacteriology, 177*(17), 5000-5008.

von Bodman, S. B., Majerczak, D. R., & Coplin, D. L. (1998). A negative regulator mediates quorum-sensing control of exopolysaccharide production in *Pantoea stewartii* subsp. *stewartii*. *Proceedings of the National Academy of Sciences of the United States of America, 95*(13), 7687-7692.

Wagner, V. E., Bushnell, D., Passador, L., Brooks, A. I., & Iglewski, B. H. (2003). Microarray analysis of *Pseudomonas aeruginosa* quorum-sensing regulons: Effects of growth phase and environment. *Journal of Bacteriology, 185*(7), 2080-2095.

Wang, Y., Zhang, S., Yu, J., Zhang, H., Yuan, Z., Sun, Y., . . . Song, H. (2010). An outbreak of *Proteus mirabilis* food poisoning associated with eating stewed pork balls in brown sauce, Beijing. *Food Control, 21*(3), 302 - 305.

Weyrich, L. S., Rolin, O. Y., Muse, S. J., Park, J., Spidale, N., Kennett, M. J., . . . Harvill, E. T. (2012). A Type VI secretion system encoding locus is required for *Bordetella bronchiseptica* immunomodulation and persistence *in vivo*. *PLoS ONE, 7*(10).

Whistler, C. A., & Pierson, L. S. (2003). Repression of phenazine antibiotic production in *Pseudomonas aureofaciens* strain 30-84 by RpeA. *Journal of Bacteriology, 185*(13), 3718-3725.

Winans, S. C., Tsai, C. S., Ryan, G. T., Flores-Mireles, A. L., Costa, E., Shih, K. Y., . . . & Chhor, G. (2016). LuxR-type quorum-sensing regulators that are antagonized by cognate pheromones. In F. J. de Bruijin (Ed.), *Stress and environmental regulation of gene expression and adaptation in bacteria* (pp. 1221-1231). Hoboken, New Jersey: Wiley-Blackwell.

Winson, M. K., Swift, S., Fish, L., Throup, J. P., Jørgensen, F., Chhabra, S. R., . . . Stewart, G. S. (1998). Construction and analysis of *luxCDABE*-based plasmid sensors for investigating *N*-acyl homoserine lactone-mediated quorum sensing. *FEMS Microbiological Letters, 163*(2), 185-192.

Winson, M. K., Swift, S., Hill, P. J., Sims, C. M., Griesmayr, G., Bycroft, B. W., . . . Stewart, G. S. (1998). Engineering the *luxCDABE* genes from *Photorhabdus luminescens* to provide a bioluminescent reporter for constitutive and promoter probe plasmids and mini-Tn5 constructs. *FEMS Microbiology Letters, 163*(2), 193-202.

Wisniewski-Dyé, F., Jones, J., Chhabra, S. R., & Downie, J. A. (2002). *raiIR* genes are part of a quorum-sensing network controlled by *cinI* and *cinR* in *Rhizobium leguminosarum*. *Journal of Bacteriology, 184*(6), 1597-1606.

Withers, H. L., & Nordström, K. (1998). Quorum-sensing acts at initiation of chromosomal replication in *Escherichia coli*. *Proceedings of the National Academy of Sciences of the United States of America, 95*(26), 15694-15699.

Wood, D. W., Gong, F., Daykin, M. M., Williams, P., & Pierson, L. S. (1997). *N*-acyl-homoserine lactone-mediated regulation of phenazine gene expression by *Pseudomonas aureofaciens* 30-84 in the wheat rhizosphere. *Journal of Bacteriology, 179*(24), 7663-7670.

Wu, S., Zhu, Z., Fu, L., Niu, B., & Li, W. (2011). WebMGA: A customizable web server for fast metagenomic sequence analysis. *BMC Genomics, 12*, 444.

Wyatt, G. R., & Kale, G. F. (1957). The chemistry of insect hemolymph. II. Trehalose and other carbohydrates. *Journal of General Physiology, 40*(6), 833-847.

Yap, D. Y., Lau, S. K., Lamb, S., Choy, B. Y., Chan, T. M., Lai, K. N., & Tang, S. C. (2010). An unusual organism for PD-related peritonitis: *Hafnia alvei*. *Peritoneal Dialysis International, 30*(2), 254-255.

Yates, E. A., Philipp, B., Buckley, C., Atkinson, S., Chhabra, S. R., Sockett, R. E., . . . Williams, P. (2002). *N*-acylhomoserine lactones undergo lactonolysis in a pH-, temperature-, and acyl chain length-dependent manner during growth of *Yersinia pseudotuberculosis* and *Pseudomonas aeruginosa*. *Infection and Immunity, 70*(10), 5635-5646.

Yoon, S. H., Ha, S. M., Kwon, S., Lim, J., Kim, Y., Seo, H., & Chun, J. (2017). Introducing EzBioCloud: A taxonomically united database of 16S rRNA and whole genome assemblies. *International Journal of Systematic Evolutionary Microbiology*. *67*,1613-1617.

Yu, D., Ellis, H. M., Lee, E. C., Jenkins, N. A., Copeland, N. G., & Court, D. L. (2000). An efficient recombination system for chromosome engineering in *Escherichia coli*. *Proceedings of the National Academy of Sciences of the United States of America97*(11), 5978-5983.

Zhang, L., Murphy, P. J., Kerr, A., & Tate, M. E. (1993). *Agrobacterium* conjugation and gene regulation by *N*-acyl-L-homoserine lactones. *Nature, 362*(6419), 446-448.

Zhang, R. G., Pappas, K. M., Pappas, T., Brace, J. L., Miller, P. C., Oulmassov, T., . . . Joachimiak, A. (2002). Structure of a bacterial quorum-sensing transcription factor complexed with pheromone and DNA. *Nature, 417*(6892), 971-974.

Zhang, W., Xu, S., Li, J., Shen, X., Wang, Y., & Yuan, Z. (2011). Modulation of a thermoregulated type VI secretion system by AHL-dependent quorum sensing in *Yersinia pseudotuberculosis*. *Archives of Microbiology, 193*(5), 351-363.

Zhang, Y., Buchholz, F., Muyrers, J. P., & Stewart, A. F. (1998). A new logic for DNA engineering using recombination in *Escherichia coli*. *Nature Genetics, 20*(2), 123-128.

Zheng, J., & Leung, K. Y. (2007). Dissection of a type VI secretion system in *Edwardsiella tarda*. *Molecular Microbiology, 66*(5), 1192-1206.

Zhu, J., Beaber, J. W., Moré, M. I., Fuqua, C., Eberhard, A., & Winans, S. C. (1998). Analogs of the autoinducer 3-oxooctanoyl-homoserine lactone strongly inhibit activity of the TraR protein of *Agrobacterium tumefaciens*. *Journal of Bacteriology, 180*(20), 5398-5405.

Zhu, J., Chai, Y., Zhong, Z., Li, S., & Winans, S. C. (2003). *Agrobacterium* bioassay strain for ultrasensitive detection of *N*-acylhomoserine lactone-type quorum-sensing molecules: Detection of autoinducers in *Mesorhizobium huakuii*. *Applied Environmental Microbiology, 69*(11), 6949-6953.

LIST OF PUBLICATIONS AND PAPERS PRESENTED

LIST OF PUBLICATIONS

1. **Tan, J. Y.**, Yin, W. F., & Chan, K. G. (2014). Quorum sensing activity of *Hafnia alvei* isolated from packed food. *Sensors*, *14*(4), 6788-6796.
2. **Tan, J. Y.**, Yin, W. F., & Chan, K. G. (2014). Gene clusters of *Hafnia alvei* strain FB1 important in survival and pathogenesis: a draft genome perspective. *Gut pathogens*, *6*(1), 29.

LIST OF PRESENTATIONS

1. **Tan, J. Y.**, See-Too, W. S., Yin, W. F., and Chan, K. G. "Quorum Sensing Studies and Construction of Mutant of Hafnia alvei, An Opportunistic Pathogen and Food Spoilage Agent." International Congress of the Malaysian Society for Microbiology (ICMSM) 2015, Bayview Beach Resort, Penang, December 7th – 10th, 2015.
2. **Tan, J. Y.**, and Chan, K. G. "*N*-acyl-homoserine lactone profile of *Hafnia alvei* FB1." Monash Science Symposium 2014, Monash University Malaysia, June 18th and 19th, 2014.